FUNCTIONAL ANALYSIS OF RNP COMPLEXES IN EUKARYOTIC MRNA TRANSLATION

By

Robert Vincent Gerbasi

Dissertation

Submitted to the Faculty of the

Graduate School of Vanderbilt University

in partial fulfillment of the requirements

for the degree of

DOCTOR OF PHILOSOPHY

in

Microbiology and Immunology

May, 2007

Nashville, Tennessee

Approved:

Professor Earl Ruley

Professor Andrew Link

Professor Mark Boothby

Professor James Patton

ACKNOWLEDGEMENTS

A special thanks to my mentor Dr. Andrew Link for all of his suggestions and hard work during the course of this dissertation. The training I received while working in his lab will provide a valuable skill-set in my postdoctoral research. Additionally, the executive functions taught to me by Dr. Link (manuscript and grant writing etc.) will continue to support my transition as an independent investigator.

I also want to thank Dr. Elizabeth Link and Dr. Tracey Fleischer for editing published manuscripts presented in this dissertation. Their guidance and suggestions greatly improved the quality of my work, and I will continue to seek the guidance of editors in the future.

I want to thank various members of the Link lab past and present namely: Dave Powell, Jennifer Jennings, Jill McAfee, Dexter Duncan, Adam Farley, and Connie Weaver. These lab mates taught me valuable molecular and proteomic techniques. Additionally, they provided interesting suggestions concerning my research.

The teaching efforts of my professors and committee members should be recognized. Of particular impact are the courses and classes taught by Dr. Earl Ruley. Reviewing some of the high-impact and flawed work in cancer biology has increased my ability to critically scrutinize my own work and the work of others. Additionally, he taught me to ask the all-important question of “who cares

about this research?" In the future, I expect that frequently asking this question will increase the impact of the projects I pursue and the guidance I can provide to other young scientists.

I want to thank Dr. Mark Boothby, Dr. Hong Fang, and Dr. Jim Patton. Your philosophical guidance in my research was extremely valuable. In particular, your suggestions to pursue projects in the most tractable genetic system available (yeast) have brought success to this dissertation. I also want to thank these professors for all of their extensive teaching efforts.

My graduate work was supported by an NIH grant to Andrew Link (GM 62487) and the Viruses Nucleic Acids and Cancer Training Grant T32 CA009385 and GM64779.

TABLE OF CONTENTS

Page

LIST OF FIGURES

CHAPTER I

INTRODUCTION

This dissertation investigated the composition and function of two distinct eukaryotic ribonucleoprotein (RNP) complexes; the ribosome and *trans*-acting proteins associated with internal ribosomal entry sites. I specifically targeted the role these RNPs perform in mRNA translation. This introduction is broken into two parts. Part I discusses the history of ribosome structure and function. Part II introduces the concept of internal ribosomal entry sites and their *trans*-acting factors. The end of both sections summarizes the advances that this dissertation has contributed to our knowledge of both complexes.

Introduction Part I: Discovery of Ribosome Structure and Function

Protein synthesis and the Central Dogma of Molecular Biology

In 1958 Francis Crick described what he called “the central dogma of molecular biology” (Crick, 1970; Crick, 1958). Crick’s dogma dictated that proteins are not made directly from genes and that the intermediary between DNA and protein is RNA (Crick, 1970; Crick, 1958). The entire process can be summarized by a pathway where DNA gives rise to RNA which in turn gives rise to proteins. The first step in the process by which DNA is generated from RNA is

called transcription. The enzymes primarily responsible for transcription are called RNA polymerases along with a number of additional proteins and cofactors.

The second step of Crick's dogma is the conversion of RNA into protein. The process by which RNA is converted to a polypeptide is called translation. Although the ribosome represents the most important catalytic component of translation, like RNA polymerases in transcription, a number of other proteins and cofactors are required for translation. Both transcription and translation are separate processes in the central dogma of molecular biology that require large, complex molecular machines (polymerases and ribosomes, respectively) and a number of factors.

This dissertation is principally concerned with the discovery of novel proteins that regulate eukaryotic translation. As such, a brief history of the ribosome and its components is appropriate. The term "ribosome" was first coined by R.B. Roberts in 1958. The ribosome was the name given to the molecular machine responsible for decoding mRNA into protein. Some of the first evidence that the ribosome was the molecular assembly responsible for translation came from the lab of Nobel Laureate George E. Palade (Palade, 1955). Palade and coworkers used electron microscopy to directly observe the synthesis of radioactive chymotrypsinogen on the endoplasmic reticulum (ER) (Palade, 1955). The position of the newly synthesized chymotrypsinogen was punctate in nature. More importantly, the newly synthesized protein was scattered along the ER at what appeared to be organized centers of protein

synthesis. The centers of protein synthesis observed by Palade and coworkers were ribosomes.

Once the ribosome was associated with the site of protein synthesis, several research groups attempted to understand different aspects of the life of ribosomes. What is the nature of the ribosomal material? How do ribosomes function to make proteins from mRNA? The landmark experiments that have attempted to answer these questions will be described below.

Composition of Ribosomes

Ribosomes consist of two subunits that have different sedimentation coefficients. In prokaryotes, the 70S ribosome is divided into a large 50S and small 30S subunit. The 30S subunit contains a 16S ribosomal RNA (rRNA) and 21 core proteins (Dzionara et al., 1970). The 50S subunit contains 23S and 5S rRNAs and 34 proteins. In eukaryotes, the 80S ribosome is divided into a large 60S and a small 40S subunit. The 60S subunit contains 46 proteins and three rRNA species (28S, 5.8S, and 5S) (Planta and Mager, 1998). The 40S subunit contains 33 ribosomal proteins associated with a single 18S rRNA (Planta and Mager, 1998). In eukaryotes, the ribosomal RNA genes are transcribed as precursor RNAs. Three of the four rRNAs are transcribed as 35S pre-RNA by RNA polymerase I (Kressler et al., 1999). Following transcription, the 35S pre-RNA transcript is processed into the 18S, 5.8S, and 28S rRNAs (Kressler et al., 1999). The 5S ribosomal RNA is transcribed independently by RNA polymerase III (Kressler et al., 1999).

Identification of Core Ribosomal Proteins

Purification of ribosomes is achieved through sucrose gradient ultracentrifugation. Ribosomes, being very dense structures, will localize to the highest concentration of a sucrose gradient. Therefore, density gradient ultracentrifugation techniques were used to isolate ribosome particles.

One of the most important factors in determining if a protein was part of the ribosome core was the association of a protein with the ribosomal RNP in a high salt buffering environment. Using this criteria, research groups purified ribosomes in the presence of 0.5M NaCl (Dzionara et al., 1970; Kruiswijk and Planta, 1974; Warner and Gorenstein, 1978). Proteins that remained associated with the ribosome under these stringent conditions were considered core ribosomal proteins.

Separation of individual core ribosomal proteins was achieved through two-dimensional denaturing gel electrophoresis (Kaltschmidt and Wittmann, 1970; Kruiswijk and Planta, 1974; Warner and Gorenstein, 1978). 2-D electrophoresis separates proteins by their isoelectric point and molecular weight. A majority of the ribosomal subunits are basic proteins with a p*I* >8. The molecular weight of the individual ribosome proteins ranged from 60kDa to 7kDa (Kaltschmidt and Wittmann, 1970).

After the ribosomal subunits were separated by 2D-gel electrophoresis, individual proteins could be excised from the gels. Trypsin was used to digest proteins from the gel slices, and Edmund degradation was used to sequence the

polypeptides (Chersi et al., 1968; Morinaga et al., 1976). Although the combination of 2D-electrophoresis and manual sequencing resulted in the identification of almost all the core subunits, emerging technologies applied later proved that there are additional core ribosome proteins (Link et al., 1999).

Components of the Ribosome Necessary for Translational Activity

The research groups of Harry Noller, Masayasu Nomura, and others have investigated the components of the prokaryotic ribosome that are necessary for mRNA translation (Noller and Chaires, 1972) (Nomura and Lowry, 1967) (Nomura and Traub, 1968). They discovered that partial digestion of the ribosomal proteins with proteases failed to completely abolish translational activity (Noller et al., 1992). However, treatment of ribosomes with ribonucleases completely abolished peptidyl transferase activity. These results suggested that the catalytic activity responsible for mRNA translation might exist in the rRNA, not the ribosomal proteins. Crystallization of the prokaryotic ribosome would later provide evidence that the site of peptidyl transferase activity was void of direct contact with ribosomal proteins. Rather, the structure of the prokaryotic 70S ribosome showed that only the 23S rRNA was in proximity to the peptidyl transferase site (Nissen et al., 2000). Collectively, the work of Noller and others would suggest that peptidyl transferase activity of the ribosome is dependent on ribosomal RNA (Nissen et al., 2000; Noller et al., 1992). Therefore, ribosomal proteins appear to be dispensable for the most important catalytic activity of the large subunit.

Based on the experiments of Nomura and others, the core components of the prokaryotic ribosome are believed to function as chaperones of the ribosomal RNA (Held et al., 1974; Mizushima and Nomura, 1970). However, the function of each individual protein has not been investigated in detail. Assembly maps of the 30S subunit suggest that ribosome formation requires a specific protein-binding-order for ribosome biogenesis (Held et al., 1974; Mizushima and Nomura, 1970). Ribosome formation is hierarchical supporting an RNA-chaperone function for ribosomal proteins. Additionally, these results suggest that ribosomal proteins are inter-dependent in their association with the ribosome. Therefore, it is likely that each core ribosome protein mediates the association of multiple neighboring proteins with the ribosomal RNA.

Structural Formation of the Ribosome

To identify the functional components of the ribosome that catalyze protein synthesis, Nomura and colleagues dissociated the ribosome into subparticles (40S and 23S). To dissociate the ribosomal proteins, the particles were centrifuged in cesium chloride, a process referred to as the “split reaction” (Hosokawa et al., 1966). Proteins that would dissociate from the core ribosome particle after centrifugation through CsCl were referred to as the “split proteins” (Hosokawa et al., 1966; Traub et al., 1967; Traub and Nomura, 1968a; Traub and Nomura, 1968b). The subribosomal particles that lost split proteins were not able to synthesize polypeptides from mRNAs (Hosokawa et al., 1966). However, reconstitution of sub-ribosomal particles with split protein-containing purifications

restored protein synthesis *in vitro* (Traub and Nomura, 1968a; Traub and Nomura, 1968b; Traub et al., 1968). These results would suggest that the ribosome can form an active RNP complex spontaneously *in vitro (Hosokawa et al., 1966).* Later studies confirmed that individually purified (recombinant) core ribosomal proteins would form active ribosomes when reconstituted with rRNA *in vitro* (Culver and Noller, 1999).

Chaperones of Prokaryotic Ribosome Assembly

Although the research groups of Noller and Nomura showed that prokaryotic ribosomes would spontaneously form active complexes *in vitro*, more recent research suggests that these ribosomes require additional cofactors to form. A search for these cofactors was initiated because the *in vitro* assembly reaction required a heat activation step. In *E. coli*, normal ribosome assembly forms at a constant, lower temperature, suggesting that a cofactor might facilitate ribosome assembly *in vivo* (Nierhaus, 1991). Recently, the heat-shock protein DnaK has been shown to drive ribosome assembly *in vitro*, bypassing the requirement for a shift in reaction temperature (Fatica and Tollervey, 2002). Therefore, prokaryotic ribosome assembly is not entirely spontaneous and requires either the activity of chaperone proteins or heat energy.

Chaperones associated with the eukaryotic core ribosome

During translation, the nascent polypeptide emerges from the polypeptide exit channel located in the large subunit. The nascent polypeptides are assumed to lack a native structure immediately after synthesis. Therefore, it has been postulated that a number of ribosome-associated chaperone proteins bind to the nascent polypeptide during synthesis to achieve proper structure (Albanese et al., 2006). For example, in eukaryotes a complex of proteins called the nascent polypeptide associated complex (NAC) includes the HSP70 chaperone Ssb1/2p, Zuo1p, and Ssz1p, and it is believed to associate with the ribosome and fold nascent polypeptides as they are being synthesized (Huang et al., 2005) (Yan et al., 1998). The precise function of the NAC complex is not completely understood. Two lines of evidence suggest that NAC functions to fold nascent polypeptides. First, NAC proteins form molecular cross-links with nascent polypeptides (Albanese et al., 2006) (Pfund et al., 1998). Second, treatment of cells with puromycin, a drug that prematurely terminates polypeptide synthesis at the ribosome, reduces the association of the NAC complex with the ribosome (Nelson et al., 1992).

A second function for the NAC complex has been proposed. Because puromycin treatment of ribosomes only partially dissociates NAC components, it is possible that this chaperone-containing complex functions to ensure that the core ribosome particle retains a correct conformation. Additionally, studies from Nancy Craig's lab suggest that Ssb1/2p functions to facilitate the translation process and is important in maintaining appropriate ribosome structure (Nelson

et al., 1992). Therefore, it is possible that Ssb1/2p may carry-out two functions: 1. the folding of nascent polypeptides, and 2. chaperoning the core ribosome particle. The recent discovery of an HSP protein that chaperones the biogenesis of nascent ribosomes supports a role for these proteins in maintaining ribosome structure or formation (Meyer et al., 2007). In summary both prokaryotic and eukaryotic ribosomes contain HSP70 chaperone proteins, although the precise function of these chaperones in protein synthesis is poorly understood.

Similarities and Differences in Prokaryotic and Eukaryotic Ribosome Formation

Cryo-electron microscopy has provided a straightforward understanding of the structural differences between eukaryotic and prokaryotic ribosomes (Spahn et al., 2004). Although the eukaryotic 60S and 40S subunits have additional rRNA and protein components compared to the prokaryotic 50S and 30S subunits, the overall structure and shape of the prokaryotic and eukaryotic ribosomes are conserved (Spahn et al., 2004) . As discussed in the proceeding section, active prokaryotic ribosomes will form *in vitro*. In contrast, attempts aimed at reconstituting eukaryotic ribosomes *in vitro* have failed. The reasons for this failure are currently unknown. In eukaryotes, ribosome biogenesis begins in the nucleolus and is completed in the cytoplasm. Over 100 different ribosome biogenesis factors have been identified that localize to the nucleolus and are postulated to function during the assembly of the ribosome (Warner, 2001) (Fatica and Tollervey, 2002) (Kressler et al., 1999; Woolford, 2002).

Eukaryotic Ribosome Biogenesis

A majority of eukaryotic ribosome biogenesis occurs in a subnuclear compartment termed the nucleolus (Warner, 2001). The (28S-25S), 18S, and 5.8S rRNAs are all transcribed as a single 35S precursor RNA by RNA polymerase I, whereas the 5S rRNA is independently transcribed by RNA polymerase III (Kressler et al., 1999). Following transcription of the 35S pre-rRNA, nucleases process the precursor RNA into 27S, 25S, 20S, and 5.8S rRNAs (Fromont-Racine et al., 2003; Granneman and Baserga, 2004; Kressler et al., 1999; Warner, 2001). Cleavage of these precursor rRNAs into mature rRNA species is facilitated by a number of small nucleolar RNAs (Fatica and Tollervey, 2002). Unlike the large subunit rRNAs (28-25S, 5.8S, and 5S), the small subunit rRNA (18S) completes a final step of processing outside the nucleolus (Kressler et al., 1999). The pre-40S particle is shuttled from the nucleolus to the cytoplasm. In the cytoplasm the pre-20S rRNA is processed into mature 18S rRNA.

Assembly of ribosomal RNAs with ribosomal proteins in the nucleolus is a complex and poorly understood process. A plethora of non-ribosomal nucleolar proteins have been identified that are critical for ribosome biogenesis (de la Cruz et al., 2005; Dosil and Bustelo, 2004; Harnpicharnchai et al., 2001). Mutation of these ribosome biogenesis factors results in ribosomal RNA processing defects. Because of all the cofactors involved in biogenesis, a complete understanding of eukaryotic ribosome formation will require decades of research.

Ribosome-associated proteins discovered through modern mass spectrometry Approaches

Although several research groups successfully identified a number of core ribosome subunits using a combination of 2D-gel electrophoresis and manual protein sequencing, it is possible that a subset of the associated proteins may have escaped detection. There are several possible reasons why these proteins may have been missed from these early screens. First, separation of complex protein mixtures using 2D-gels has been problematic in the past because complex samples often contain proteins with overlapping isoelectric points (p*I*) and similar molecular weights (MW). 2-D gel electrophoresis has a limited fractionation range. As a result, proteins with extreme pI and MW are typically absent. Additionally, the technology used to identify proteins often presented technical hurdles. Because Edmund degradation requires near-homogeneity, proteins with overlapping mobilities in 2D gels would have provided confusing protein sequences. Additional problems with 2D analysis include the fragile nature of the gels, and various buffering issues. Collectively, the combination of 2D-gel electrophoresis and Edmund degradation correctly defined the identity of a majority of the ribosomal proteins (Dzionara et al., 1970; Higo et al., 1982; Ishiguro, 1976; Kaltschmidt and Wittmann, 1970; Kruiswijk and Planta, 1974; Otaka et al., 1982; Zinker and Warner, 1976). However, common difficulties that are encountered when using these techniques most likely left a population of ribosome-associated proteins undiscovered.

In the mid-1990s, mass spectrometry approaches were developed that aimed to identify the composition of complex protein samples without the use of gels (McCormack et al., 1997). This approach was later developed for analyzing complex protein mixtures termed direct-analysis-of-large-protein-complexes (DALPC) (Link et al., 1999). The approach was renamed to multidimensional-protein-identification-technology (MUDPIT) (Washburn et al., 2001). The approach coupled multidimensional liquid chromatography with tandem mass spectrometry to identify proteins in very complex mixtures. The technique provided advantages over previous approaches used to identify components of multi-protein complexes. First, MUDPIT circumvented the need for separation of proteins by gels. Peptides lost during extraction from gel slices could result in failure to identify proteins. In MUDPIT, peptides are directly loaded onto a multi-dimensional-chromatography column. Second, MUDPIT identifies proteins in a sample that do not stain in gels. Therefore, the technique reduces the biased imposed by manual visualization of protein bands.

Perhaps the most important advantage of MUDPIT is the multi-dimensional nature of the chromatography columns used in the technique. First, the peptides are loaded onto a strong-cation-exchange column. The peptides are released with successive increases in salt concentration and transferred to a reversed phase column. Peptides will bind to the reversed phase column based on their relative hydrophobicity. Peptides are dissociated with a gradient of increasing acetonitrile concentration. The multi-dimensional nature of MUDPIT chromatography dramatically increases the number of peptides that are detected.

This most likely occurs by separating abundant peptides from less abundant peptides that are competing for ionization and detection by the mass spectrometer.

The MUDPIT approach successfully identified a number of the known core components of the ribosome (Link et al., 1999). In addition, novel ribosome-associated proteins were discovered that co-purified with the eukaryotic ribosome. Among Yates and Link's initial screen, Asc1p/RACK1 associated with the ribosome under high salt conditions. Asc1p was associated with yeast ribosome while RACK1 was associated with human ribosomes. An exceptionally high number of unique Asc1p and RACK1 mass spectra were associated with ribosomes under high salt conditions. 2-D gel analysis of yeast ribosomal proteins showed Asc1p was stoichiometric to other core ribosome components. Because Asc1p and RACK1 bound to the ribosome under stringent conditions and appeared to be stoichiometric with other core ribosomal proteins, it was speculated that these proteins might be core components of the ribosome (Link et al., 1999).

ASC1 Gene Structure is Consistent with other Core Ribosome Protein Encoding Genes

If *ASC1* encodes a ribosome-associated protein, then the structure of the *ASC1* gene should contain features that are shared among other ribosomal protein encoding genes. The codon adaptive index (CAI) is a measurement of the relative adaptiveness of the codon usage of a gene toward the codon usage of highly expressed genes (Jansen et al., 2003; Sharp and Li, 1987). In yeast,

the ribosomal protein coding genes have a CAI ranging from 0.6 to 0.9 with 1.0 being the highest value (Planta and Mager, 1998). *ASC1* has a CAI of 0.71(Gerbasi et al., 2004). Therefore, the codon adaptiveness of *ASC1* parallels that of other ribosomal protein encoding genes. Another feature of the *ASC1* gene structure that is consistent with that of ribosomal protein encoding genes is the presence of an intron. Introns occur in only small percentage (<3%) of genes in yeast. However, 66% of the ribosomal genes contain an intron (Planta and Mager, 1998). Therefore, the structure of the *ASC1* gene shares similar features with other ribosomal protein encoding genes.

Proposed Functional roles of *ASC1* in yeast

The name *ASC1* is an acronym that stands for "absence of growth suppression in a *cyp1* mutant" (Chantrel et al., 1998). *CYP1* is a yeast transcription factor that activates the expression of a number of genes in response to hypoxia (Creusot et al., 1988). Mutant yeast strains with *cyp1 alleles* fail to grow in environments that are oxygen poor (Kwast et al., 1998). *ASC1* was discovered in a screen for suppressor mutations that would rescue growth in a low oxygen environment in a *cyp1* mutant yeast background (Chantrel et al., 1998). Therefore, it was hypothesized that *ASC1* functioned as a repressor of *CYP1*-mediated gene expression.

The genetic data suggesting that *ASC1* functioned as a repressor of Cyp1-mediated gene expression prompted investigation into the function of *ASC1* as a potential transcriptional repressor. Interestingly, yeast strains with

asc1 alleles have elevated levels of mRNAs that are usually expressed during amino acid starvation (Hoffmann et al., 1999). These results strongly suggest that *ASC1* functions to represses gene expression in yeast.

Structure and Proposed functions of RACK1 in human cells

RACK1 was originally identified in a screen for proteins that interact with activated Protein Kinase C (Ron et al., 1994). The primary structure of RACK1 contains repeats of tryptophan and aspartic acid residues. As such, RACK1 belongs to the WD-40 family of proteins. WD-40 proteins are predicted to form a β-propeller structure and have promiscuous binding properties (Smith et al., 1999; van Nocker and Ludwig, 2003). Because Asc1p/RACK1 is very abundant (330,000 molecules/yeast cell) and has promiscuous binding properties, a high level of background protein interactions are predicted (Ghaemmaghami et al., 2003; Smith et al., 1999). Many of the reported interactions with Asc1p/RACK1 may not be physiological. Two proteins that are consistently reported to interact with RACK1 are the protein kinases PKC and SRC (Cox et al., 2003; Lopez-Bergami et al., 2005; Ron et al., 1994; Ron et al., 1999; Schechtman and Mochly-Rosen, 2001). It is postulated that RACK1 functions as an adapter protein to bring these two kinases in proximity to their substrates. Experiments showing RACK1 is associated with the ribosome and binds to these kinases has fueled speculation that RACK1 provides a link between signal transduction and translation (Ceci et al., 2003; Nilsson et al., 2004).

Conserved sequence and structure of Asc1p/RACK1 across eukaryotes

Yeast Asc1p and Human RACK1 share a 54% sequence identity, strongly suggesting that the two proteins are orthologs. The sequence of the protein appears to be conserved across the eukarya, but is absent from prokaryotic proteomes suggesting that *ASC1* performs a function unique to eukaryotes. Asc1p and RACK1 contain multiple WD-repeats. WD-repeat containing proteins are often associated with scaffolding functions. Many of the WD-repeat containing proteins have also been implicated in signal transduction (Dell et al., 2002; Liu et al., 2001; Slessareva et al., 2006). However, in yeast many of the ribosome biogenesis factors are WD-repeat containing proteins (de la Cruz et al., 2005; Dosil and Bustelo, 2004; Harnpicharnchai et al., 2001; Iouk et al., 2001; Pestov et al., 2001; Saveanu et al., 2003; Schaper et al., 2001). Therefore, it is possible that one of *ASC1* and RACK1 functions is to facilitate ribosome biogenesis.

A Defined Structural and Functional Role for Asc1p/RACK1

The structural and functional relationship of Asc1p with the ribosome became the primary focus of this dissertation. The history of functional and biochemical claims made regarding Asc1p and RACK1 are very diverse. The possibility that Asc1p and RACK1 perform all of the reported functions is unlikely. This dissertation investigated the structural and functional relationship of Asc1p and RACK1 with the ribosome.

RACK1 co-fractionated with ribosomes from all eukaryotic organisms tested including: worm, fly, mouse, and human (Gerbasi et al., 2004). More importantly, mammalian RACK1 co-fractionated with ribosomes of yeast that lacked the Asc1p protein. In contrast, mammalian RACK1 was excluded from wild-type yeast ribosomes that harbor Asc1p (Gerbasi et al., 2004). This suggested that these two proteins were competing for the same site in the yeast ribosome. Additionally, these data were consistent with RACK1 and Asc1p functioning as a core component of the ribosome and not a transient ribosome-interacting protein. The conclusion that RACK1 is a core component of the ribosome has been validated structurally by two separate studies during the course of this dissertation (Manuell et al., 2005; Sengupta et al., 2004).

This dissertation discovered multiple functions for Asc1p in translation. Ribosomes deficient in Asc1p have higher translational activity *in vitro*, suggesting that *ASC1* represses mRNA translation (Gerbasi et al., 2004). Additionally, yeast strains with *asc1*-mutations have elevated levels of specific proteins *in vivo* when grown at 30°C, suggesting that Asc1p functions to repress the translation of mRNAs (Gerbasi et al., 2004).

Proteomic analysis showed that Asc1p-deficient ribosomes were enriched in chaperone proteins relative to wild-type ribosomes. From these results, a hypothesis that Asc1p stabilizes the structure of the ribosome was developed. Polysome profiling and pulse-chase analysis showed that Asc1p facilitates the structure of nascent ribosomes at elevated temperatures. Therefore, this dissertation demonstrates that Asc1p is a structural component of the ribosome

that represses mRNA translation when cells are grown under standard laboratory conditions (30°C) and facilitates nascent ribosome formation at elevated temperatures.

asc1-deficient yeast recover from growth at the non-permissive temperature by increasing their ribosome population

*asc1*Δ null yeast fail to grow at elevated temperatures. An *asc1*Δ null yeast strain recovered from growth at elevated temperatures. *asc1*-deficient yeast have a diminished population of ribosomes after growth at 39°C for 16 hours in comparison to wild-type. Shifting the yeast to fresh media at 30°C after long-term incubation at the non-permissive temperature (NPT) stimulated translational initiation immediately. However, the complete restoration of the ribosome pool was not achieved until 4-20 hours of growth at 30°C. Importantly, *asc1*-deificent yeast exhibited a severe growth-lag at 30°C after a period of growth at 39°C. Therefore, this dissertation demonstrates that a proliferation lag in *asc1*-deficient yeast is associated with a reduced ribosome pool, but not repressed translational initiation *per se*.

Introduction Part II: Eukaryotic Translational Initiation Mechanisms

In prokaryotes, the small ribosomal subunit is recruited directly to mRNAs via a sequence in the leader region of the message (Shine and Dalgarno, 1975). However, the mechanism of eukaryotic translational initiation is much different. The combined work of Nahum Sonenberg, Marilyn Kozak, and Tatyana Pestova developed the scanning model of eukaryotic translational initiation (Kozak,

1980a; Pestova et al., 1998; Sonenberg et al., 1979a; Sonenberg et al., 1979b). In this model, ribosomes bind to a structure at the very 5'-end of the mRNA and scan the 5'UTR (Kozak, 1978; Kozak, 1980a; Kozak, 1980b). Once ribosomes reach an AUG start codon, the large subunit joins the small subunit and translational initiation begins (Kozak and Shatkin, 1976).

In order for the scanning model to be correct, a molecular structure would have to be present on mRNAs to recruit the ribosome. This unique structure on mRNAs was the 7-methyl-guanosine cap (Furuichi et al., 1975a; Furuichi et al., 1975b; Furuichi et al., 1976). These modified bases were found at the distal 5'-end of messages (Furuichi et al., 1975a; Furuichi et al., 1975b; Furuichi et al., 1976; Shatkin, 1976). After the discovery of the cap structure, it was assumed by Sonenberg and colleagues that an RNP complex might specifically recognize the modified base structure. Using 7-methyl-guanosine affinity chromatography, Sonenberg and colleagues were able to capture a specific protein complex bound to the cap (Sonenberg et al., 1979a). This complex was the eIF4F complex (Gingras et al., 1999). The complex consisted primarily of three proteins: eIF4E, eIF4G, and eIF4A (Shatkin, 1985).

Dissection of eIF4F showed that eIF4E was the protein that bound directly to the cap structure (Sonenberg et al., 1979b). eIF4A is a stoichiometric component of the complex that contains RNA-helicase activity (Gingras et al., 1999). eIF4G is a large scaffolding protein with multiple functions (Gingras et al., 1999). eIF4G tethers the small subunit to the cap structure through interactions with the ribosome-bound initiation factor eIF3. Therefore, the cap

binding complex eIF4F and its individual protein components scaffold interactions with the small ribosomal subunit and the mRNA.

Evidence for the scanning mechanism was generated first by Kozak and colleagues, and later by Pestova and others (Kozak, 1980a; Kozak, 1980b; Kozak and Shatkin, 1978; Pestova et al., 1998). Kozak found that the first AUG (start codon) was usually the first amino acid translated into the growing polypeptide chain (Kozak, 1980a). However, if the AUG codon was placed in different locations along the 5'UTR, the start site of translation would be affected (Kozak, 1980a). Additionally, if the 5'UTR of a given mRNA contained a small upstream open reading frame, translational initiation would often terminate before reaching the start codon (Kozak, 1980a). This result suggested that the ribosome scanned the 5'UTR to search for an AUG codon. If the ribosome finds a stop codon in the 5'UTR, the ribosome falls off the message and initiation fails.

Although Kozak's experiments supported the scanning mechanism of translational initiation, they did not provide direct evidence that the ribosome would localize to a particular AUG codon. To test the scanning model further, Pestova used a "toeprinting" technique to capture the position of the ribosome on the 5'UTR (Pestova et al., 1998). Toeprinting is an *in vitro* technique that defines the position of the ribosome on a given mRNA under a specific set of conditions. The ribosome was positioned directly on top of the start codon in a reconstituted *in vitro* translation system (Pestova et al., 1998).

Cap-independent Translation Initiation in Eukaryotes

The picornaviruses are small viruses that contain an RNA genome. These viruses are completely dependent on the host cell machinery (including host ribosomes) to translate their mRNAs into protein. Although the scanning model made sense for cellular mRNAs, the model failed to describe all of the mechanistic details of picornaviral mRNA translation. For example, picornaviral mRNAs do not contain a 7-methyl-guanosine-cap structure. Therefore, the eIF4F complex would not be bound to these viral mRNAs. How do these viral mRNAs translate into protein if they are lacking a cap structure to recruit the ribosome? Sonenberg and colleagues reasoned that there must be a structure in the 5'UTR of picornaviral mRNAs that is responsible for recruiting the ribosome (Jang et al., 1989; Pelletier and Sonenberg, 1988). The 5'UTR of poliovirus was shown to initiate cap-independent mRNA translation in HeLa cells (Pelletier and Sonenberg, 1988). Pelletier and Sonenberg referred to these cap-independent 5'UTRs as ribosomal landing pads, which were later renamed to Internal Ribosomal Entry Sites (IRESs). After the discovery of the first IRES, it was shown that a cellular mRNA also contained an IRES (Yang and Sarnow, 1997). The discovery of additional cellular IRESs would follow (Pyronnet et al., 2000; Qin and Sarnow, 2004; Stoneley and Willis, 2004).

After the first IRES was discovered, it was hypothesized that a number of IRES-*trans*-acting factors (ITAFs) might bind the IRES RNA to facilitate cap-independent translation (Stoneley and Willis, 2004). The first ITAF discovered

was the LA protein (Meerovitch et al., 1989). LA binds to the poliovirus IRES and enhances cap-independent translation (Meerovitch et al., 1993).

Using RNA affinity chromatography, research groups have discovered additional ITAFs (Blyn et al., 1996; Hunt et al., 1999). Proteins that function as viral ITAFs often function as cellular ITAFs (Blyn et al., 1997; Evans et al., 2003; Gamarnik and Andino, 2000; Hunt and Jackson, 1999; Pickering et al., 2004). This common family of ITAFs includes: PCBP2, UNR, PTB, and others. Because viral and cellular IRESs share few sequence or structural similarities, it is likely that several additional ITAFs exist that have remained undiscovered.

ITAFs Function in Collaboration

After some of the first ITAFs were characterized, the research groups of Jackson and Willis performed screens to discover additional ITAFs (Hunt et al., 1999; Mitchell et al., 2001). Both groups found that a complex of ITAFs bind to viral and cellular IRESs. Additionally, these larger ITAF assemblies have been shown to have additive or synergistic stimulation of cap-independent translation. Therefore, it is unlikely that ITAFs act alone in stimulating the translation of IRES-containing mRNAs.

Proposed Mechanisms for IRESs and ITAFs in mRNA Translation

During IRES-mediated translation, the ribosome (and associated proteins) must localize to the IRES RNA. In order for the ribosome to be recruited to this RNP complex, there must be an affinity of the ribosome for either the IRES RNA,

the proteins complexed with IRES RNA, or the IRES-ITAF RNP combination. Structural analysis of the cricket-paralysis-virus-IRES (CPV-IRES) suggests that the viral RNA can recruit the ribosome without the assistance of other proteins (Spahn et al., 2004). Unfortunately, the CPV-IRES exhibits mechanisms of translational initiation that are different from all mRNAs studied thus far (Pestova and Hellen, 2003; Wilson et al., 2000). Therefore, structural analysis of the CPV-IRES-RNA interaction with the ribosome may only provide a single exceptional example of an IRES-RNA initiation mechanism but is probably inadequate to derive a general model of IRES-mediated translational initiation.

A second model for IRES-mediated translational initiation has developed. In this model, ITAFs bind to IRES RNA and function to mold the RNA into an active structure (Mitchell et al., 2003). Once the IRES RNA has achieved an appropriate secondary structure, it attracts the ribosome and translational initiation begins. Experimental support for this model exists through cross-linking studies (Mitchell et al., 2003). Through these cross-linking studies, it was shown that ITAFs will modify the secondary structure of IRES RNA (Mitchell et al., 2003). Therefore, it is possible that ITAFs function to remodel the IRES RNA into a structural form that attracts the ribosome.

The Ornithine Decarboxylase (ODC) IRES

The ODC enzyme is a critical enzyme in polyamine biosynthesis, catalyzing the synthesis of putrescine from ornithine. The functional role of polyamines in the cell is not yet well understood. However, because polyamines

are small cationic molecules, they are expected to bind negatively charged molecules (DNA, RNA, and some proteins). Therefore, the effects of polyamines on cell metabolism are most likely pleiotropic. ODC is mutated and/or over-expressed in several forms of cancer (LaMuraglia et al., 1986; Martinez et al., 2003; O'Brien et al., 1997). Inhibitors of ODC suppress DNA synthesis and the growth of tumors (Fillingame et al., 1975; Tutton and Barkla, 1986). Therefore, there is a positive correlation between enhanced ODC activity and cell proliferation. For this reason, the development of ODC inhibitors is of considerable pharmacological interest.

The effects of ODC on cell cycle maturation has led several research groups to investigate the possibility that ODC might be synthesized at specific points in the cell cycle (Pyronnet et al., 2000; Pyronnet et al., 2005; Pyronnet and Sonenberg, 2001). Interestingly, ODC is highly expressed during the G2/M transition, a time when a majority of protein synthesis is repressed (Pyronnet et al., 2000). The research groups of Pyronnet and Sonenberg showed that the ODC 5'UTR contained an IRES that was translated through the G2/M phase of the cell cycle (Pyronnet et al., 2000). Later, it was shown that IRESs in general translate through the G2/M boundary, while cap-dependent translation is stalled (Qin and Sarnow, 2004).

Discovery of ODC ITAFs

Using site-directed mutagenesis, Sonenberg and Pyronnet discovered an element in the 5'UTR of ODC that was necessary for IRES activity (Pyronnet et al., 2000). They postulated that some set of ITAFs might bind to and stimulate the activity of the ODC IRES (Pyronnet et al., 2005). In this dissertation, I utilized RNA-affinity chromatography combined with mass spectrometry to identify RNA-binding proteins that bind the wild-type, but not the mutant ODC IRES RNA first described by Pyronnet and Sonenberg (Pyronnet et al., 2000).

RNA affinity combined with mass spectrometry analysis identified clear differences in the proteins that bind to either the wild-type or mutant ODC IRES RNA. Specifically, multiple peptides were detected corresponding to the protein sequences of ZNF9 and PCBP2. PCBP2 and ZNF9 bound to the ODC IRES in independent biochemical tests; validating the interaction with the ODC IRES RNA. Additionally, PCPB2 and ZNF9 activate the translation of the ODC IRES suggesting that these two proteins function as ITAFs of the ODC IRES.

Proposed functional roles for ZNF9 are diverse (Chen et al., 2003; Crosio et al., 2000; Rajavashisth et al., 1989). Defining a functional role for ZNF9 is of medical interest because the ZNF9 gene is mutated in patients with type-2 myotonic dystrophy. Specifically, ZNF9 accumulates CCTG expansions in intron 1 (Liquori et al., 2001). Similarly, patients with type-1 myotonic dystrophy accumulate CTG expansions in the non-coding region of a separate gene (Carango et al., 1993). The similarities in the expansion sequences of type-I and type-II myotonic dystrophy have led to an RNA-toxicity hypothesis (Cho and

Tapscott, 2007; Kuyumcu-Martinez and Cooper, 2006). In this hypothesis, CCTG and CTG repeats sequester RNPs that are essential for cell survival. Experimental evidence supporting these models is provided through animal models (Kanadia et al., 2003; Kanadia et al., 2006).

The discovery that ZNF9 complexes with the ODC IRES RNP and enhances ODC IRES activity suggests that the wild-type protein functions as an ITAF. Disruptions in ZNF9 protein production due to the CCTG expansion in intron 1 could disrupt the natural function of the gene by inhibiting ZNF9 mRNA splicing. Therefore, it is possible that mutations in ZNF9 disrupt cellular IRES activity. Disruptions in ZNF9 structure and function may contribute to the pathogenesis of type-2 myotonic dystrophy through interference of IRES-dependent translational initiation.

The results described above established that ZNF9 and PCBP2 function as ITAFs of the ODC IRES. The success of these experiments suggest that RNP discovery is now a feasible task. In moving forward to new projects, these experiments provide a valuable protocol for discovering proteins that complex with specific RNA sequences. Therefore, experiments performed in this portion of the dissertation may enhance the speed at which future RNP complexes are discovered and characterized.

CHAPTER II

YEAST ASC1P AND MAMMALIAN RACK1 ARE FUNCTIONALLY ORTHOLOGOUS CORE 40S RIBOSOMAL PROTEINS THAT REPRESS GENE EXPRESSION

The following chapter was published in **Molecular and Cellular Biology 24(18):8276-87 Sept. 2004**. All experiments were performed by Vincent Gerbasi with the exception of the 2D-Difference-in-gel-electrophoresis (2D-DIGE) experiments shown in Figure 1-5. 2-D DIGE experiments were performed by David Freedman and Salisha Hill. Connie Weaver prepared some of the critical reagents required for some of the experiments.

Abstract

Translation of mRNA into protein is a fundamental step in eukaryotic gene expression requiring the large (60S) and small (40S) ribosome subunits and associated proteins. Using modern proteomic approaches, we previously identified a novel 40S-associated protein named Asc1p in budding yeast and RACK1 in mammals. The goals of this study were to establish Asc1p/RACK1 as a core, conserved, eukaryotic ribosomal protein and to determine the role of Asc1p/RACK1 in translational control. We provide biochemical, evolutionary, genetic, and functional evidence showing that Asc1p/RACK1 is indeed a conserved, core component of the eukaryotic ribosome. We also show that purified Asc1p-deficient ribosomes have increased translational activity

compared to wild-type yeast ribosomes. Further, we demonstrate that *asc1Δ* null strains have increased levels of specific proteins *in vivo*, and that this molecular phenotype is complemented by either Asc1p or RACK1. Our data suggest that one of Asc1p/RACK1's functions is to repress gene expression.

Introduction

The eukaryotic 80S ribosome consisting of small (40S) and large (60S) subunits is the catalytic and regulatory macromolecular complex responsible for the decoding of mRNA into polypeptides. Together, the small and large ribosomal subunits contain the 18S, 28S (25S in yeast), 5.8S, and 5S rRNAs along with a large number of proteins. The structure and function of the ribosome has been extensively studied for decades, and a 15 Å cyro-electron microscopic map of the yeast ribosome is available (Spahn et al., 2001). While the catalytic activity of the ribosome's 28S rRNA in peptide bond formation is well established, the function and regulatory activity of the ribosomal proteins is still largely unknown (Doudna and Rath, 2002).

Advanced mass spectrometry analysis has facilitated the identification of novel ribosomal proteins. In a proteomic screen of *Saccharomyces cerevisiae* 40S, 60S, and 80S components, we identified a novel component of the 40S and 80S subunits, Asc1p (*ASC1*, YMR116C, *CPC2*, *BEL1*), which remains associated with the small subunit in the presence of 1M KCl (Link, 1999). Under these stringent conditions, transient translation factors and ribosome biogenesis factors present under lower salt concentrations are shed from the 40S. In these

experiments, Asc1p was present at equimolar concentration to the other ribosomal proteins (Link, 1999). Using established criteria for defining ribosomal proteins, Asc1p can be classified as a novel, core, 40S ribosomal component (Kruiswijk and Planta, 1974). We also demonstrated that RACK1 (Receptor for Activated C Kinase), a protein with 52% sequence identity to Asc1p, is localized to the 40S, 80S, and polysomes in human cells (Link, 1999). These observations have been confirmed by several other studies (Angenstein et al., 2002; Ceci et al., 2003; Chantrel et al., 1998; Inada et al., 2002; Shor et al., 2003).

RACK1 was originally identified as a protein with sequence similarity to the guanine nucleotide-binding protein β subunit and other proteins containing Trp-Asp (WD) repeat domains (Guillemot et al., 1989). RACK1 was later shown to associate both *in vitro* and *in vivo* with activated PKC βII (Hoffmann et al., 1999) and is hypothesized to function as an anchoring protein that localizes activated PKC to the insoluble cell fraction. A plethora of independent studies have attempted to define the molecular function of RACK1. Yeast 2-hybrid and co-immunoprecipitation methods show RACK1 interacting with a large number of cellular proteins with roles in signal transduction (Chang et al., 1998; Cox et al., 2003; Dell et al., 2002; Gallina et al., 2001; Geijsen et al., 1999; Hennig et al., 2001; Hermanto et al., 2002; Kiely et al., 2002; Koehler and Moran, 2001; Kubota et al., 2002; Liliental and Chang, 1998; McCahill et al., 2002; Mourton et al., 2001; Ozaki et al., 2003; Reinhardt and Wolff, 2000; Rigas et al., 2003; Tcherkasowa et al., 2002; Yarwood et al., 1999). Because of its apparent ability

to interact with a number of signaling molecules, RACK1 is perceived to play a crucial role in a multitude of biological processes.

Consistent with our previous results showing association of Asc1p/RACK1 with the ribosome, more recent studies have implicated *ASC1* and RACK1 in translational control. General translational inhibition occurs upon amino acid starvation when the eIF2α kinase Gcn2p is activated (Dever et al., 1992). Yeast deficient in Gcn2p fail to initiate the amino-acid starvation response. An *asc1* mutation has been shown to restore the amino-acid-starvation response in a *gcn2Δ* strain (Hoffmann et al., 1999). Further, *Schizosaccharomyces pombe* *cpc2Δ* (*asc1Δ*) null mutants appear to have a subset of genes that are transcriptionally and translationally repressed relative to wild type (Shor et al., 2003). The *cpc2*Δ(*asc1*Δ) null strains were also sensitive to puromycin, a drug that causes premature termination of translation, suggesting that translational fidelity has been reduced (Shor et al., 2003). Moreover, in mammalian COS cells, transient over-expression of RACK1 stimulated translation *in vivo* (Ceci et al., 2003).

In this study we provide biochemical, evolutionary, genetic, and functional data showing that Asc1p/RACK1 is a core 40S ribosomal protein in eukaryotes. Further, our results suggest that Asc1p and RACK1 function to repress gene expression. This novel expression phenotype provides insight into a potential regulatory mechanism in eukaryotic gene expression.

Materials and Methods

Plasmids and Yeast Strains

Strain construction, genetic manipulations, and yeast media preparation were carried out by standard methods (Sherman et al., 1986). To construct plasmid p*ASC1*, a 2.13 kb *Bam*HI and *Xba*I yeast genomic fragment from lambda clone λPM5992 (ATCC70652) containing the entire *ASC1* locus was cloned into the *Bam*HI-*Xba*I sites of pRS416 (Christianson et al., 1992; Olson et al., 1986; Riles et al., 1993). Plasmid pME1867 (renamed pRACK1 in these studies) containing the rat cDNA for RACK1 expressed under the control of the *ASC1* promoter and terminator sequences in a pRS316 vector backbone, was a gift from Gerhard Braus (Hoffmann et al., 1999). To construct plasmid pET100-*ASC1*, the PCR primers A-ASC1: (CACCATGGCATCTAACGAAGTTTTAG), B-ASC1: (TTAAGTTCCAAGCCTTAACCATTTTGTCGTTACCGGC), C-ASC1: (ACAAAATGGTTAAGGCTTGGAACTTAAACCAATTCC), and D-ASC1: (TTAGTTAGCAGTCATAACTTGCC) were used in a crossover PCR reaction to amplify an intronless *ASC1* DNA fragment encoding the complete Asc1p protein (Chantrel et al., 1998). The intronless *ASC1* fragment was cloned into the pET100/D-TOPO bacterial expression vector (Invitrogen) to create plasmid pET100-*ASC1* encoding an N-terminally-tagged 6xHis::*ASC1* fusion protein expressed from a T7 promoter. To construct plasmid p426-GPD::6xHis-*ASC1*, a Klenow treated 1.1 kb *Nde*I-*Sac*I fragment from plasmid pET100-*ASC1*

containing the 6xHis-*ASC1* fusion was cloned into the *Sma*I site of p426GPD (Mumberg et al., 1995). All constructs were confirmed by DNA sequencing.

The yeast strains used were: **BY4743** *MATa/MATα his3Δ1/his3Δ1 leu2Δ0/leu2Δ0 met15Δ0/MET15 LYS2/lys2Δ0 ura3Δ0/ura3Δ0* (Winzeler et al., 1999), **YDM36556** *MATa/MATα his3Δ1/his3Δ1 leu2Δ0/leu2Δ0 met15Δ0/MET15 LYS2/lys2Δ0 ura3Δ0/ura3Δ0 Δasc1::Kan^R/Δasc1::Kan^R* (Winzeler et al., 1999), **AL150** YDM36556 + pRS416, **AL156** YDM36556 + p*ASC1*, **AL141** YDM36556 + pRACK1, **AL190** BY4743 + pRS316, **AL191** BY4743 + p*ASC1*, **AL140** BY4743 + pRACK1, **AL143** YDM36556 + (p426-GPD::6xHis-*ASC1*), **AL146** YDM36556 + (pYES-DEST52), **AL103** *MATa his7 ura3-52*, **AL030** *MATa his7 ura3-52 asc1Δ* (Link, 1999), **AL185** YDM36556 + p180 (5'UTR GCN4 lacZ reporter plasmid) (Hinnebusch, 1985), **AL183** BY4743+ p180. Strains containing chromosomal deletions of *asc1* were confirmed by PCR of yeast genomic DNA, PCR of yeast cDNA, and absence of Asc1p by 2D-gel electrophoresis.

Polysome Analysis

Yeast cell extracts were prepared essentially as described (Mikulits et al., 2000). Briefly, yeast strains were grown in SC-URA media to an O.D. $_{600}$ of 0.6, and 5 mL of cells were lysed with 0.5 mm glass beads in 250 µL of lysis buffer (10 mM Tris-HCl, pH 8.0, 140 mM NaCl, 1.5 mM $MgCl_2$, 0.5% NP40 and 200 U/mL RNASIN (Promega). Extracts were centrifuged in a microcentrifuge for 1 min. at 20,000 X g. Supernatants were supplemented with 250 µL of 2X

translation stop buffer (20 mM DTT, 665 µg/mL heparin, 150 µg/mL cyclohexamide) and 1 tablet of mini-Complete™ protease inhibitor (Roche) per 5 mL of buffer. The supplemented extracts were centrifuged for 5 min. at 20,000 X g. Supernatants (200µl) were gently layered on top of a 15-40% sucrose gradient cast in 10 mM Tris-HCl, pH 7.5, 140 mM NaCl, 1.5 mM $MgCl_2$, 10 mM DTT, 100 µg/mL cyclohexamide, and 0.5 mg/ml heparin. Gradients were centrifuged in a Beckman table-top ultracentrifuge (TlS 55) for 75 min at 50,000 rpm. Fractions were collected from the top of the gradients and partitioned for RNA isolation, Western blotting, or DALPC. RNA was isolated from sucrose gradient fractions and yeast strains, with TRI-reagent LS (MRC) according to the manufacturer's protocol. RNA from gradient fractions was loaded onto non-denaturing 1% agarose gels cast in 1X TAE and stained with ethidium bromide.

Western Analysis and DALPC

Western analysis was performed on polysome profile fractions from *S. cerevisiae* cells**,** human HEK293 cells, mouse NT2 cells, and *in vitro* translation extracts from *S. cerevisiae* strains. Sucrose gradient fractions or *in vitro* translation extracts were mixed with Laemmeli buffer, heated for 5 min. at 100°C, loaded onto NuPAGE 10% Bis-Tris gels, and separated using 1X MOPS SDS running buffer (Invitrogen). For Western analysis, NuPAGE gels were transferred to nitrocellulose membranes and blocked overnight in Tris-buffered saline containing 0.1% Tween (TBST) and 10% non-fat dry milk. Western blots were probed with either affinity-purified rabbit polyclonal antibodies to Asc1p

generated against full-length recombinant 6xHis-tagged Asc1p (Bethyl Laboratories, Montgomery, Texas), mouse RACK1 monoclonal antibodies (BD Biosciences), Aip1p polyclonal antibodies kindly provided by David Amberg (Rodal et al., 1999) or Rpl3p monoclonal antibodies kindly provided by Jonathan Warner (Vilardell and Warner, 1997). Western blots were washed three times in TBST and then incubated with the appropriate HRP-tagged secondary antibody (Promega). Blots were developed with ECL Plus reagent (Amersham-Pharmacia). Asc1p antibody specificity was confirmed by Western blotting of Asc1p positive control antigen and whole-cell lysates from wild-type and *asc1Δ* null yeast strains (data not shown). The mass spectrometry approach termed Direct Analysis of Large Protein Complexes (DALPC) experiments on *Drosophila melanogaster* embryos and *C. elegans* strain N2 pooled ribosomal and non-ribosomal fractions were performed essentially as described previously (Link, 1999; Sanders et al., 2002).

Genetic Complementation of yeast *asc1Δ* strains

Yeast strains were grown in either SC-URA or SC+URA to an O.D. $_{600}$ of 0.6. Cells were counted with a hemocytometer, adjusted to equal concentration, and serially diluted (10 fold). Five µL of each 10-fold serial dilution (10^8-10^5) was spotted onto SC-URA plates. Plates were incubated at 30 and 37˚C for 72 hrs and photographed.

In vitro translation assays

To prepare translation extracts, 2 L of yeast were grown in YPD to an O.D. $_{600}$ of 2. Cells were washed five times in ribosome buffer lacking protease inhibitors (30 mM HEPES pH 7.4, 100 mM potassium acetate, 2 mM magnesium acetate, 2 mM fresh DTT, and 8.5% mannitol). After washing, 8 g of cells (wet weight) were lysed in 15 mL of ribosome buffer containing mini-Complete™ protease inhibitor (Roche) with 48 g of 0.5 mm glass beads. Cells were lysed in 50 mL sterile falcon tubes by rigorous rocking in 6 inch arcs for 1 min intervals (5 times) with 1 min intervals on ice between each rocking. Extracts were cleared by centrifugation 2X at 20,000 X g for 10 minutes. Five mL of extract was loaded onto a 75 mL bed-volume Sepharose G-25 column. The sample was fractioned with an isocratic buffer (ribosome buffer + protease inhibitors) flowing at 0.5 ml/min. The flow-through fractions (0.5 mL) with an O.D. $_{260}$ > 90 were pooled and used for the *in vitro* translation assays (Asano et al., 2002).

T3 lucpA plasmid originally created by Peter Sarnow's lab (Iizuka et al., 1994) was kindly provided by Alan Sachs. T3 lucpA was purified with a Qiagen mini-prep and linearized with *Bam*HI. The linearized plasmid was purified using a Qiaquick PCR clean-up kit (Qiagen). Capped luciferase mRNAs were synthesized with the Amplicap T3 high yield message maker kit (Epicentre) using the purified, linearized, T3 lucpA DNA as template. The capped luciferase mRNAs were purified prior to *in vitro* translation with RNAEASY spin columns (Qiagen). Uncapped luciferase mRNA was purchased from Promega. Total yeast RNA from wild-type yeast strain BY4743 grown to an O.D. $_{600}$ of 1.0 was

isolated with TRI-REAGENT(MRC). Following isolation of total RNA, polyA-mRNAs were isolated with an Oligotex mRNA isolation kit (Qiagen). *In vitro* translation assays were conducted as described previously (Tarun and Sachs, 1995).

Assay for B-galactosidase activity

The p180 plasmid containing the 5'UTR of GCN4 cloned in front of the lacZ gene was transformed into yeast strains BY4743 and YDM36556 (Hinnebusch, 1985). Strains were grown in SC-URA to an O.D. $_{600}$ of 0.6. Cells were then pelleted by centrifugation at 9,000 X g for 5 min. Cells were lysed by bead-beating in 1X lysis buffer provided by the manufacturer (Promega). After lysis, extracts were centrifuged at 20,000 X g for 2 min. Following centrifugation, supernatants were assayed for β-galactosidase activity using the manufacturer's protocol (Promega) and measured for absorbance at O.D. $_{420}$ and O.D. $_{280}$. Relative β-galactosidase activity was standardized by dividing the β-gal activity (absorbance at O.D. $_{420}$) by the respective absorbance at O.D. $_{280}$ for each individual sample.

Isolation of recombinant Asc1p

One liter of *E. coli* strain BL21 containing plasmid pET100-*ASC1* was grown to an O.D. $_{600}$ of 0.6 in LB medium. Protein expression was induced with IPTG at 37°C for 1 h. Cells were harvested and lysed by sonication, and the recombinant protein was purified according to the PROBOND kit native purification instructions (Invitrogen). To prepare Asc1p protein for *in vitro*

translation reactions, recombinant Asc1p protein was dialyzed exhaustively against ribosome buffer containing protease inhibitors.

Two-dimensional difference gel electrophoresis (2D DIGE) analysis

One liter of each strain of yeast was grown in SC-URA to an O.D. $_{600}$ of 0.6. Cells were harvested and lysed by bead-beating in lysis buffer (10 mM Tris-HCl, pH 8.0, 140 mM NaCl, 1.5 mM $MgCl_2$, 0.5% NP40 and 200 U/mL RNASIN (Promega)). After lysis, extracts were centrifuged at 20,000 X g for 10 min. Extracts were then partitioned for protein and mRNA analysis. Samples designated for 2D analysis were digested with RNAseA and DNAse and centrifuged again at 20,000 X g for 10 min prior to protein extraction. Three independent samples for each strain were prepared and analyzed.

2D-DIGE analysis using a mixed-sample internal standard was carried out essentially as described previously (Alban et al., 2003; Friedman et al., 2004). Triplicate protein samples for each strain were individually labeled with either Cy3 or Cy5. To control for bias in the fluorescent dyes, we reversed the Cy3 and Cy5 dyes used to label the whole cell extracts in one of each of the experimental replicates from the 4 strains being compared. The Cy2-labeled mixed-sample internal standard was comprised of an equal portion of all 12 extracts used in the experiment. The Cy2 standard was used to normalize protein abundances across different gels and to control for gel-to-gel variation (Alban et al., 2003;

Friedman et al., 2004). An equal amount of Cy3-labeled sample, Cy5-labeled sample, and Cy2-internal control were mixed together and run on individual 2D gels. Triplicate Cy2/3/5 samples were then loaded onto a total of six 24 cm pH 4-7 immobilized pH gradient strips (Amersham Biosciences) and subjected to 2D gel electrophoresis using the IPGphor and DALT-twelve systems per the manufacturer's protocols (Amersham Biosciences).

2D-DIGE gels were scanned with a Typhoon 9410 variable mode imager using the recommended mutually-exclusive emission and excitation wavelengths for each Cy dye (Amersham Biosciences). 2D-DIGE analysis was performed using DeCyder version 5.0 software (Amersham Biosciences), which employs a triple co-detection algorithm to generate the same protein spot-feature boundary for individual Cy2, Cy3, and Cy5 signals. The Cy3/Cy2:Cy5/Cy2 ratios were then calculated and compared among the six DIGE gels, allowing for the application of Student's t-test statistical analyses to triplicate samples from all strains despite being separated on different DIGE gels (Alban et al., 2003; Friedman et al., 2004).

In our analysis of *in vivo* protein levels, we consider 2D gel features to be a protein only if the spot was confirmed with both Cy labels and was present on every gel. Only proteins with $\geq$1.5 fold differences in abundance were considered significant. Differences in protein levels between wild-type and *asc1*Δ *null* samples were considered statistically significant only if the difference fell within the 95% confidence interval as determined by the Student's t-test.

Identification of 2D DIGE proteins

A SyproRuby (Molecular Probes) post-stain image (similarly acquired with a Typhoon 9410) was used to ensure accurate robotic protein excision for subsequent trypsin in-gel digestion using the ProSpot spot-handling workstation (Amersham Biosciences). Protein identifications were made using matrix-assisted laser desorption/ionization, time-of-flight mass spectrometry (MALDI-TOF MS) and TOF/TOF tandem mass spectrometry using a Voyager 4700 MALDI-TOF/TOF mass spectrometer (Applied Biosystems). Protein identifications were based on the acquired mass spectral data combined with database interrogation using the MASCOT algorithm (Matrix Science).

Multiplex RT-PCR and real-time quantitative RT-PCR

Lysate-matched RNA extracts from the 2D DIGE protocol were analyzed for levels of mRNA transcripts encoding identified proteins. The extracts were treated with molecular biology grade DNAse (Invitrogen) prior to reverse transcription. RNA was reverse-transcribed using oligo dT priming (Perkin-Elmer) and Superscript II (Invitrogen). Specific PCR primers were designed to the cDNA transcripts of interest with dsGENE software (Accelrys). Triplex PCR was performed using previously described protocols (Gerbasi et al., 2003). Primer pairs used for RT-PCR were *TDH3 (GAPDH)* (5' TCTTCCATCTTCGATGCTGCCG and 5' AGCCTTGGCAACGTGTTCAACC),

*APE2: (*5’ ACCAAAGGAAACCCAGGATGCG and 5’ AGCAGCTTTTTCAACGTCTGCG), *AIP1: (*5’ CGTCCTTGTGAGCATTCAACGC and 5’ TCTTCGCGCAAAACCCTCGTAC), *DKA1: (*5’ AAGCACGGCATTCTGGAGGATG and 5’ TCTTGGGGAACGTACGCATTCG), *ENO2: (*5’ TAGAGCCGCTGCTGCTGAAAAG and 5’ TTGGAGCAACACCACCTTCGTC) *TPS1*: (5’ TACAGGTTGCAGTGCCAAGTCG and 5’ ATTGTGCGGCACCTGTGAACTC), *ALD3*: (5’ AAAGCTGCCAGGGCTGCTTTTG and 5’ TATTGAACTTGTCGACCGCCCC), *CTT1*: (5’ ACACCAGACACTGCAAGAGACC and 5’ TACGCGTTCATACTAGCCCACG). PCR samples were taken at cycles 17, 20, 23, 26 and 30. PCR products were run on 6% polyacrylamide gels cast in 0.5X TBE, and stained with ethidium bromide.

For real-time RT-PCR, cDNA samples were prepared as described above. cDNAs were amplified in an IQ SYBR green supermix using the manufacturer’s recommended protocol (BioRad). Samples were analyzed in a Biorad iCycler with the following temperature cycle: 95°C for 10 seconds, 64°C for 1minute. PCR samples were cycled 32X. To quantitate relative mRNA levels between yeast strains, mRNA levels were divided by the calculated *TDH3* (GAPDH) mRNA levels for each strain as a standard. For all cDNAs amplified, a step-wise melting curve protocol of 0.5°C was performed after PCR to confirm the presence of a single PCR product.

Results

Mammalian RACK1 and *S. cerevisiae* Asc1p are orthologous ribosomal proteins

In a past study we showed that Asc1p localizes to the 40S and 80S subunits in *S. cerevisiae* and RACK1 localizes to the 40S and polysomes in human HELA cells (Link, 1999). Sequence similarity and ribosome localization suggested that the two proteins are orthologous. To further examine if RACK1 and Asc1p are biochemically orthologous ribosomal proteins, we performed a series of competitive and non-competitive polysome profiling experiments in *S. cerevisiae*.

Figure 1-1.

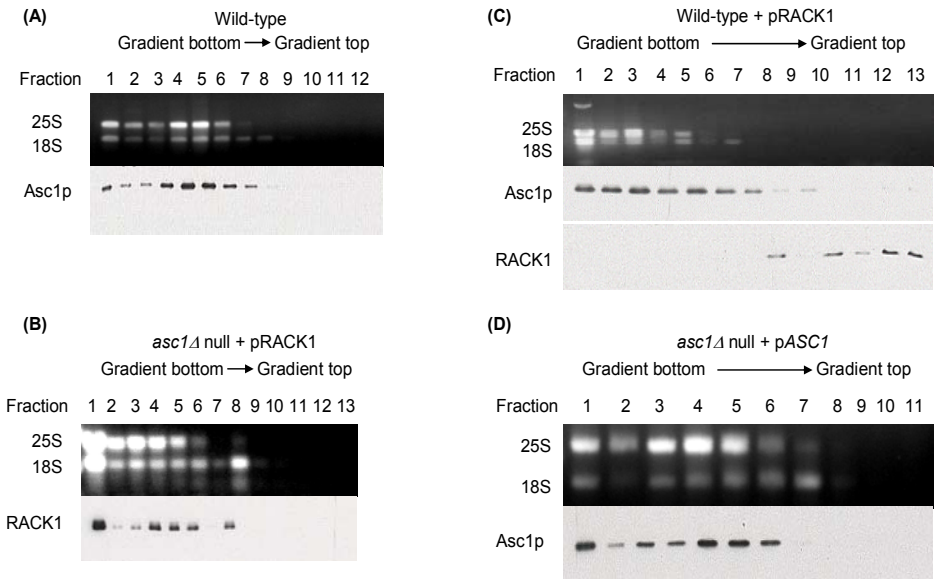

Figure 1-1. Polysome profiles show Asc1p and RACK1 are biochemically orthologous ribosomal proteins. (A) Polysome profile shows yeast Asc1p localizes to the polysome fractions and is absent in the non-ribosomal fractions. Cell lysate from yeast wild-type strain AL190 was fractionated by sucrose gradient centrifugation and fractions were collected. An aliquot of each fraction was analyzed by agarose gel electrophoresis to identify fractions with 25S and 18S ribosomal RNAs. Western analysis of the fractions using anti-Asc1p antibodies shows Asc1p is in the ribosome fractions (1-8) and is absent from the non-ribosomal fractions (9-12). (B) Polysome profile showing RACK1 expressed in a yeast *asc1Δ* null strain localizes to the ribosomal fractions and is absent in the non-ribosomal fractions. Cell lysate from yeast strain AL141 was fractionated by sucrose gradient centrifugation and analyzed as described in (A) except anti-RACK1 antibody was used for the Western analysis. (C) Polysome profile showing exclusion of RACK1 from ribosomal fractions in a wild-type yeast strain. Cell lysate from yeast strain AL140 was fractionated by sucrose gradient centrifugation and analyzed as described in (A) except Western analysis used anti-RACK1 and anti-Asc1p antibodies in separate Western blots. (D) Polysome profile of an *asc1Δ* null strain complemented by expression of *ASC1*. Cell lysate from yeast strain AL156 was fractionated by sucrose gradient centrifugation and analyzed as described in (A).

Results from polysome profiling showed that in wild-type *S. cerevisiae*, Asc1p localized to ribosomal fractions, but was absent from non-ribosomal fractions (Fig. 1-1A). We reasoned that if RACK1 and Asc1p are orthologs, then in the absence of Asc1p, RACK1 should localize to ribosomes in yeast. When we expressed rat RACK1 (99% identical to human RACK1) in an *asc1Δ* null yeast strain, we found that RACK1 localizes to ribosomal fractions in a polysome profile but was absent from non-ribosomal fractions (Fig. 1-1B). This result indicated that RACK1 associated with the yeast ribosome similar to Asc1p and therefore might perform similar functions within the ribosome. Interestingly, when we expressed RACK1 in a wild-type yeast background we found that Asc1p was still included in ribosomal fractions but RACK1 was excluded (Fig. 1-1C). Because these results suggest that Asc1p and RACK1 compete for the same ribosomal position, we refer to this phenomenon as species-competitive-protein-exclusion (compare Figures 1-1B and C).

Figure 1-2.

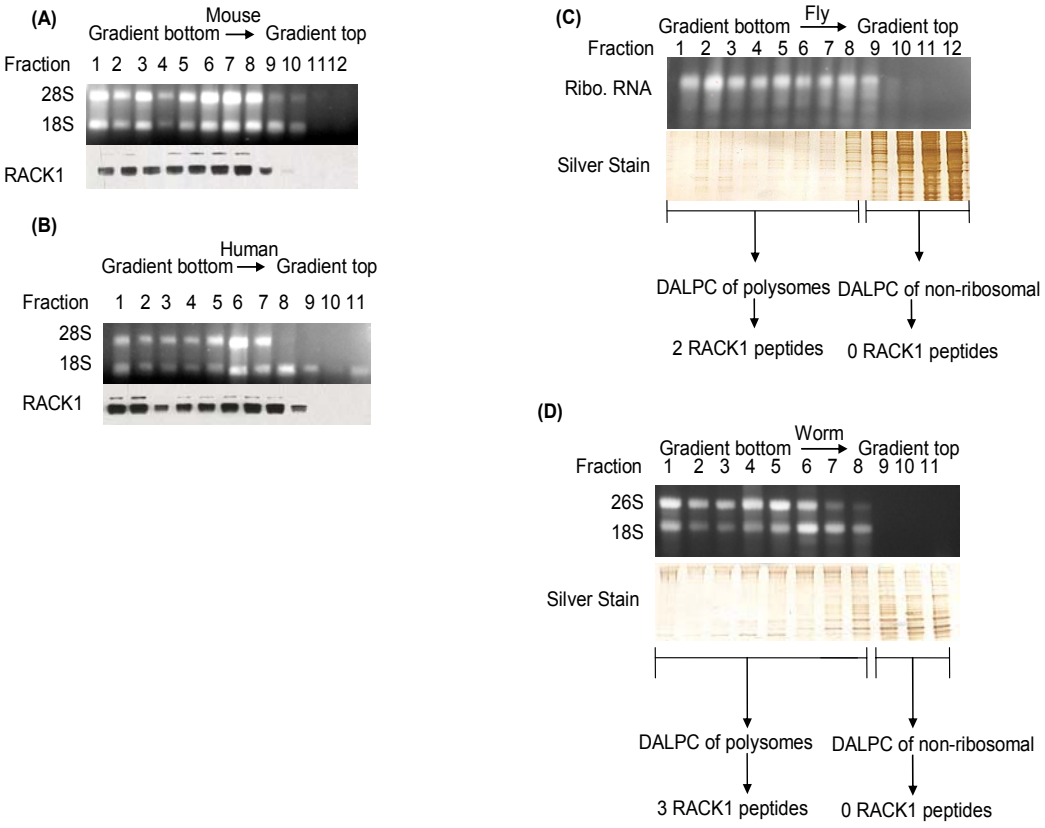

Figure 1-2. Polysome profiling of RACK1 protein shows polysomal localization in four eukaryotic species. (A) Mouse polysome profile shows RACK1 localizes to the polysome fractions and is absent in the non-ribosomal fractions. A cell lysate from mouse NT2 cells was fractionated by sucrose gradient centrifugation and fractions were collected. An aliquot of each fraction was analyzed by agarose gel electrophoresis to show fractions with 28S and 18S ribosomal RNAs. Western analysis of the fractions using anti-RACK1 antibodies shows the distribution of RACK1. (B) Human polysome profile shows RACK1 localizes to the polysome fractions and is absent in the non-ribosomal fractions. A cell lysate from human HEK293 cells was fractionated by sucrose gradient centrifugation and analyzed as described in 2(A). (C) DALPC analysis of fruit fly polysome profile shows RACK1 localizes to the polysome fractions and is absent in the non-ribosomal fractions. Each fraction was analyzed by SDS-PAGE to visualize the amount of protein in each fraction. Polysome and non-ribosomal fractions were separately pooled, digested with trypsin, and proteins identified by the DALPC-mass spectrometry approach (Link, 1999; Sanders et al., 2002; Yik et al., 2003). The Drosophila 28S and 18S rRNA typically co-migrate as a doublet (Ishikawa, 1977). (D) DALPC analysis of nematode polysome profile shows *ASC1*/RACK1 localizes to the polysome fractions and is absent in the non-ribosomal fractions. A lysate from wild-type worms was fractionated by sucrose gradient centrifugation and fractions were collected. An aliquot of each fraction was analyzed by agarose gel electrophoresis to identify fractions with 28S and 18S ribosomal RNAs. Protein samples were analyzed as described in panel (C).

Localization of RACK1 to ribosomes is evolutionarily conserved in eukaryotes

Since the polysome profiling experiments suggested that Asc1p and RACK1 were biochemically orthologous ribosomal proteins, we wanted to investigate whether RACK1 is a conserved eukaryotic ribosomal protein. Alignment of yeast Asc1p with four putative orthologs from different species, *C. elegans* (NP_501859), *D. melanogaster* (NP_477269), *M. musculus* (BAA06185) and *H. sapiens* (NP_006089), revealed a high sequence similarity between the different proteins. To test if localization of these Asc1p/RACK1 orthologs is conserved among eukaryotic species, we performed polysome profiling on extracts from mouse, human, fly, and nematode (Fig. 1-2 A-D respectively). By Western analysis, a RACK1 monoclonal antibody recognized a major and minor band in the ribosomal fractions of *M. musculus,* and *H. sapiens*. In both organisms, the RACK1 antibody failed to detect a protein in the non-ribosomal fractions. Because the RACK1 antibody poorly recognized a cognate fly and worm protein, we analyzed *D. melanogaster* and *C. elegans* polysomes and non-ribosomal fractions by the mass spectrometry approach termed Direct Analysis of Large Protein Complexes (DALPC) (Link, 1999; Sanders et al., 2002; Yik et al., 2003) (Fig. 1-2 C-D). DALPC identified RACK1 peptides in the polysomal but not the non-ribosomal fractions for both *D. melanogaster* and *C. elegans*. Together our data show that in the four eukaryotes tested**,** *ASC1*/RACK1 were found in the ribosomal fractions and were absent from the non-ribosomal fractions. Collectively, these results suggest that both the

sequences and localization of *ASC1*/RACK1 to ribosomal fractions are conserved in eukaryotes.

Figure 1-3.

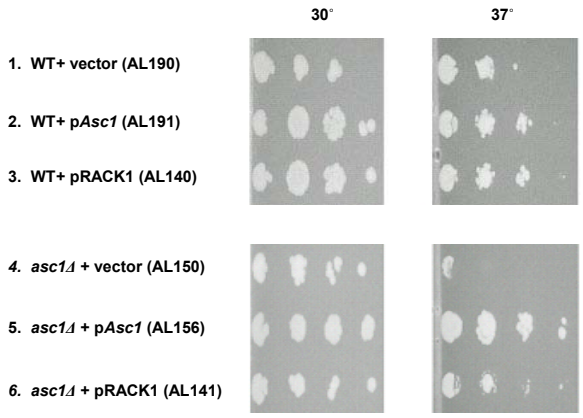

Figure 1-3. *ASC1* and RACK1 genetically complement the temperature-sensitive growth defect in a yeast *asc1Δ* null strain.
The indicated yeast strains were grown to logarithmic phase in liquid media, spotted in a dilution series onto SC-Ura plates, and grown at two different temperatures for 72 hours and then photographed. Strains 1-3 are wild-type controls. Strains 4-6 are experiments performed in the *asc1Δ* null background. The genotypes of the strains are described in "Materials and Methods".

S. cerevisiae ASC1 and mammalian RACK1 are genetically orthologous

Because polysome profiling experiments in yeast and higher eukaryotes indicated that Asc1p and RACK1 were biochemically conserved orthologous ribosomal proteins, we wanted to test to see if *ASC1* and RACK1 are genetically orthologous genes. We found an *asc1Δ* null yeast strain had a temperature-sensitive growth defect (Fig. 1-3, line 4). Using a plate dilution assay, we tested whether *CEN* plasmids expressing *ASC1* (p*ASC1*) or RACK1 (pRACK1) at the endogenous level of *ASC1* could complement the temperature-sensitive phenotype in an *asc1Δ* null strain. Complementation in the *asc1Δ* null strain was complete for *ASC1* and partial for RACK1 (Fig. 1-3, line 5 and 6). These results are in excellent agreement with a previous study (Hoffmann et al., 1999). Polysome profile analysis of the yeast *asc1Δ* null + p*ASC1* complementing strain demonstrated that *ASC1* expression is restored and the complementing Asc1p protein localized to the ribosomes (Fig. 1-1D). These data indicate that yeast *ASC1* and RACK1 are genetically orthologous.

Figure 1-4.

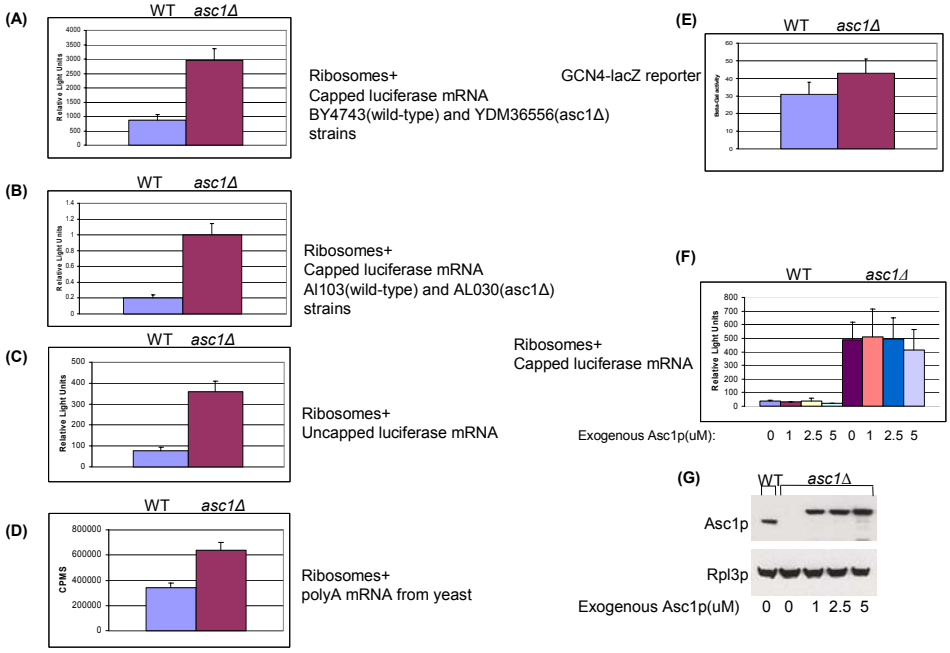

Figure 1-4. Translational activity in *asc1Δ* extracts is up-regulated.

(A) *In vitro* translation of capped and polyadenylated luciferase reporter mRNA with extracts that were prepared from wild-type BY4743 and the isogenic *asc1Δ* null strain YDM36556. Translational activity was determined by measuring luminescence (relative light units) after 30 min of incubation at 26°C. Error bars indicate the standard deviation. (B) *In vitro* translation of capped and polyadenylated luciferase reporter mRNA with extracts that were prepared from wild-type AL103 and the isogenic *asc1Δ* null strain AL030. (C) *In vitro* translation of uncapped and polyadenylated luciferase reporter mRNA with extracts that were prepared from wild-type BY4743 and the isogenic *asc1Δ* null strain YDM36556. (D) *In vitro* translation of polyA-enriched mRNAs with extracts that were prepared from wild-type BY4743 and the isogenic *asc1Δ* null strain YDM36556. The extracts were incubated with whole wild-type yeast mRNA and ^{35}S methionine. Translational activity was determined by measuring the counts per min (CPM) after 30 min of incubation at 26°C. (E) *In vivo* analysis of GCN4 translation. Wild-type BY4743 and *asc1Δ* null YDM36556 strains were transformed with a 5'UTR GCN4 lacZ reporter plasmid (p180) (Hinnebusch, 1985). Cells were grown in SC-URA to an O.D. $_{600}$ of 0.6 and assayed for B-galactosidase activity as described in materials and methods. (F) *In vitro* translation of capped and polyadenylated luciferase reporter mRNA in the presence of an increasing concentration of recombinant Asc1p protein. Protein extracts were prepared from wild-type BY4743 and the isogenic *asc1Δ* null strain YDM36556. The extracts were incubated with luciferase mRNA and the indicated amounts of recombinant Asc1p protein. Translational activity was determined by measuring luminescence (relative light units) after 30 min of incubation at 26°C. (G) Western analysis of *in vitro* extracts using anti-Asc1p and anti-Rpl3p antibodies. As a loading control for the *in vitro* translation assay, Asc1p and Rpl3p levels were measured. Poly-His-tagged recombinant Asc1p migrates more slowly than endogenous Asc1p. Rpl3p levels suggest that 60S subunit levels were similar between wild-type and *asc1Δ* translation extracts.

Asc1p deficient ribosomes have increased translational activity *in vitro*

Because our data indicated that RACK1 and Asc1p are conserved eukaryotic ribosomal proteins and earlier studies had implicated Asc1p in the amino-acid starvation response, we wanted to determine the role of Asc1p/RACK1 in translation. To evaluate the activity of Asc1p in translation, we performed *in vitro* translation assays using extracts from wild-type and *asc1Δ* null yeast strains (Tarun and Sachs, 1995). In three independent experiments translating a capped and polyadenylated luciferase reporter mRNA, the *asc1Δ* null strain ribosomes had a 3-10 fold higher translational activity compared to wild-type ribosomes (Fig. 1-4A and F). To show that the increased translational activity was not strain dependent, *in vitro* translation assays were performed using extracts from genetically independent wild-type and *asc1⊿* null strains (Link, 1999). Similar to the earlier strains, the second *asc1Δ* null strain had a higher *in vitro* translational activity compared to an isogenic wild-type strain (Fig. 1-4B).

To test that the *asc1Δ* null increased translational activity phenotype was independent of the reporter molecule, we translated uncapped luciferase, capped luciferase, wild-type polyA mRNAs, and a GCN4 5'UTR-lacZ reporter. We found that translational activity is elevated in the *asc1Δ* null strain compared to the wild-type strain (Fig. 1-4A through F).

In an attempt to modulate the higher translational activity of the ribosomes lacking Asc1p, we added recombinant Asc1p protein to our *in vitro* extracts. Expression of the recombinant protein in *asc1⊿* null strains complemented the

temperature-sensitive growth defect. However, addition of exogenous Asc1p protein to the *in vitro* translation extracts failed to repress translational activity (Fig. 1-4F).

Since the recombinant protein failed to restore translational activity to wild-type levels, we sought to determine if our recombinant protein was added at wild-type stoichiometric levels. Western analysis of *in vitro* translation extracts showed the levels of exogenous Asc1p equal to or above that found in wild-type ribosome preparations (Fig. 1-4G). When relative levels of Rpl3p protein were compared between extracts, the amounts of ribosomes appeared to be similar (Fig. 1-4G). These data suggest that equal amounts of ribosomes were present in each extract for translation. Collectively, these data show that ribosomes lacking Asc1p have increased (derepressed) translation activity, suggesting that Asc1p acts as a translational repressor.

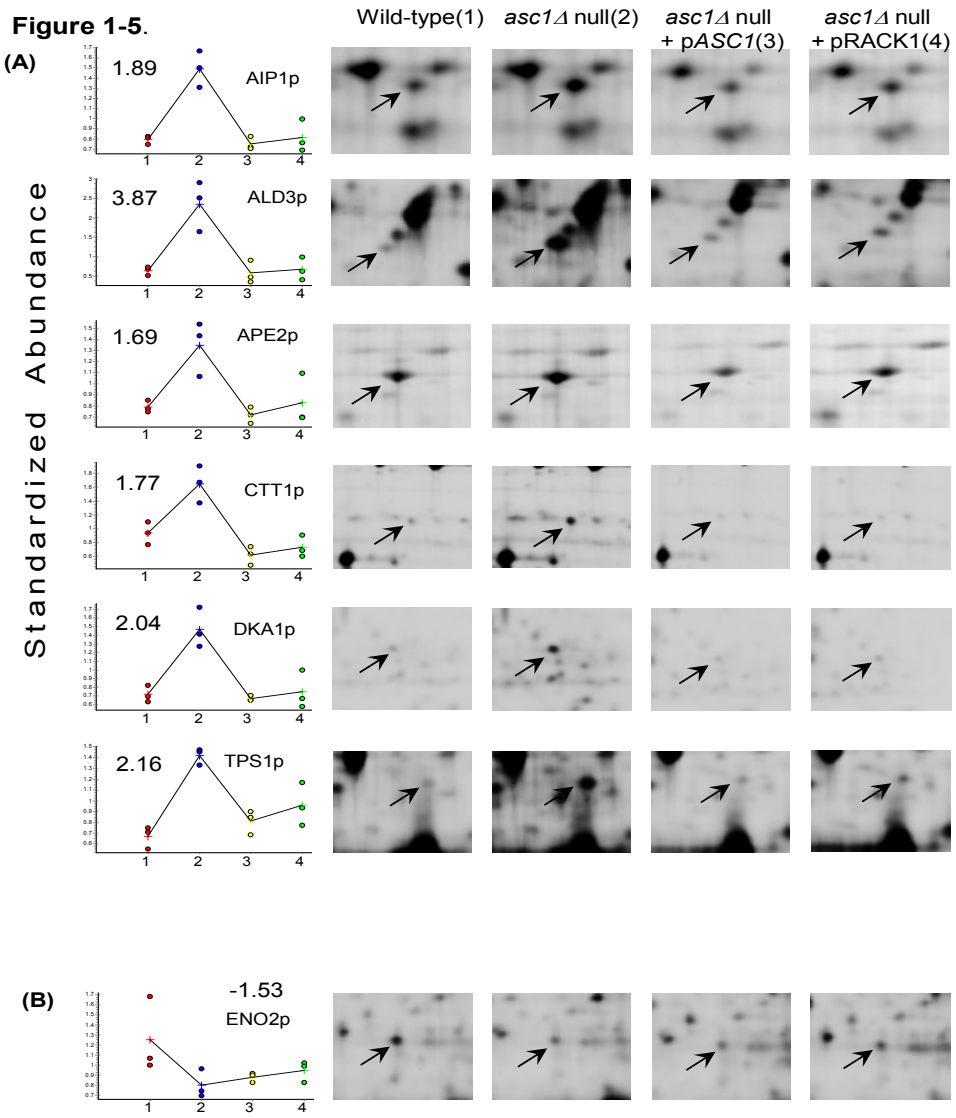

Figure 1-5. *In vivo* changes of protein levels in *asc1Δ* null strains.

(A) Up-regulated proteins in the *asc1Δ* null strain are complemented by either Asc1p or RACK1. Graphs of standardized protein abundance in wild-type (1), *asc1Δ* null (2), *asc1Δ* null + p*ASC1* (3) , and *asc1Δ* null + pRACK1 (4) complemented strains are shown. Representative 2D-gel images are shown as a reference for protein levels for each strain and show an arrow pointing to the Cy3 or Cy5-labeled protein identified. For the graphs, each dot indicates the standardized protein abundance of a specific protein for a given strain in a single independent experiment. Each dot is calculated by dividing the Cy3 or Cy5 density by the Cy2 density (internal standard) for the respective protein position. Numbers on the graphs indicate the fold difference in average standardized abundance between the *asc1Δ* null and wild-type strain. A (+) marks the average standardized abundance for a given strain and is representative of 3 independent experiments. The black line connects the average standardized protein abundance with one another. (B) The down-regulated protein in the *asc1Δ* null strain is not complemented by either Asc1p or RACK1. The graph shows standardized protein abundances in wild-type (1), *asc1Δ* null (2), *asc1Δ* null + p*ASC1* (3), and *asc1Δ* null + pRACK1 (4) complemented strains. A description of the graphs and 2D-gel images are similar to those in (A).

Asc1p or RACK1 functionally complement increased protein levels in *asc1Δ* null strains

Because the *in vitro* data above suggested that Asc1p functions as a translational repressor, we sought to analyze *in vivo* changes in protein levels between wild-type, *asc1Δ* null, *asc1Δ* null + p*ASC1*, and *asc1Δ* null + pRACK1 complemented strains. We employed 2D-difference gel electrophoresis (2D-DIGE) to quantify any changes in the *in vivo* proteins levels for a large population of proteins (Alban et al., 2003; Friedman et al., 2004). In the 2D-DIGE experiments, whole cell lysates were prepared from three independent cultures for each of the four strains described above (e.g. 12 independent samples). The lysates were labeled prior to electrophoresis with the spectrally resolvable fluorescent dyes Cy3 or Cy5. To normalize for protein abundance differences across multiple 2D gels, a mixed internal standard pool containing equal amounts of each experimental sample was labeled with a Cy2 fluorescent dye. The pooled standard represented the average of all samples being compared. Independent Cy2, Cy3, and Cy5 samples were mixed and resolved on the same 2D gels. As a consequence, each gel contained an image with a highly similar spot pattern, simplifying and improving the confidence of inter-gel spot matching and quantification (Alban et al., 2003). To control for bias in the fluorescent dyes, we reversed the Cy3 and Cy5 dyes used to label the whole cell extracts in one of the experimental triplicates from the 4 strains being compared.

In our analysis of *in vivo* protein levels, we interpreted a 2D gel feature as a protein only if the spot was confirmed with both Cy3 and Cy5 labels and was present on every gel. The total number of proteins analyzed (approximately 1500) included multiple isoforms of some individual proteins. Only proteins with ≥1.5 fold differences in abundance were considered significant and included in our analysis. In addition, differences in protein levels between wild-type and *asc1Δ null* samples were considered statistically significant only if the difference fell within the 95% confidence interval as determined by the Student's T-test.

2D-DIGE analysis indicated that among ~1500 yeast proteins detected, 27 proteins are ≥1.5 fold more abundant in the *asc1Δ* null strain relative to wild-type ($p<0.05$) (Fig. 1-5A). Among these 27 elevated proteins, the differences in abundance between the wild-type and *asc1Δ* null strain ranged from 1.5 to 4.44 fold. Six of the seven up-regulated had sufficient material for unambiguous identification by mass spectrometry (Figure 1-5A). For *AIP1* up-regulated in the *asc1Δ* null strain, we performed Western analysis using the same extracts used for the 2D-DIGE experiments. The relative abundance of Aip1p from the four strains was consistent with results from the 2D-DIGE experiments. Only 3 of 1500 proteins demonstrated a statistically significant ($p<0.05$) down-regulation in the *asc1Δ* null in comparison to wild-type (Fig. 1-5B). One of the three proteins had sufficient material for identification by mass spectrometry (Figure 1-5B). Both the *asc1Δ* null + p*ASC1* and *asc1Δ* null + pRACK1 strains restored elevated proteins back to wild-type levels for 24 of 27 of the up-regulated proteins (Fig. 1-5A). In contrast, levels of the three down-regulated proteins were not

complemented by the *asc1Δ* null + p*ASC1* or the *asc1Δ* null + pRACK1 strains (Fig. 1-5B). These results are consistent with our *in vitro* experiments suggesting a repressive role for Asc1p in translation. Additionally, these data provide further evidence that Asc1p and RACK1 are functionally orthologous ribosomal proteins.

To discern between transcriptional and post-transcriptional regulation of gene expression for the seven identified proteins, we compared 2D-DIGE protein abundance data with mRNA levels from the four strains. The mRNA levels encoding six up-regulated (AIP1p, ALD3p, APE2p, CTT1p, DKA1p, and TPS1p) and one down-regulated (ENO2p) protein were measured in wild-type, *asc1Δ* null, and complemented strains using multiplex RT-PCR and real-time RT-PCR. By triplex RT-PCR we observed no apparent difference in transcript levels for any of the seven genes analyzed (Fig. 1-6A). By real-time quantitative PCR, the average differences in levels of *AIP1, ALD3, APE2, CTT1, DKA1*, and *TPS1* transcript abundance were variable but not statistically significant in the *asc1Δ* null strain relative to wild-type and complemented strains ($p<0.05$) (Fig. 1-6B). However, ENO2 transcript levels were down-regulated in the *asc1Δ* null strain relative to wild-type ($p<0.05$) (Fig. 1-6A). Collectively these results support a negative role for Asc1p/RACK1 in gene expression.

Figure 1-6.

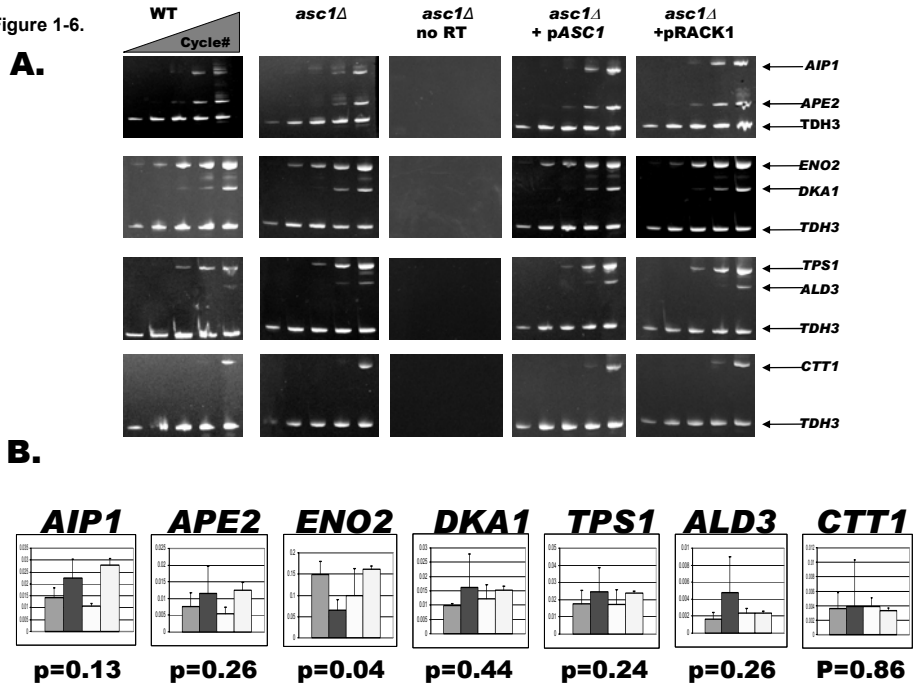

Figure 1-6. Analyzing mRNA transcript levels in *asc1Δ* null, *asc1Δ* null +p*ASC1*, *asc1Δ* null + pRACK1 and wild-type strains.
(A) Triplex RT-PCR of mRNA transcripts in *asc1Δ* null, *asc1Δ* null +p*ASC1*, *asc1Δ* null + pRACK1 and wild-type strains used for 2D-DIGE analysis. As a negative control, *asc1Δ* null RNA was amplified with no reverse-transcriptase. *AIP1, ALD3, APE2, CTT1, DKA1*, *ENO2*, and *TPS1* mRNA transcript abundances were measured by triplex semi-quantitative RT-PCR using total RNA prepared from 2D-DIGE experiments. cDNA transcripts were co-amplified with *TDH3 (GAPDH)* as a standard. One of three independent samples is shown here. PCR cycles 17, 20, 23, 26, and 30 are shown in order from left to right for each sample. (B) Quantifying mRNA levels in *asc1Δ* null strains. The graph shows the quantified mRNA levels for the seven genes from four different strains in (A). Transcript levels for all seven proteins identified by MALDI-TOF were quantified by real-time PCR of cDNA transcripts. As a standard, mRNA transcript levels for each gene were divided by *TDH3 (GAPDH)* transcript levels in each sample. Error bars indicate the standard deviation of the mean. P-values for each gene were determined through a student's T-test between the calculated wild-type and *asc1Δ* null transcript levels.

Discussion

RACK1/ Asc1p is the 33rd ribosomal protein of the small (40S) eukaryotic subunit

In the classical experiments of Kruiswijk and Planta, proteins are considered "core" ribosomal components if they remain associated in the presence of 0.5M KCl (Kruiswijk and Planta, 1974). Asc1p fulfills this requirement by associating with the ribosome in the presence of 1M KCl (Link, 1999). The localization of Asc1p/RACK1 to the 40S, 80S, and polysomal fractions has been observed by several independent studies (Angenstein et al., 2002; Ceci et al., 2003; Chantrel et al., 1998; Inada et al., 2002; Link, 1999; Shor et al., 2003). Here we have demonstrated the localization of Asc1p and RACK1 to polysomes in five different eukaryotic species. Further, we demonstrate that yeast Asc1p and mammalian RACK1 compete for localization to the yeast ribosome. Moreover, we show that RACK1 functionally complements the phenotype of an *asc1Δ* null mutant. These data, taken together with other studies, strongly suggest that Asc1p and RACK1 are orthologous core ribosomal proteins. Consequently, we propose a more appropriate name for yeast *ASC1* is *RPS33*, the 33rd ribosomal protein in the *S. cerevisiae* 40S small subunit. By corollary, RACK1 should be classified as a mammalian 40S core ribosomal protein.

ASC1 has several other features that are common to *S. cerevisiae* ribosomal genes. Although only a small percentage of *S. cerevisiae* genes contain an intron, 66% of the yeast ribosomal genes contain an intron. Two

previous studies have shown that *ASC1* contains an intron (Chantrel et al., 1998; Hoffmann et al., 1999). The codon adaptation index (CAI) is a measurement of the relative adaptiveness of the codon usage of a gene towards the codon usage of highly expressed genes *(Jansen et al., 2003; Sharp and Li, 1987))*. CAI values range from 0 to 1, with higher values indicating a higher proportion of the most abundant codons. The average CAI for all yeast genes is 0.18 while the average CAI for ribosomal genes is 0.71. *ASC1* has a CAI of 0.77 suggesting it is highly expressed. Several studies have measured the transcriptional expression of *ASC1* and found it to be expressed at levels equivalent to ribosomal genes (Velculescu et al., 1997; Wodicka et al., 1997). A recent study measured the abundances of a large number of yeast proteins (Ghaemmaghami et al., 2003). The estimated abundances for ribosomal proteins ranged from 4.5E+03 to 6.02E+05 molecules per log-phase cell with average of 7.0E+04 molecules per cell. Asc1p was found to be present at approximately 3.33E+05 molecules per log-phase cell which is in the same range as other ribosomal proteins (Ghaemmaghami et al., 2003). These results agreed with an earlier study showing Asc1p is an abundant yeast protein that is highly enriched in ribosomal fractions (Garrels et al., 1997). In ribosome fractions, Asc1p is present at equimolar concentration to the other ribosomal proteins (Link, 1999). All of these reports indicate *ASC1* is a highly expressed yeast gene with characteristics similar to other ribosomal genes.

ASC1/RACK1 exerts a repressive effect on specific protein synthesis

We found that absence of yeast Asc1p resulted in elevated translational activity. However, this molecular phenotype could not be complemented *in vitro* by adding recombinant Asc1p. While it is possible the recombinant Asc1p fusion protein is not folded properly or is lacking critical modified residues, the fusion protein does complement an *asc1Δ* null strain. Failure of a core eukaryotic ribosomal protein to complement when added exogenously is not surprising since eukaryotic ribosome assembly is thought to occur as a stepwise process in the nucleolus (Fromont-Racine et al., 2003; Tschochner and Hurt, 2003). In contrast, translational initiation factors can be added exogenously to restore activity to wild-type levels in *in vitro* translation assays (Choi et al., 1998; Tarun et al., 1997).

To identify the molecular function of *ASC1* and RACK1 *in vivo,* we employed a quantitative, global proteomic analysis of WT, *asc1*Δ null, yeast p*ASC1*, and mammalian p*RACK1* complemented strains. We reasoned that if Asc1p and RACK1 function as repressive, ribosomal proteins, we might observe a global up-regulation of protein levels in *asc1*Δ null strains. Further, this up-regulation should be complemented by expression of yeast p*ASC1* or mammalian pRACK1 in an *asc1*Δ null background. Indeed, we found that *asc1*Δ null strains have elevated levels of some proteins, and this molecular phenotype can be complemented by either yeast p*ASC1* or mammalian pRACK1. The changes in protein levels appear to be independent of mRNA levels and therefore likely occur through a post-transcriptional mechanism.

The *in vitro* translation assays using various mRNA templates suggest that translation activity is globally increased for ribosomes lacking Asc1p. However, *in vivo* assessment of protein levels in *asc1Δ* null strains shows that only a specific population of proteins (27 of 1500) are significantly up-regulated. Although *in vitro* translation assays suggested a 2-10-fold increase in translational activity for the *asc1Δ* null strain ribosomes, *in vivo* post-transcriptional analysis indicated that specific protein levels were up-regulated between 1.5 and 4.44 fold (compare Figures 1-4 and 1-5). The *in vitro* translation assays are by nature an artificial environment for translating mRNAs. Therefore, a 1:1 correlation with the *in vivo* results should not be expected. Despite the observed discrepancy between *in vitro* and *in vivo* results, both assays suggest a general trend of increased translational activity for the *asc1Δ* null strain. Taking the results of both assays into consideration, we propose that Asc1p functions as a translational repressor.

Recent reports suggest that Asc1p/RACK1 function to stimulate eukaryotic translation (Ceci et al., 2003; Shor et al., 2003). We speculate that these observations arise from indirect phenomena, initiated by the translational up-regulation of regulatory proteins. For example, in this study we observe a reduction of ENO2 protein and mRNA levels in the *asc1Δ* null strain (Fig. 1-6 A and B). It is conceivable that this reduction in transcript levels arises from the translational up-regulation of a transcriptional repressor.

A previous study observed an increase in specific mRNA levels in *asc1Δ* null strains relative to wild-type strains (Hoffmann et al., 1999). Interestingly,

these up-regulated mRNAs in *asc1Δ* null strains are regulated by the transcription factor Gcn4p (Hoffmann et al., 1999). However, in the same study *asc1Δ* null strains did not show a translational up-regulation of GCN4. Here we observe an up-regulation of *GCN4* translational activity relative to wild-type (Figure 1-4E). Because a multiplicity of co-activators contributes to *GCN4*-mediated transcription, it is possible that specific mRNAs are elevated in *asc1Δ* null strains through the translational up-regulation of specific *GCN4* co-activators (Kanadia et al., 2003). Our results support a model where Asc1p and RACK1 are core components of the 40S ribosomal subunit that modulate the translation of mRNAs. Because our results show that average mRNA levels are often higher, but not statistically different in *asc1Δ* null strains, it is possible that Asc1p and RACK1 play an indirect role in transcriptional repression.

A number of proteins have been reported to interact with RACK1 in mammalian systems. Although we have not addressed this question, we observe RACK1 in ribosomal fractions when analyzing mammalian species. It is possible that RACK1 dissociates from the ribosome to perform other functions. Precedent for such phenomena has recently been reported for the ribosomal protein L13A (Mazumder et al., 2003). Several studies have reported an association of RACK1 with the BII isoform of PKC (BII PKC) (Hoffmann et al., 1999; Stebbins and Mochly-Rosen, 2001). Interactions of RACK1 with signal transduction proteins may direct ribosomes to specific cellular locations where localized translation of proteins is required. Further experiments will be required to test these different models.

Acknowledgements

We thank Tracey Fleischer and David Powell for numerous discussions during this project. We thank Tony Weil, Kathy Friedman and Elizabeth Link for comments during the preparation of this manuscript. We thank Jennifer Jennings for assistance in the mass spectrometry experiments and Rodney Gabriel for media preparation. We thank Corbin Williams for assistance with 2D-DIGE experiments. We thank Linda Riles and Mark Johnston for yeast lambda clone 5992 (ATCC70652); John Warner for antibodies to the yeast ribosomal protein Rpl3p; Alan Hinnebusch for the GCN4 reporter plasmid p180; Gerhard Braus for plasmid pME1867; Tony Weil for yeast vectors pRS416 and p426GPD; and Alan Sachs for plasmid T3 lucpA and *in vitro* translation protocols. We would like to thank the Vanderbilt Academic Venture Capital Fund. This project was supported by NIH grant GM64779 to A.J.L. V.R.G. is supported by NIH training grant T32 CA009385. C.W. is supported by NIH grants GM64779 and HL68744. A.J.L. is supported by NIH grants GM64779, HL68744, NS43952, ES11993, and CA098131.

CHAPTER III

ASC1 FACILITATES YEAST RIBOSOME BIOGENESIS AT ELEVATED TEMPERATURES

Chapter 3 is a manuscript in preparation. All experiments performed in this chapter were performed by Vincent Gerbasi.

Summary

Asc1p and Rack1 are orthologous components of the yeast and human 40S ribosomal subunit (respectively). Cryo-EM studies show the mRNA exit channel of the 40S ribosome is lacking significant electron density in Rack1 deficient ribosomes. To dissect the function of Asc1p in protein synthesis, we compared the protein composition of wild-type and *asc1Δ* null yeast strains. Asc1p-deficient ribosomes have a marked increase in their association with the ribosome-associated chaperone Ssb1/2p. Based on this observation, we reasoned that Asc1p-deficient ribosomes might be unstable. Shifting an *asc1Δ* null strain to elevated growth temperatures resulted in a strong growth inhibition and a rapid reduction in total ribosome levels. Experiments testing the stability of Asc1p-deficient ribosomes suggest that *ASC1* facilitates nascent ribosome formation (biogenesis) at elevated temperatures. Yeast deficient in *ASC1* recovered from growth at elevated temperatures. Recovery was associated with increasing the ribosome density (density of ribosomes per cell), but not the ability to stimulate translational initiation *per se*. These studies strongly suggest that

ASC1 is involved in ribosome assembly and that ribosome density is a critical checkpoint for cell proliferation.

Introduction

The precise function of core ribosomal proteins remains obscure. Studies of prokaryotic ribosomes suggest that core ribosomal proteins are not entirely necessary for aspects of protein synthesis (Nissen et al., 2000; Noller et al., 1992). For example, high-resolution structures of the prokaryotic ribosome have confirmed that the active site of peptide bond formation is tightly wrapped in ribosomal RNA but is quite far (>18 angstrom) from any of the ribosomal proteins (Nissen et al., 2000).

Systematic gene disruption has shown that many of the ribosomal proteins orchestrate different steps in ribosome biogenesis (Ferreira-Cerca et al., 2005; Jakovljevic et al., 2004; Leger-Silvestre et al., 2004). Ribosomal proteins (RP) are necessary for different steps of ribosome maturation including ribosomal RNA processing in the nucleolus, late maturation of ribosomal RNA in the cytoplasm, and transport of ribosomes to the cytoplasm (Ferreira-Cerca et al., 2005; Jakovljevic et al., 2004; Leger-Silvestre et al., 2004). Although these studies revealed roles of several RP in biogenesis, the functional roles for other ribosome components will be obtained from focused studies on individual proteins.

Our understanding of ribosome protein function in mammalian systems is not as well developed. However, conditional deletion of RPS6 in mice combined

with fasting results in a dramatic loss of free 40S subunits and a subtle reduction of 80S subunits and polyribosomes in the liver (Volarevic et al., 2000). The combination of fasting and RPS6 depletion was associated with reduced liver cell proliferation (Volarevic et al., 2000). In agreement with these data, yeast cells suppress ribosome synthesis and cell proliferation during starvation (Kief and Warner, 1981). Therefore, there is an established link between ribosome synthesis, cell proliferation, and nutrient deprivation.

Ribosomes deficient in Asc1p have an abnormal structure and are missing electron density at the mRNA exit channel of the 40S subunit (Nilsson et al., 2004; Sengupta et al., 2004). Yeast *asc1Δ* null strains are viable but have a temperature sensitive phenotype (Gerbasi et al., 2004). The *asc1Δ* null strains provide an opportunity to study the functional consequences of this altered ribosome structure and the overall contribution of the gene to cell proliferation.

In this study, we performed a proteomic comparison of wild-type and Asc1p-deficient yeast ribosomes. Surprisingly, ribosomes deficient in Asc1p are enriched in the chaperone protein Ssb1/2. This prompted us to investigate the stability of Asc1p-deficient ribosomes relative to wild-type. Asc1p-deficient ribosomes formed at 30°C *in vivo* are stable at elevated temperatures. However, an *asc1Δ* null strain showed a ribosome biogenesis defect at elevated temperatures. These data strongly suggest that Asc1 is involved in chaperoning ribosome biogenesis. The temperature-sensitive phenotype of an *asc1Δ* null strain is reversible. However, an *asc1Δ* null strain exhibits a severe growth-lag after shifting from the non-permissive to the permissive temperature. This growth

lag is associated with a diminished ribosome pool. While translation initiated immediately after shifting *asc1Δ* null cells from the non-permissive to the permissive temperature, recovery of the ribosome population was delayed. These data strongly suggest that translational initiation alone is insufficient to drive cell proliferation but that proliferation requires an adequate density of ribosomes to proceed.

Results

Proteomic analysis of Asc1p-deficient core ribosome particles

Cryo-electron microscopy has shown that yeast ribosomes lacking Asc1p are missing electron density at the 40S mRNA exit channel. Despite this structural disruption in the small subunit, *asc1Δ* null strains have normal growth rates under permissive conditions (Gerbasi et al., 2004). Unexpectedly, the null strains have elevated levels of a subset of proteins (Gerbasi et al., 2004).

To improve our understanding of Asc1p function in the ribosome, we performed a proteomic comparison of wild-type and Asc1p-deficient ribosomes using semi-quantitative mass spectrometry (Link et al., 1999) (Washburn et al., 2001). Total cellular ribosomes were purified over discontinuous gradients in 200mM salt from a wild-type or cognate *asc1Δ* null strain grown to semi-logarithmic phase at 30°C. Mass spectra corresponding to ribosomal proteins from the wild-type and the *asc1Δ* null strains were obtained using MUDPIT (Link et al., 1999; Washburn et al., 2001). The mass spectrometry data were processed and analyzed using our bioinformatic graphical comparative analysis

software tools (BIGCAT) (Fleischer et al., 2006). To estimate the relative abundance of each protein from the mass spectrometry data, we used a normalized label-free method of quantification (Fleischer et al., 2006; Powell et al., 2004). A protein abundance factor (PAF) was calculated for each identified protein to quantify its relative amount in the samples.

Figure 2-1

A.

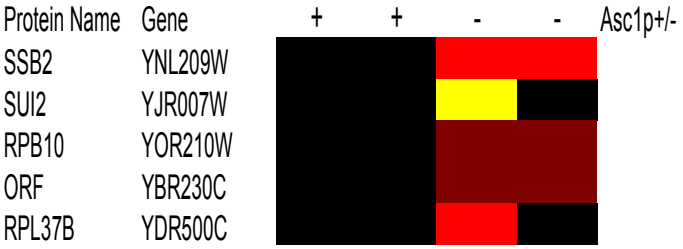

B.

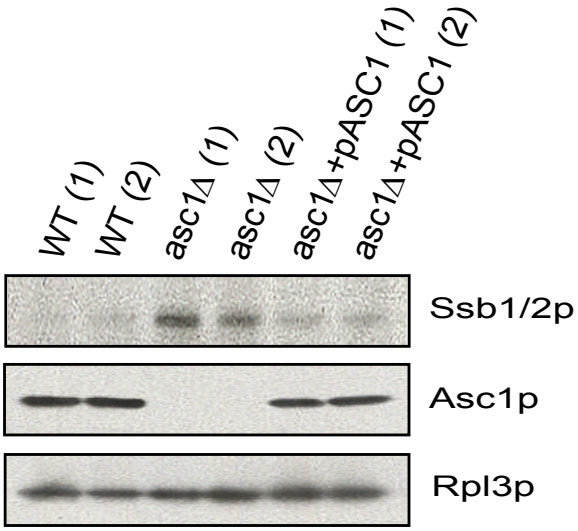

Figure 2-1: Asc1p-deficient ribosomes are enriched with chaperones

(A) Wild-type (+) or *asc1Δ* null (-) yeast core ribosome particles were isolated in duplicate as described in Materials and Methods. Core ribosome particles were then subjected to MUDPIT analysis (Link et al., 1999; Washburn et al., 2001). Results acquired from each MUDPIT sample was then analyzed using BIGCAT software (McAfee et al., 2006). The heat map shows proteins that have the highest PAF values in the Asc1p-deficient ribosomes that were not detected in the wild-type samples. Red indicates a protein with a high protein abundance factor (PAF) score (an estimate of the relative abundance of each protein in a given sample), yellow indicates proteins with an intermediate PAF score, and black indicates the protein was not detected (PAF=0). Ssb1/2p scored the highest PAF among proteins unique to the Asc1p-deficient ribosomes. **(B)** Core ribosome particles were isolated in duplicate from wild-type, *asc1Δ*, or *asc1Δ* + pASC1. Ribosome samples were subjected to SDS-PAGE and immunoblotting for Ssb1/2p, Asc1p, or Rpl3p levels.

Interestingly, ribosomal particles deficient in Asc1p lacked only a few sub-stoichiometric interactions. Comparison of proteins detected between the wild-type and *asc1⊿* null strain ribosomes suggested that mutant ribosomes were deficient in Asc1p, but not other core components of the ribosome. In contrast, the Asc1p-deficient ribosomes were enriched in the ribosome-associated chaperone protein Ssb1/2p (average PAF value of 3.30) (Figure 2-1A). Additionally, Asc1p-deficient ribosomes were enriched in RPB10 and the undefined yeast gene product YBR230C. Both of these proteins contained PAF scores that were considerably lower than Ssb1/2p. Because the PAF value indicates the confidence of a given protein identification, we chose not to pursue these additional interactions further. To test if Ssb1/2p enrichment in Asc1p-deficient ribosomes was due to the absence of Asc1p, we analyzed Ssb1/2p levels from wild-type, *asc1Δ*, and *asc1Δ*+ pASC1 (complemented) yeast strains by isolating ribosomes and performing immunoblot analysis. Densitometry of the immunoblots showed that Asc1p-deficient ribosomes contained an 80% increase of Ssb1/2p protein relative to wild-type (Figure 2-1B). Further, Ssb1/2p ribosomal protein levels were complemented when ASC1 was expressed from a low-copy plasmid in the *asc1Δ* null yeast. Therefore, alteration in 40S structure induced by a loss of Asc1p is associated with increased levels of Ssb1/2p in the ribosome.

asc1-deficient yeast rapidly lose ribosomes and polyribosomes at elevated temperatures

A subset of HSP70-like chaperone proteins are ribosome-associated and parallel the expression profiles of core ribosomal proteins when yeast cells are subjected to stressful conditions (Albanese et al., 2006). These chaperones linked to protein synthesis (CLIPS) include Ssb1/2p (Albanese et al., 2006). Previous studies have shown that Ssb1/2 binds to the ribosome in a conformation-dependent manner and maintains ribosome structure through an unknown mechanism (Nelson et al., 1992; Pfund et al., 1998).

Figure 2-2

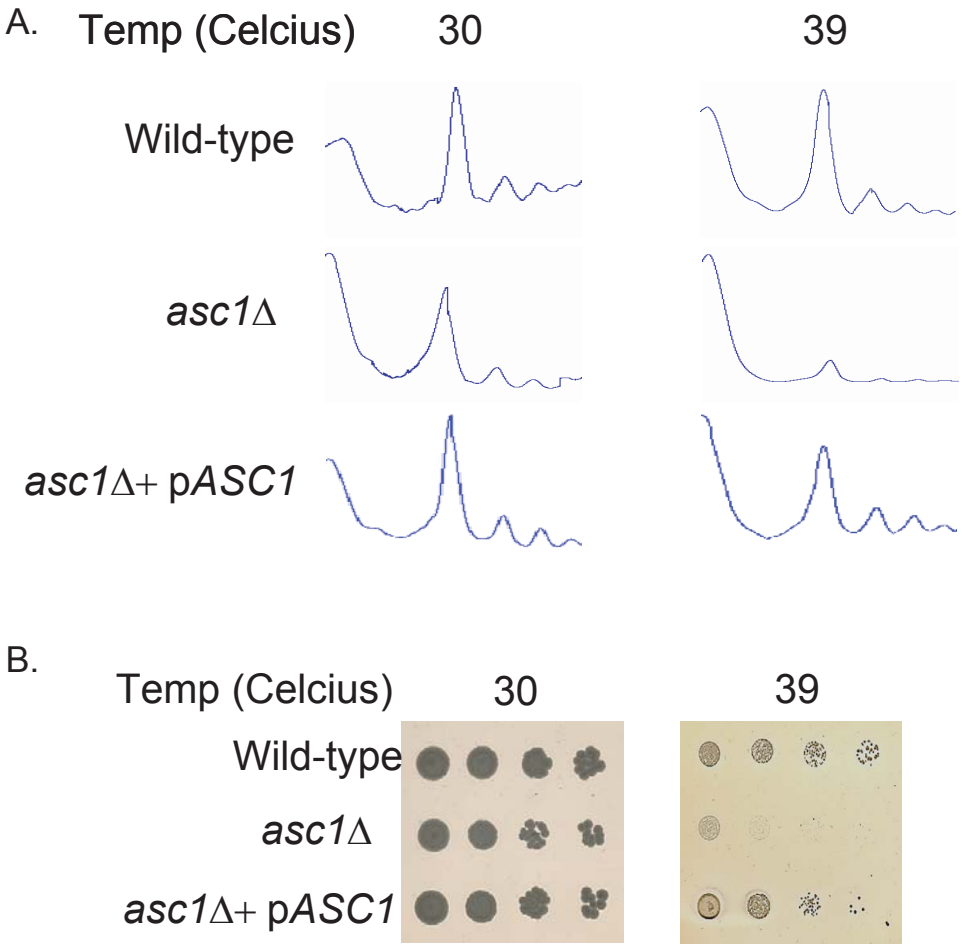

Figure 2-2: asc1-deficient yeast grow slowly and lose ribosomes at the non-permissive temperature

(A) Wild-type, *asc1Δ*, or *asc1Δ* + pASC1 yeast were grown in SC-URA at 30°C. Cells were then transferred to either 30°C or 39°C for 2 h. Cells isolated at the indicated temperatures were then subjected to polysome profiling analysis as described in materials and methods. An equivalent number of O.D. 260 units were loaded onto each sucrose gradient. **(B)** Wild-type, *asc1Δ*, or *asc1Δ* + pASC1 were analyzed for growth at 30°C or 39° C using a plate dilution assay. Growth of *asc1Δ* yeast was strongly inhibited at 39°C. This phenotype was complemented by expression of ASC1 on a low-copy plasmid.

Asc1p-deficient ribosomes were enriched in Ssb1/2p. Because Ssb1/2p has been implicated in stabilizing ribosome structure, we reasoned that this chaperone enrichment might be due to reduced ribosome stability in the *asc1Δ* null mutant. To test this hypothesis, we analyzed the level and activity of ribosomes in wild-type, *asc1Δ*, and *asc1Δ* +pASC1 strains. Ribosome levels and activity were accessed by polyribosome profiling. Our results show that an *asc1Δ* null strain contains normal levels of ribosomes and polyribosomes at 30°C (Figure 2-2A). However, shifting *asc1Δ* yeast to 39°C resulted in a severely diminished ribosome and polyribosome population. Polyribosome levels were reduced in a similar proportion to monosome (80S peak) levels, consistent with a defect in ribosome biogenesis (Ferreira-Cerca et al., 2005). The abnormal polysome profile of the *asc1Δ* yeast at the non-permissive temperature was complemented by expressing *ASC1* on a low-copy plasmid (Figure 2-2A). We found that growth of *asc1Δ* null yeast at 39°C was severely impaired (Figure 2-2B). Negative control strains that are temperature sensitive but have no reported function in mRNA translation or ribosome biogenesis failed to grow at 39°C, but did not lose ribosomes when grown at the non-permissive temperature (Audhya et al., 2000). Collectively, these data show that *asc1Δ* null yeast have reduced cell proliferation and a severely diminished ribosome population when grown at 39°C.

Figure 2-3

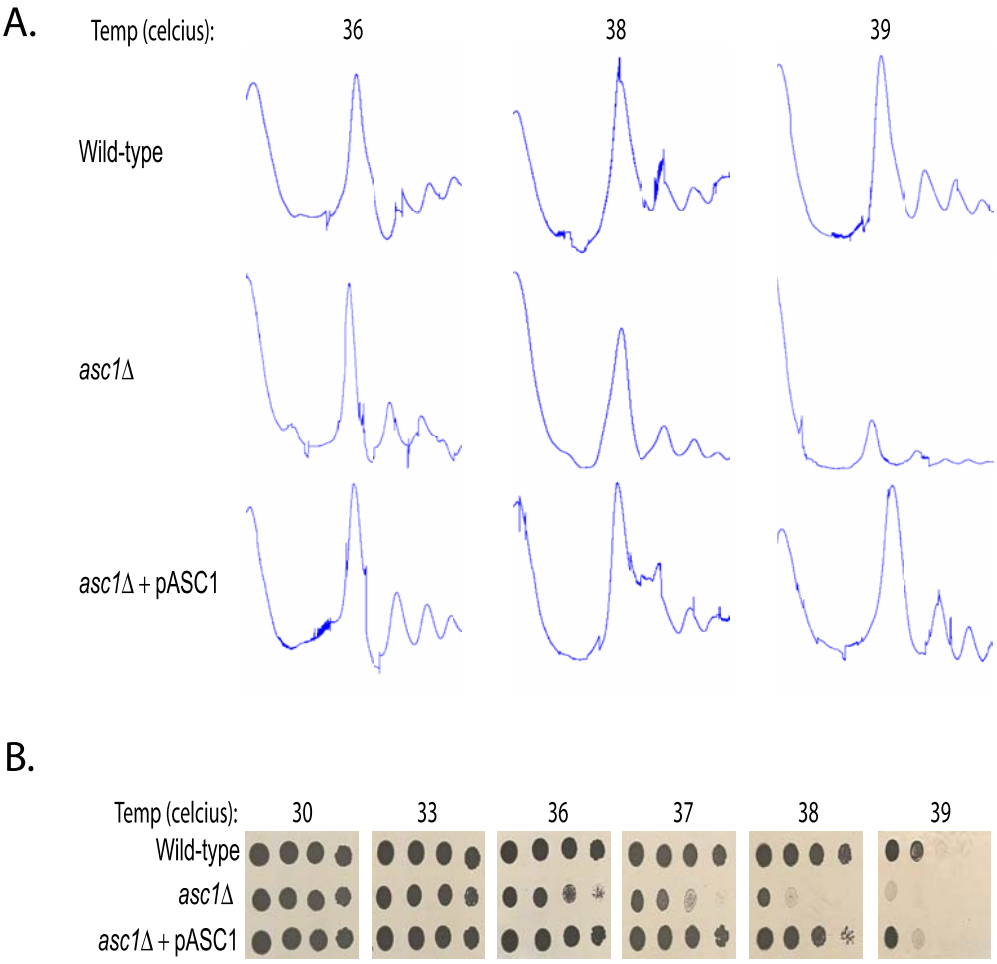

Figure 2-3: Correlation between temperature, ribosome loss, and degree of growth inhibition in asc1-deficient yeast

(A) Wild-type, *asc1Δ*, or *asc1Δ* + pASC1 yeast were grown as described in Figure 2-2. Yeast were then shifted for 2 h to 36°C, 38°C, or 39°C and subjected to polysome profiling analysis. **(B)** Wild-type, *asc1Δ*, or *asc1Δ* + pASC1 yeast were grown at either 30°C, 33°C, 36°C, 37°C, 38°C or 39°C in a plate dilution assay for 48 h.

Association between growth temperature, ribosome loss, and cell proliferation in asc1-deficient yeast

The severity of ribosome loss and growth suppression was assessed over a gradient of temperatures in wild-type, *asc1Δ* null, and a complemented *asc1Δ* null yeast strains. The extent of ribosome and polyribosome depletion in *asc1Δ* null yeast correlated with the temperature at which the yeast were grown (Figure 2-3A). As before, expressing ASC1 on a low-copy plasmid in the *asc1Δ* null yeast complemented the observed reduction in ribosomes and polyribosomes (Figure 2-3A). Additionally, we observed a correlation between the extent of growth suppression and growth temperature in the *asc1Δ* null yeast (Figure 2-3B). These data establish an association between growth temperature, extent of ribosome loss, and proliferation rate in *asc1Δ* null yeast.

Figure 2-4

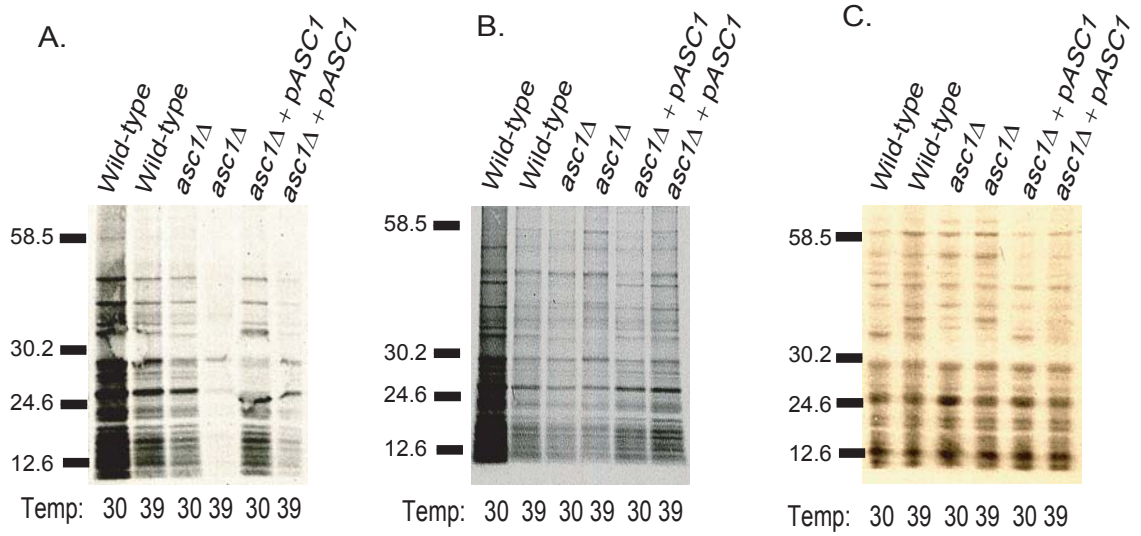

Figure 2-4: Asc1p is critical for nascent ribosome stability at the non-permissive temperature

(A) Ribosomal proteins from wild-type, *asc1Δ*, or *asc1Δ* + pASC1 yeast complemented with ASC1 on a low-copy plasmid (*asc1Δ* + pASC1) were radiolabeled with a mixture of 35S-methionine and 35S-cysteine at 30°C or 39°C for 4 hours. Ribosomal particles were isolated from the radiolabeled cells and subjected to SDS-PAGE and radiography. **(B)** Ribosomal proteins from strains described in **(A)** were radiolabeled in media containing 35S-methionine and 35S-cysteine at 30°C. The cell labeling was quenched with 50mM cold cysteine and methionine and cells were shifted to either 30°C or 39°C for four hours. Core ribosome particles were isolated and analyzed as described in **(A)**. **(C)** Yeast strains described in **(A)** were radiolabeled at 30°C for 4 hours. Core ribosome particles were isolated from cell lysates that were incubated *in vitro* for 2 hours at either 30°C or 39°C.

A role for *ASC1* in ribosome biogenesis

The *asc1Δ* null yeast strain showed a temperature-sensitive reduction in the density of ribosomes per cell. The ribosome and polyribosome population was severely diminished within 2 hours of growth at the non-permissive temperature. This rapid reduction in the ribosome population led us to question the fate of these Asc1p-deficient ribosomes at the non-permissive temperature. To analyze the synthesis and stability of Asc1p-deficient ribosomes, we isolated ribosomal particles from cells radiolabeled with 35S-methionine and cysteine (Figure 2-4A). The *asc1Δ* null strain exhibited a severe reduction in radiolabeled core ribosomal proteins at the non-permissive temperature compared to the wild-type and complemented *asc1Δ* null strain (Figure 2-4A). The data suggested that *ASC1* functioned during ribosome synthesis and/or stability at elevated growth temperatures. That Asc1p-deficient ribosomes were not detected in this assay suggests that these mutant yeast either fail to synthesize ribosomal proteins, or fail to form the ribosome complex at the non-permissive temperature.

To distinguish between a ribosome stability or biogenesis role for *ASC1* at non-permissive temperatures, we analyzed ribosome stability using pulse-chase. Wild-type, *asc1Δ* null, and complemented *asc1Δ* null yeast strains were pulse labeled with 35-S methionine and cysteine at 30°C, treated with excess cold methionine and cysteine, and shifted to either 30°C or 39°C for 4 hours. Ribosomes from *asc1Δ* null yeast grown at 30°C were stable at 39°C (Figure 2-4B). Additionally, *in vitro* analysis of ribosome stability at 30 or 39°C revealed no difference between wild-type and complemented strains (Figure 2-4C).

Therefore, our results support a model where *ASC1* stabilizes nascent but not mature ribosomes at elevated temperatures.

Figure 2-5

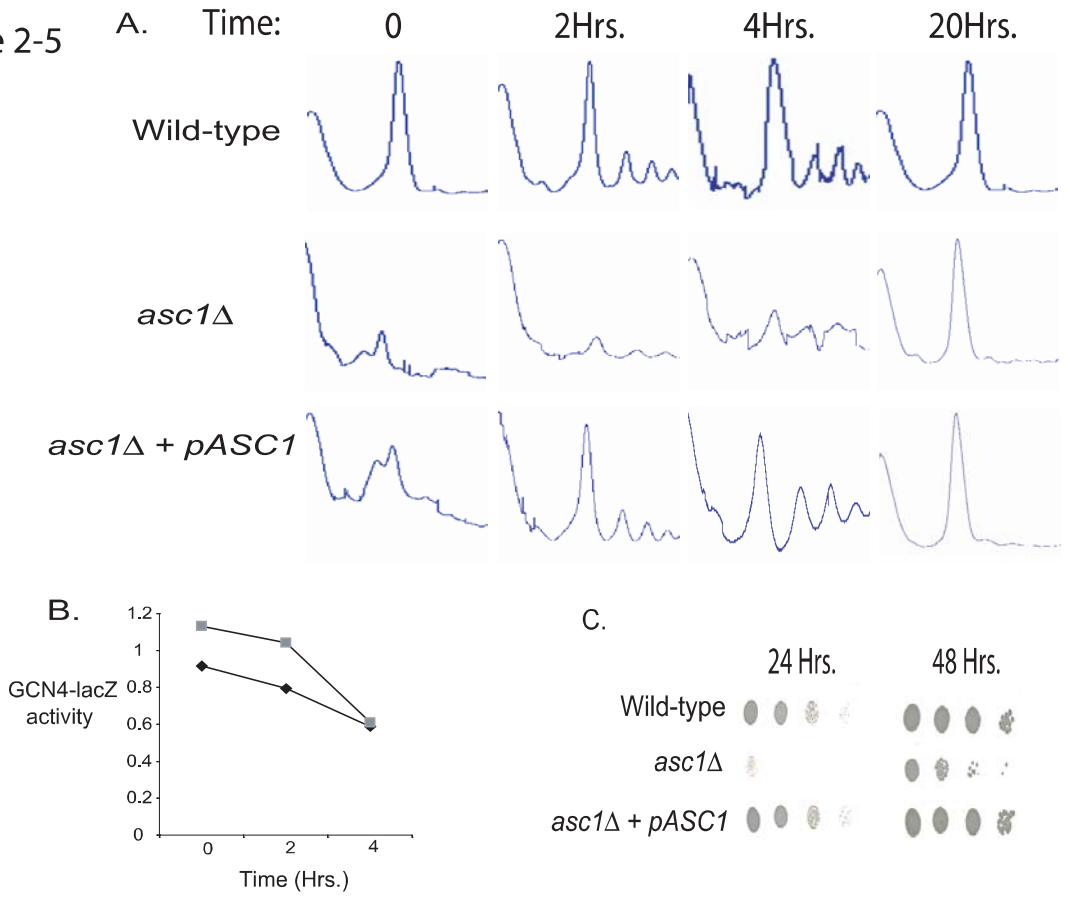

Figure 2-5: A growth lag in recovering asc1-deficient yeast is associated with reduced ribosome density, not repressed translational initiation

(A) Wild-type, *asc1Δ*, or *asc1Δ* + pASC1 yeast were grown for 16 h at 39°C. Cells were then shifted to fresh media at 30°C and grown for either 0, 2, 4, or 20 h. Cells isolated at the indicated time points were subjected to polysome profiling analysis as described in Figures 2-2 and 2-3. **(B)** Wild-type (Grey boxes) or *asc1Δ* (Black diamonds) yeast expressing a GCN4-reporter construct were grown for 16 h at 39°C. Following growth at the non-permissive temperature, yeast were shifted to 30°C for 0, 2, or 4 h. Cells recovering at the indicated time points were assayed for B-gal activity as described in materials and methods. **(C)** Wild-type, *asc1Δ*, or *asc1Δ* + pASC1 yeast were grown in SC-URA for 16 h at 39°C. Cells were then diluted onto a plate and analyzed for growth after either 24 or 48 h at 30°C.

asc1Δ null yeast recover from the non-permissive temperature by replenishing the ribosome pool

After 16 hours of growth at 39°C, *asc1Δ* null yeast had a severely diminished pool of ribosomes relative to wild-type or complemented strains (Figure 2-5A). All the yeast strains tested exhibited fewer polysomes after growth for 16 hours at 39°C (Figure 2-5A). We presume that this loss of polysomes is due to nutrient depletion (Ashe et al., 2000; Hinnebusch, 2005). Two hours after shifting the cells to fresh media at 30°C, wild-type, *asc1Δ* null, and complemented yeast re-formed polysomes (Figure 2-5A). Although *asc1Δ* null yeast formed polysomes after 2 hours of growth at the permissive temperature, the total ribosome population was still considerably lower than wild-type or complemented strains at this time point (Figure 2-5A). After four hours of recovery, the *asc1Δ* null yeast exhibited a mild increase in the ribosome pool (Figure 2-5A). At twenty hours of recovery, *asc1Δ* null yeast exhibited a ribosome pool that was indistinguishable from wild-type and complemented strains (Figure 2-5A).

That *asc1Δ* null yeast formed polysomes within two hours of recovery at the permissive temperature suggested that the yeast were able to reinitiate mRNA translation immediately after growth at the non-permissive temperature. In yeast, translation of the transcription factor GCN4 is most active when general translational initiation is repressed following nutrient starvation (Hinnebusch, 2005). Conversely, yeast growing in a nutrient-rich environment suppress GCN4 mRNA translation and actively initiate the translation of a majority of mRNA

transcripts (Hinnebusch, 2005). Therefore, GCN4 translational activity is an effective inverse indicator of overall translational initiation (Holmes et al., 2004). We used a GCN4 reporter assay as an additional test of initiation competency in yeast recovering from long-term growth at the non-permissive temperature. Wild-type and *asc1Δ* null yeast harboring a GCN4 reporter were grown at 39°C for 16 hours. After growth at the non-permissive temperature, cells were shifted to fresh media at 30°C and assayed for GCN4 activity at several time points. Consistent with our previous observations, asc1-deficient yeast contained a 20% increase in GCN4 reporter activity relative to wild-type at the 0-time-point (Gerbasi et al., 2004). Both wild-type yeast and *asc1Δ* null strains gradually repressed GCN4 reporter activity during recovery at the permissive temperature (Figure 2-5B). These data strongly suggest that *asc1Δ* null yeast recovering from the non-permissive temperature are competent to initiate mRNA translation. Additionally, these data suggest that initiation of mRNA translation in recovering *asc1Δ* null yeast precedes expansion of the ribosome population.

Polysome profiling and reporter assays suggested that *asc1Δ* null yeast recovering from growth at the non-permissive temperature were able to initiate mRNA translation immediately, but required long-term growth at the permissive temperature to completely replenish the ribosome population. Because *asc1Δ* null yeast exhibited a significant lag in recovering the ribosome population, we tested the ability of *asc1Δ* null yeast to proliferate after shifting from the non-permissive to the permissive temperature using a plate-dilution assay. The *asc1Δ* null yeast strain had a significant growth lag during recovery compared to

wild-type and complemented strains (Figure 2-5C). However, the *asc1Δ* null yeast strain reached a level of growth that was near that of the wild-type and *asc1Δ* null complemented strain after 48 hours (Figure 2-5C). Taken together, these results show that the growth lag of *asc1Δ* null yeast is associated with a diminished ribosome pool, but not suppressed translational initiation *per se*.

Discussion

Enrichment of Chaperones in Asc1p-deficient Ribosomes

The function of many ribosomal proteins remains unknown. Here we used mass spectrometry to analyze the composition of a eukaryotic ribosome that was missing a single core component of the 40S. We find that loss of Asc1p enhances the association of the CLIPS chaperone Ssb1/2p with the ribosome. It has been established that Ssb1/2p binds to the ribosome in a conformation-dependent manner (Pfund et al., 1998). It is tempting to speculate that the abnormal structure of 40S ribosomes in an *asc1Δ* null strain triggers binding of this chaperone. Recently, a role for one of the HSP70 chaperones in ribosome biogenesis has been shown (Meyer et al., 2007). Therefore, it is possible that chaperone-like proteins facilitate critical steps in ribosome biogenesis and/or stability.

ASC1 is critical for ribosome biogenesis at elevated temperatures

Asc1p has been confirmed as a core component of the 40S subunit by several independent studies (Gerbasi et al., 2004; Manuell et al., 2005; Sengupta et al., 2004). Here we show that loss of *ASC1* disrupts the biogenesis of ribosomes at the non-permissive temperature. *In vivo* and *in vitro* analysis of ribosome stability showed that Asc1p-deficient ribosomes formed at the permissive temperature will retain their structure at the non-permissive

temperature. However, *asc1*-deficient yeast failed to label ribosomal proteins at the non-permissive temperature, suggesting that *ASC1* functions during the synthesis of nascent ribosomes (biogenesis), but does not effect the stability of mature ribosomes. The precise mechanistic step at which *ASC1* orchestrates ribosome biogenesis is currently unknown. However, our results suggest that *ASC1* facilitates a temperature-sensitive step of the ribosome biogenesis sequence. It is possible that a sub-set of ribosomal proteins may have evolved to play functional roles in stabilizing ribosome structure after or during exposure to stresses such as heat-shock. This may help to explain why yeast that do not express some 40S subunit proteins fail to present a growth defect under optimal growth conditions (Ferreira-Cerca et al., 2005).

Do nascent ribosomes constitute a major portion of ribosomes detected in a polyribosome profile?

In the polysome profiling experiments performed in Figures 2-2 and 2-3, an *asc1Δ* null strain exhibited a loss of the total ribosome pool within two hours at the non-permissive temperature. That *asc1Δ* null yeast contain stable, mature ribosomes, but fail to form nascent ribosomes at the non-permissive temperature, suggests that much of the total ribosome population might consist of nascent ribosomes.

There is a small pool of ribosomes that remain in *asc1Δ* null yeast after growth for 16 hours at the non-permissive temperature. Why does this small pool of ribosomes persist? Two possibilities are either loss of nascent ribosome

synthesis in *asc1Δ* null yeast may be incomplete or mature Asc1p-deficient ribosomes may be able to persist long-term (>16 hours). If mature ribosomes constitute a small population of the total ribosome pool in *asc1*-deficient yeast grown at the non-permissive temperature, it is conceivable there is a high rate of ribosome turnover. It is tempting to speculate that there are distinct populations of ribosomes; one group that persists long-term, and another that is turned-over rapidly or sequestered in a cellular compartment. The process of ribosome degradation/recycling is poorly understood. However, core components of the ribosome are heavily ubiquitinated (Spence et al., 2000). Perhaps ubiquitination, or a combination of post-translational modifications decides the fate of the nascent or mature ribosome pool.

Growth behavior of *asc1Δ* null yeast establishes an association between ribosome density and cell proliferation

The *asc1Δ* null yeast strain grown for 16 hours at 39°C exhibits a severely diminished ribosome and polyribosome pool. Interestingly, *asc1Δ* null yeast form polyribosomes and suppress GCN4 mRNA translation within two hours of introduction to fresh media at 30°C. However, at the two-hour recovery-time-point, the *asc1Δ* null yeast did not appear to significantly increase the total ribosome pool. This suggests that the limited remaining pool of yeast ribosomes in *asc1Δ* null yeast are able to initiate mRNA translation immediately, but are not able to rapidly replenish the ribosome population. The ribosome pool of *asc1Δ* null yeast appeared to be growing after four hours of recovery from the non-

permissive temperature. However, *asc1Δ* null yeast recovering from growth at the non-permissive temperature did not completely replenish the ribosome pool until four to twenty hours of growth at the permissive temperature. Because *asc1Δ* null yeast exhibited a severe growth lag that was associated with a reduced ribosome pool, but not suppressed translational initiation, these studies support a link between cell proliferation and ribosome density that is independent of translational initiation.

Implications for mammalian cells

Activation of various signaling pathways in mammalian cells leads to stimulation of the TOR kinase. TOR activity is associated with increased translation of 5′ terminal oligopyrimidine tract (TOP) containing mRNAs (Raught et al., 2001). TOP-containing mRNAs code for core ribosomal proteins, ribosome biogenesis factors, and other proteins with functional roles in translation (Raught et al., 2001). Suppression of TOR activity with rapamycin inhibits cell proliferation by mechanisms that are not completely understood. These studies and others establish a strong association between ribosome density and the capacity for cells to proliferate (Guertin et al., 2006; Jorgensen et al., 2004; Rudra and Warner, 2004; Rudra et al., 2005; Volarevic et al., 2000). Taken together, stimulation of cell proliferation by TOR activity might manifest through increasing the ribosome pool (Guertin et al., 2006). The success of rapamycin as a therapeutic compound suggests that direct pharmacological

inhibition of ribosome biogenesis might function as an effective inhibitor of cell proliferation.

Acknowledgments

We would like to thank Jonathan Warner, Todd Graham, and Elizabeth Craig for sharing reagents. We would like to thank Jill McAfee, Nicholas Campbell, and Jennifer Jennings for technical assistance. We would also like to thank Elizabeth Link for editorial assistance. V.R.G was supported by NIH training grant This project was supported by NIH grant GM64779 to A.J.L.

Experimental Procedures

Yeast Strains and other Reagents

Construction of strains AL190 (BY4743 with pRS316), AL150 (YDM36556 with pRS416), and AL156 (YDM36556 with p*ASC1*) has been described previously (Gerbasi et al., 2004). Temperature sensitive strains used as negative controls; AAY102 *(stt4-ts)* and AAY104 *(pik1-ts)* were described in a previous publication (Todd Graham source)(Audhya et al., 2000). Antibodies against Rpl3p and Ssb1/2p were kindly provided by Jonathan Warner and Elizabeth Craig (respectively). Construction of plasmid p*ASC1* is described in a previous publication (Gerbasi et al., 2004).

Core Ribosome Preparation

Cells were pelleted by centrifugation at 3,000 rpm for 15 min. Cell pellets were washed in 25mL of water and re-centrifuged. Cell pellets were resuspended in standard buffer (10mM Tris pH 7.4, 5mM 2-mercapto ethanol, 50mM Ammonium Chloride, and 5mM Magnesium Acetate) at 25% W/V. Cells were lysed by bead beating. Cell extracts were centrifuged for 30 min at 20,000x g. Supernatants were subjected to ultracentrifugation for 2h at 45,000 rpm in an SA-600 rotor at 4^{o}C. Following centrifugation, supernatants were discarded and ribosome pellets were suspended in 6mL of wash buffer (10mM Tris pH 7.4, 5mM 2-mercapto ethanol, 166mM ammonium chloride, and 33mM magnesium acetate).

Suspended ribosome pellets were centrifuged through 6mL discontinuous sucrose gradients (5% and 20% sucrose suspended in wash buffer) for 18 h at 20,000 rpm in an SW-41 rotor. Ribosome pellets were suspended in 100mM ammonium bicarbonate for mass spectrometry or SDS-PAGE analysis.

Polysome Profiling

Polysome profiling was performed as described previously (Fleischer et al., 2006).

Mass Spectrometry Analysis of Core Ribosome particles

Core ribosome particles were reduced, alkylated, and trypsinized in 100mM ammonium bicarbonate at pH 8.0 as described previously (Sanders et al., 2002). The tryptic peptide fragments were desalted using a C-18 reversed-phase salt trap (Michrom). After desalting, the tryptic peptides were subjected to reverse-phase microcapillary LC-ESI-MS/MS using a LTQ mass spectrometer (Thermo Electron, Inc) to acquire tandem mass spectra of the eluted proteins (Link et al., 1999; Washburn et al., 2001). Acquired tandem spectra were identified using SEQUEST and the *Saccharomyces cerevisiae* database (Updates as of May 2006). Data was processed and organized using the BIGCAT software analysis suite (McAfee et al., 2006). Cluster figures of identified proteins were generated using the BIGCAT cluster option (McAfee et al., 2006).

GCN4 Reporter Assays

Construction of yeast strains (AL185 (YDM36556 plus p180 [GCN4 5' untranslated region -*lacZ* reporter plasmid) and AL183 (BY4743 with p180) were described previously (Gerbasi et al., 2004). Yeast were grown for 16 h at 39°C in SC-URA media. Following growth for 16 h, the yeast strains were shifted to new media at 30°C for 0, 2, or 4 h. GCN4 reporter activity was assayed as described previously (Gerbasi et al., 2004).

Yeast Proliferation Assays

Yeast dilution assays were performed as described previously (Gerbasi et al., 2004).

35-S Methionine/Cysteine Labeling

50mL of yeast cells were grown to an $O.D._{600}$ of 0.6. Cells were harvested by centrifugation and suspended in 1mL of SC-URA containing 300uCi of 35-S cysteine and methionine (ICN). Cells were labeled for 4 h at either 30 or 39°C. For pulse-chase analysis, cells were treated with 50mM cold methionine and cysteine prior to incubation at either 30°C or 39°C for an additional 4 h. For *in vitro* analysis of ribosome stability, cells were labeled for 4 h at 30°C in SC-URA media containing 300uCi of 35-S cysteine and methionine (ICN). After labeling of total cellular proteins, cells were lysed by bead-beating in standard buffer (see ribosome preparation). Cell extracts were incubated at either 30°C or 39°C for 2

h prior to centrifugation of core ribosome particles as described in the core ribosome preparation protocol.

CHAPTER IV

THE MYOTONIC DYSTROPHY TYPE-2 PROTEIN ZNF9 IS PART OF AN ITAF COMPLEX THAT PROMOTES CAP-INDEPENDENT TRANSLATION

All experiments performed in this chapter of the dissertation were performed by Vince Gerbasi. The manuscript has been accepted for publication in **Molecular and Cellular Proteomics**.

Summary

The 5' untranslated region (5'UTR) of the ornithine decarboxylase (ODC) mRNA contains an internal ribosomal entry site (IRES). Mutational analysis of the ODC IRES has led to the identification of sequences necessary for cap-independent translation of the ODC mRNA. To discover novel IRES-*trans*-acting-factors (ITAFs), we performed a proteomic screen for proteins that regulate ODC translation using the wild-type ODC mRNA and a mutant version with an inactive IRES. We identified two RNA-binding proteins that associate with the wild-type ODC IRES, but not the mutant IRES. One of these RNA-binding proteins, PCBP2, is an established activator of viral and cellular IRESs. The second protein, ZNF9 (myotonic dystrophy type-2 protein), has not previously been shown to bind IRES-like elements. Using a series of biochemical assays, we validated the interaction of these proteins with ODC mRNA. Interestingly, ZNF9 and PCBP2 biochemically associate with each other and appear to function as part of a larger holo-ITAF / RNP complex. Our functional studies show that PCBP2 and ZNF9 stimulate translation of the ODC IRES. Importantly, these

results may provide insight into the normal role of ZNF9 and why ZNF9 mutations cause myotonic dystrophy.

Introduction

Most eukaryotic translation initiation involves the interaction of the 43S preinitiation complex (comprised of the 40S ribosomal subunit plus initiation factors, Met-tRNA$_i$, and GTP) with the 7-methyl-guanosine cap complex at the 5'end of the mRNA (Sachs et al., 1997). During such cap-dependent translation initiation, the 43S preinitiation complex is recruited to the 5'-cap structure and scans the 5' untranslated region (UTR). Recognition of the AUG start codon is followed by joining of the 40S-Met-tRNA$_i$ complex to the 60S large ribosomal subunit to form the 80S initiation complex. In contrast, translation mediated by an internal ribosomal entry site (IRES) does not require the 5'-cap structure. Instead, translation initiates at internal sites in the mRNA (Chen and Sarnow, 1995; Jang et al., 1989; Pelletier and Sonenberg, 1988).

IRESs are *cis*-acting RNA sequences found in the 5' region of a subset of eukaryotic mRNAs. Originally discovered in viral mRNAs, IRESs were later found in cellular transcripts (McCormack et al., 1997). It is postulated that 3-5% of all human mRNAs are translated in a cap-independent manner (Johannes et al., 1999; Qin and Sarnow, 2004). Some translational initiation factors used in cap-dependent initiation also stimulate translation of some, but not all, IRES-containing transcripts. There are examples of IRES-containing mRNAs that appear to recruit ribosomes directly, independent of the classical initiation factors

(Hellen and Sarnow, 2001; Ji et al., 2004; Wilson et al., 2000). Each IRES may employ a unique mechanism of translational initiation.

Evidence from studies of both viral and cellular IRESs has led to several hypotheses as to how and why IRESs initiate translation of their cognate mRNAs. First, IRESs may be an efficient alternative to cap-dependent translation initiation; an observation supported by multiple studies (Johannes et al., 1999; Johannes and Sarnow, 1998; Pyronnet et al., 2000; Qin and Sarnow, 2004). Second, specific RNA binding proteins may be dedicated to facilitating IRES-mediated translation initiation. This model has gained favor through the discovery that viral and cellular IRESs share a common set of RNA-binding proteins that stimulate their translation (Blyn et al., 1996; Blyn et al., 1997; Evans et al., 2003; Hunt et al., 1999; Mitchell et al., 2001; Walter et al., 1999). Finally, there is evidence that a subset of IRESs can recruit ribosomes directly through a complex RNA secondary structure (Pestova and Hellen, 2003; Wilson et al., 2000).

The sequences and structures of viral and cellular IRESs vary widely although they often contain pyrimidine-rich sequences. The conserved pyrimidine tract is found proximal to the start codon (Sachs et al., 1997). Mutagenesis of pyrimidines proximal to the start codon or in other locations throughout an IRES reduces activity and results in the disruption of specific protein-RNA interactions (Mitchell et al., 2005; Pyronnet et al., 2000). Thus, these pyrimidine-rich sequences in IRESs are necessary for complete IRES activity and recruitment of *trans*-acting factors.

The IRES *trans*-acting-factor PTB binds pyrimidine-rich sequences in viral and cellular IRESs (Mitchell et al., 2001; Mitchell et al., 2005; Singh et al., 1995). It functions with UNR, another ITAF, to enhance the activity of viral and cellular IRESs (Hunt et al., 1999; Mitchell et al., 2001). In addition, several other RNA-binding proteins have been shown to bind and enhance the activity of IRESs (Pickering et al., 2004). However, the high sequence variability between IRESs suggests that there is a wide array of ITAFs, many of which are unknown.

Pancreatic tumor cells alternatively splice the 5'UTR of ODC to generate an IRES that is translated in a cap-independent and cell-cycle dependent manner (Pyronnet et al., 2000; Pyronnet et al., 2005; Pyronnet et al., 1996). Pyrimidine tracts in the ODC 5' UTR that are necessary for IRES activity have been identified by site-directed mutagenesis (Pyronnet et al., 2000). Mutations that disrupt either RNA secondary structure or interactions with *trans*-acting factors compromise IRES activity. As such, we chose the ODC IRES as the target in our search for novel proteins that modulate cellular IRES activity.

To identify potential proteins that associate with the ODC IRES, we utilized a proteomic approach (Link, 1999). Using RNA-affinity capture and mass spectrometry, we found that two nucleic acid-binding proteins, PCBP2 and ZNF9, associate with the wild-type ODC IRES. Mutations in the IRES sequence that compromise ODC IRES function reduce binding to these two proteins. PCBP2 is a known IRES-binding protein that enhances cap-independent translation (Blyn et al., 1996; Blyn et al., 1997; Evans et al., 2003; Gamarnik and Andino, 2000; Walter et al., 1999). The function of ZNF9 is unknown, although its non-coding

region is mutated in patients with type-2 myotonic dystrophy (Liquori et al., 2001). Our results suggest that one function of ZNF9 is to enhance cap-independent translation.

Experimental Procedures

Reagents

3'-biotinylated RNAs used for affinity capture reactions were purchased from Dharmacon. The wild-type ODC RNA sequence was: 5'-UUUCUGUCUUAUUGUUUC-3'(Pyronnet et al., 2000). The mutant ODC RNA sequence was: 5'-AAACUGUCUUAUUGAAAC-3' (Pyronnet et al., 2000). RAJI human B-cell lymphocytes were grown in RPMI 1640, 10% FCS, 1% PS, at 37°C and 5% CO_2. Human 293T cells were grown in DMEM, 10% FBS, and 1% PS at 37°C and 5% CO_2. Antibodies raised against PCBP2 were kindly provided by Raul Andino. α-V5 antibodies were purchased from Invitrogen. α-PKC and α-actin antibodies were purchased from Santa Cruz Biotechnology Inc. To clone the ZNF9 cDNA, total RNA was isolated from human RAJI B-cells. cDNA was generated using Superscript II (Invitrogen) primed with oligo dT. The ZNF9 cDNA was amplified using the primers: 5'-GGCAAGGACCCTCAAAATAAAC-3' (forward) and 5'-TGTAGCCTCAATTGTGCATTC (reverse). The 620 bp RT-PCR product was cloned in-frame into the pcDNA3.1/V5-His-TOPO plasmid to create the plasmid pcDNA-ZNF9-V5 expressing a ZNF9-V5 fusion. The plasmid

pcDNA3.1/V5-His-TOPO/lacZ expressing a lacZ-V5 fusion was obtained from Invitrogen.

RNA affinity chromatography

To generate the RNA affinity-chromatography resin, 100 μL of streptavidin-agarose beads (Pierce) were incubated with 30 nmol of wild-type or mutant 3'-biotinylated RNA in binding buffer (12 mM HEPES in diethylpyrocarbonate-treated water pH8.0, 15 mM KCl, 15 mM dithiothreitol, 5 mM $MgCl_2$, 10% glycerol, with 1 mini-Complete™ protease inhibitor (Roche)/50 mL binding buffer) at 4˚C for 30 min with gentle mixing. Following incubation of biotinylated RNA with the steptavidin beads, the chromatography resin was washed with binding buffer (200x bead volumes) to remove excess biotinylated RNA. To generate cell extracts, 10^9 cells were suspended in 3 mL binding buffer and lysed in 2 mL tubes with 0.5 mm glass beads using a bead-beater (Biospec, Inc). The supernatant was removed from the glass beads into sterile microcentrifuge tubes and centrifuged at 20,000x g for 15 min. The cleared supernatant was incubated with the agarose-coupled RNA affinity resin for 30 min at 4˚C with gentle mixing. After incubation, the chromatography resin was washed with binding buffer (200x bead volumes) to remove non-specific proteins. Proteins were eluted from the RNA affinity resin with 1 mL washes of increasing salt concentration (150 mM, 250 mM, 350 mM, and 600 mM NaCl) in binding buffer. Each salt wash was then subjected to a 10% TCA precipitation. Protein pellets were suspended in 100

mM ammonium bicarbonate prior to SDS-PAGE, trypsinization, and mass spectrometry analysis.

Experiments utilizing a competitive, non-biotinylated RNA were performed essentially as described above with the exception that a wild-type RNA affinity column was incubated with cell extract then washed twice with 30 nmols of non-biotinylated ODC RNA suspended in 1 mL of binding buffer. Proteins that remained associated with the resin were eluted with 4 separate salt washes (150 mM, 250 mM, 350 mM, and 600 mM NaCl) and prepared for mass spectrometry analysis as described below.

Mass spectrometry analysis of RNA binding proteins

Eluted proteins from the RNA affinity-capture experiments were reduced, alkylated, and trypsinized in 100 mM ammonium bicarbonate as described previously (Sanders et al., 2002). The tryptic peptide fragments were desalted using a C-18 reverse-phase salt trap (Michrom) and were subjected to reverse-phase (RP) microcapillary LC-ESI-MS/MS. A fritless, microcapillary column (100 μm i.d.) was packed with 10 cm of 5 μm C_{18} reverse-phase material (Synergi 4u Hydro RP80a, Phenomenex). The trypsin-digested peptides were loaded onto the RP column equilibrated in buffer A (0.1% formic acid and 5% acetonitrile). The column was placed in-line with an LTQ linear ion trap mass spectrometer (Thermo Electron, Inc). Peptides were eluted using a 60 min linear gradient from 0 to 60% buffer B (0.1% formic acid, 80% acetonitrile) at a flow rate of 0.3 μl/min.

During the gradient, the eluted ions were analyzed by one full precursor MS scan (400-2000 *m/z*) followed by five MS/MS scans of the five most abundant ions detected in the precursor MS scan while operating under dynamic exclusion. The program extractms2 was used to generate the ASCII peak list and identify +1 or multiply charged precursor ions from the native mass spectrometry data file. Tandem spectra were searched with no protease specificity using SEQUEST-PVM (Sadygov et al., 2002) against the Refseq human protein database (released May 2005) containing 28,818 entries. For multiply charged precursor ions ($z \geq +2$), an independent search was performed on both the +2 and +3 mass of the parent ion. Data were processed and organized using the BIGCAT software analysis suite (Fleischer et al., 2006). A weighted scoring matrix was used to select the most likely charge state of multiply charged precursor ions (Fleischer et al., 2006; Link, 1999). From the database search, fully tryptic peptide sequences with Sequest cross-correlation scores ≥ 1.5 for +1 ions, ≥ 2 for +2 ions, and ≥ 2 for +3 ions were considered significant and used to create the list of identified proteins. To estimate the relative abundance of a protein from the mass spectrometry data, a protein abundance factor (PAF) was calculated for each identified protein (Fleischer et al., 2006; Powell et al., 2004). To calculate PAF values, the total number of non-redundant spectra that correlated significantly with each cognate protein was normalized to the molecular weight of the protein ($x10^4$) (Fleischer et al., 2006; Powell et al., 2004).

Mass spectrometry analysis of trypsinized proteins from SDS-PAGE gels

Protein bands corresponding to the predicted molecular weights of PCBP2 and ZNF9 were excised from silver-stained gels and sliced into 1 mM cubes. The gel pieces were dehydrated in acetonitrile and then rehydrated in 100 mM ammonium bicarbonate. After rehydration, the samples were brought to a 1:1 equal volume of ammonium bicarbonate and acetonitrile. Gel pieces were lyophilized to dryness. The samples were suspended in digestion buffer (50 mM ammonium bicarbonate, 0.5 mM $CaCl_2$, and 0.0125 μg/μl trypsin). The gel pieces remained in digestion buffer for 45 min on ice. Following incubation, 20 μl of additional digestion buffer without trypsin was added, and the gel pieces were incubated for 18 h at 37°C. Trypsinized peptides were extracted three times from the gel pieces with 50 μl washes of 25 mM ammonium bicarbonate and acetonitrile (1:1). The pooled supernatants were frozen and lyophilized. The dried peptides were resuspended in 10 μl of 0.1% formic acid and subjected to the LC-ESI-MS/MS analysis described above.

Sucrose gradient analysis of ZNF9

Sucrose gradient analysis was performed as described previously (Link et al., 2005).

Reporter assays and RNA-interference

To analyze the activity of the bicistronic reporter (Pyronnet et al., 2000), 293T cells were transfected with either 10 μg of the bicistronic reporter plus 10 μg pcDNA-ZNF9-V5 or 10μg of the bicistronic reporter plus 10 μg of pcDNA3.1/V5-His-TOPO/lacZ. Each transfection cocktail contained 60 μL of Lipofectamine 2000 (Invitrogen). All reporter assays were performed in triplicate. All transfections were performed in Optimem minimal medium as recommended by the manufacturer (Invitrogen). After 4 h of transfection, the Optimem medium was replaced with full medium containing serum. Cells were harvested 48 h after transfection and assayed for luciferase and chloramphenicol-acetyl-transferase (CAT) activity (Nordeen et al., 1987). Reporter assays employing RNA-interference were similar to the assays described above. On day 1, 293T cells were simultaneously transfected with 10 μg of the bicistronic reporter and 400 nM siRNAs specific for either laminA/C (Elbashir et al., 2001), ZNF9 (5'-GCUAUUCUUGUGGAGAAUU-3'), PCBP2 (5'-GCAUUCCACAAUCCAUCAUUU-3'), or a combination of ZNF9 and PCBP2 siRNAs using 60 μL of lipofectamine 2000. All siRNAs used in this study were purchased from Dharmacon Inc. siRNAs for PCBP2 targeted both isoforms detected in our mass spectrometry analysis. On day 2, 293T cells were re-transfected with 400 nM of the same siRNAs except that 60 μL of oligofectamine per transfection was used instead of the lipofectamine 2000. Twenty-four h after the second transfection, the cells were harvested and assayed for luciferase and CAT activity. Experiments were performed in triplicate. A Student's two-tailed t-

test was performed to test the statistical significance of the difference between the experimental and control results.

Electrophoretic mobility shift assays

EMSAs were performed essentially as described previously (Rychlik et al., 2003). We used oligoribonucleotides corresponding to the wild-type ODC IRES RNA sequence (5'-UUUCUGUCUUAUUGUUUC-3') and the mutant sequence (5'AAACUGUCUUAUUGAAAC3'). Briefly, 50 pmol of an oligonucleotide was end-labeled with 50 pmol of γ-ATP using T4 polynucleotide kinase. Two pmol of the radiolabeled oligonucleotide was incubated with 10 μg of human cell extract in the presence of binding buffer (20 mM HEPES (pH 7.9), 2 mM $MgCl_2$, 10% glycerol, 50 mM KCl, and 1 mM EDTA) at room temperature for 30 min. Supershifting experiments used either α-PCBP2 or control antibodies at 1 μg of polyclonal antibody per EMSA reaction. Following formation of RNP complexes, the EMSA reactions were electrophoresed on 6% native polyacrylamide gels at 145 V for 3 h. The gels were dried and exposed to autoradiographic film to visualize RNP complexes.

Immunoprecipitation-RT-PCR

293T cells were transfected with 5 μg of the bicistronic ODC IRES reporter or 5 μg of the reporter plus 5 μg of pcDNA-ZNF9-V5 using Lipofectamine 2000 (Invitrogen). Following transfection, cell extracts were prepared and

immunoprecipitated with either 10 μg of α-V5 antibody, 10 μg of α-PCBP2 antibody, or 10 μg of pre-immune serum as a negative control in the presence of 50 μL of protein G beads (Pierce). Immunoprecipitations (IPs) were performed at 4˚C for 30 min prior to washing with 100x bead volumes of 12 mM HEPES pH 8.0, 15 mM KCl, 0.25 mM dithiothreitol, 5 mM $MgCl_2$, 0.1 mM PMSF, 40 U of RNasin, and 10% glycerol. The IPs were subjected to RNA extraction and RT-PCR of mRNA. RNA extraction and cDNA synthesis were performed as described previously (Gerbasi et al., 2004). The sequences of the primers used to amplify the ODC IRES cDNA product were: 5'-TGAGGCATTTCAGTCAGTTG-3' (forward) and 5'-GGATGAGCATTCATCAGGC-3' (reverse). The sequences of the primers used to amplify the GAPDH product were: 5'-GGAGAAGGGTGTTAAGGTGG-3' (forward) and 5'-GATCTCATGGTTGTCCACG-3' (reverse). The sequences of the primers used to amplify the RPL32 product were: 5'-CCTTGTGAAGCCCAAGATC-3' (forward) and 5'-AATGTTGGGCATCAAGATCTG-3' (reverse). PCR was performed as described previously (Gerbasi et al., 2004). Samples were taken after 24 PCR cycles, electrophoresed on 6% native polyacrylamide gels, and stained with ethidium bromide.

Co-Immunoprecipitation analysis of PCBP2 and ZNF9-V5

2.5 X 10^8 293T cells were transfected with plasmid pcDNA-ZNF9-V5 or no plasmid (negative control) using lipofectamine 2000 (Invitrogen). Cells from either the ZNF9 or control transfections were lysed by bead-beating with 0.5 mm

glass beads in 1 mL of lysis buffer (12 mM HEPES in diethylpyrocarbonate-treated water pH 8.0, 15 mM KCl, 15 mM dithiothreitol, 5 mM $MgCl_2$, 10% glycerol, plus 1 Complete™ EDTA-free protease inhibitor (Roche)/50 mL). The supernatant from the cell extract was then removed from the glass beads into sterile microfuge tubes and centrifuged at 20,000x g for 15 min. Supernatants were transferred to new microfuge tubes and incubated with 10 μg of α-PCBP2 antibody and 50 μL protein G beads. The immunoprecipitations were then incubated with gentle agitation overnight at 4ºC. The precipitations were then washed with 100x column volumes of lysis buffer. The beads were then suspended in 50 μL of 2x Laemmli buffer, boiled for 2 min, subjected to SDS-PAGE, immunoblotted, and probed with α-V5 antibodies. Ten microliters of each extract was assayed for actin levels by immunoblotting to quantitate protein levels prior to immunoprecipitation of the samples.

RT-PCR of cells transfected with siRNAs

293T cells were transfected with siRNAs using previously described protocols (Elbashir et al., 2001). Individual samples of 293T cells were transfected with siRNAs specific to either lamin A/C, PCBP2, or ZNF9. Following transfection, RNA was extracted using TRI-REAGENT (MRC) as described by the manufacturer. cDNA products coding for GAPDH, PCBP2, or ZNF9 were amplified by RT-PCR as described previously (Gerbasi et al., 2004) and analyzed at cycle 24 by native gel electrophoresis and ethidium bromide staining. The sequences of the primers used to amplify the PCBP2 product were: 5'-

GCCTGCAGTTTTTGGCTTTC (forward) and 5'-TCACAAAGAAAAAGCTCCAGT-3' (reverse). The sequences of the primers used to amplify the ZNF9 product were: 5'-GGCAAGGACCCTCAAAATAAAC-3' (forward) and 5'-TGTAGCCTCAATTGTGCATTC (reverse). The primers used to amplify the GAPDH product were: 5'-GGAGAAGGGTGTTAAGGTGG-3' (forward) and 5'-GATCTCATGGTTGTCCACG-3' (reverse).

Results

The sequence of the ODC IRES is important for formation of RNPs and stimulation of translation

Mutation of a pyrimidine (PY) tract in the 5'UTR of the ODC mRNA has been shown to inhibit IRES activity (Pyronnet et al., 2000). We refer to this 18-base sequence in the ODC 5'UTR as the IRES regulatory element (RE). To analyze the effects on secondary structure caused by these mutations in the RE, we compared the wild-type and PY-mutated ODC IRES structures using an RNA folding algorithm (Brodskii et al., 1995; Brodsky et al., 1993). Although minor structural differences were predicted, the pyrimidine tract mutations are not expected to result in a complete restructuring of the ODC IRES. Because mutations in the pyrimidine tract are predicted to have only a minor effect on the structure of the ODC IRES RNA, we hypothesized that these mutations might directly disrupt protein-RNA interactions.

Figure 3-1

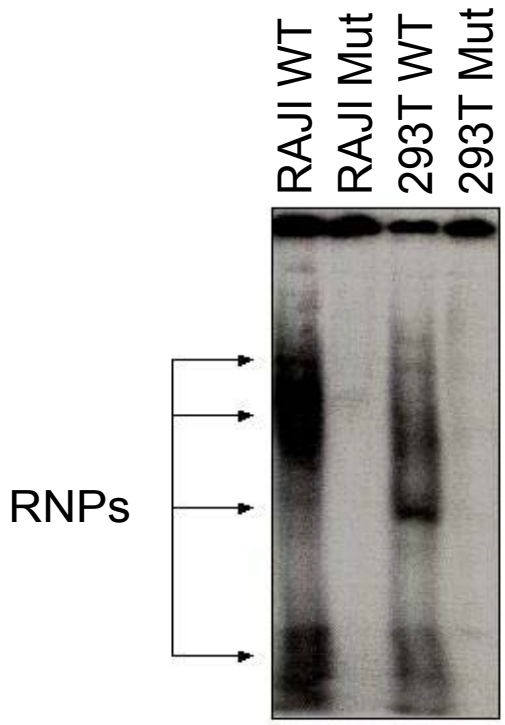

Figure 3-1: Wild-type, not mutant form, of the ODC IRES forms RNPs *in vitro*

Oligonucleotides containing sequence from either wild-type (WT) ODC IRES RNA or mutant (Mut) ODC IRES RNA were end-labeled with γ-ATP, incubated with extract from either RAJI lymphocytic B-cells or 293T cells, and electrophoresed on native polyacrylamide gels in an EMSA assay. Arrows point to RNP complex(s) that formed between the radiolabeled oligonucleotides and proteins in the RAJI and 293T cell lysates. The mutant ODC IRES has been shown to have repressed translational activity compared to the wild-type IRES (Pyronnet et al., 2000).

To test this hypothesis, we performed electrophoretic mobility shift assays (EMSAs) with human cell extracts and radiolabeled RNAs containing the wild-type or PY-mutant RE (Pyronnet et al., 2000). Interestingly, we found that the wild-type, but not the PY-mutant RE, formed RNP complexes in an EMSA (Figure 3-1). We conclude that an RNA-binding protein or a group of RNA-binding proteins associates with the ODC IRES RE and that this association requires the wild-type pyrimidine tract.

Figure 3-2

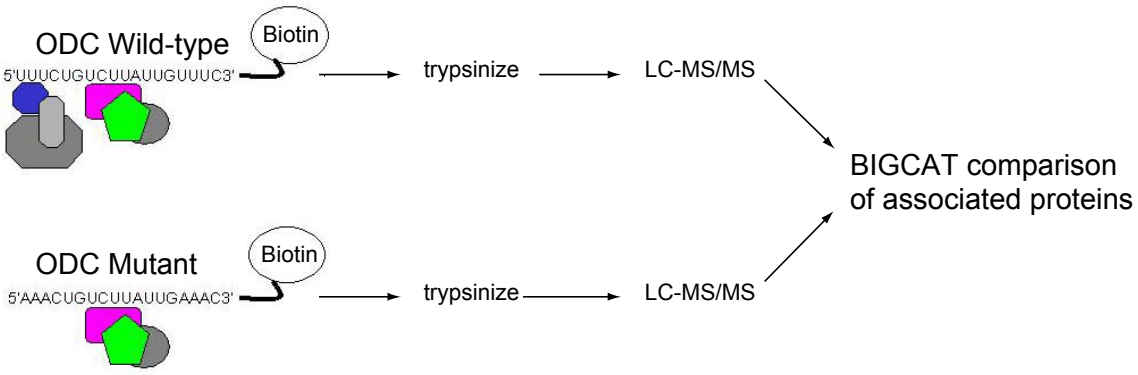

Figure 3-2: Schematic of proteomic screen for proteins associated with ODC wild-type (active) and a mutant IRES (repressed) element

Two separate RNA affinity chromatography samples were generated. In the top sample, the wild-type form of the ODC IRES RNA was used to affinity capture human RNA-binding proteins. In the bottom sample, a mutated version of the ODC IRES RNA was used in a control reaction. After isolation of proteins from the wild-type and mutant IRES affinity capture reactions, proteins were trypsinized, desalted, and analyzed by microcapillary LC-MS/MS mass spectrometry. Acquired tandem mass spectra were searched against the human proteome using the Sequest algorithm. Identified proteins bound to the wild-type and the mutant RNA affinity resin were then processed and compared using the BIGCAT software suite (McAfee et al., 2006).

The ODC IRES recruits specific RNA-binding proteins.

Since this ODC PY mutation reduced translation mediated by the IRES (Pyronnet et al., 2000) and reduced the ability of the RE to recruit RNA-binding proteins, we hypothesized that these RNA-binding proteins represent ITAFs that bind to and stimulate the ODC IRES. Using RNA affinity capture combined with LC-MS/MS mass spectrometry, we designed a proteomic screen to identify proteins from human cells that bind to the wild-type IRES RE, but not the mutant (Figure 3-2).

Figure 3-3

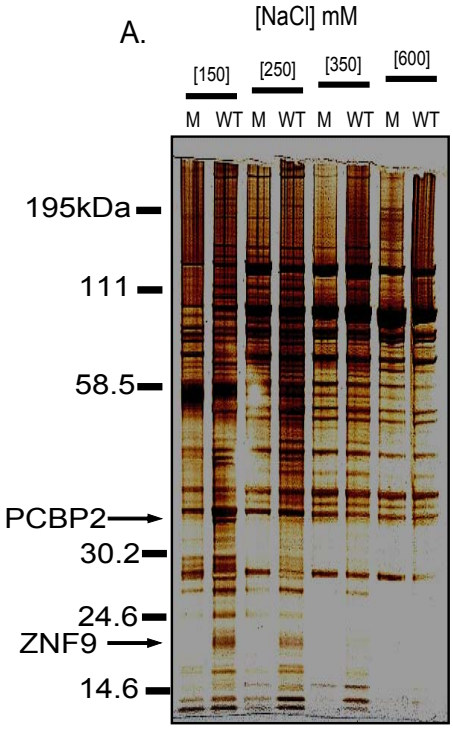

B.

Protein	Accession	MW (kDa)
ZNF9	NP_003409	19.5
PCBP2	NP_114366	38.2
LOC389395	XP_371824	12.8
PGD	NP_002622	53.1
TLX2	NP_001525	10.3
LSM8	NP_057284	10.4
U2AF2	NP_009210	53.5
FLJ10514	NP_060592	73.6
KRTHA3B	NP_002270	46.2
LOC392647	XP_374414	31.3

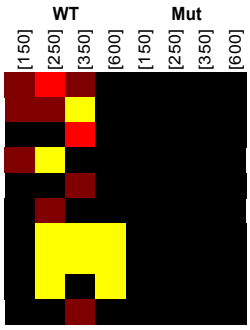

C.

Protein	Accession
ZNF9	NP_003409
PCBP2	NP_114366

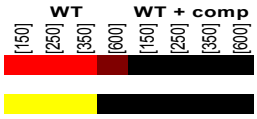

Figure 3-3: Proteomic identification of proteins associated with the ODC IRES RNA (A) Proteins bound to either the wild-type (WT) IRES or mutant (M) IRES RNA affinity capture reactions were eluted with 150, 250, 350, and 600 mM NaCl. Five μg of total protein from each salt fractionation was subjected to SDS-PAGE and detected by silver staining. The arrows point to gel bands that were in-gel digested and shown to contain spectra corresponding to PCBP2 and ZNF9, respectively **(B)** The heat map shows the ten most abundant proteins associated with the wild-type RNA affinity column that were not detected from the mutant RNA affinity column. Ten μg of protein from each salt fractionation in **(A)** was trypsinized, desalted, and analyzed by LC-MS/MS. The acquired tandem mass spectra were searched against a human protein database using the Sequest algorithm. Proteins identified from the wild-type (left side) and mutant (right side) RNA affinity capture reactions were displayed using BIGCAT's Clusterer visualization application (McAfee et al., 2006). Red indicates a protein with a high protein abundance factor (PAF) score (an estimate of the relative abundance of each protein in a given sample), yellow indicates proteins with an intermediate PAF score, and black indicates the protein was not detected (PAF=0). **(C)** The heat map shows that ZNF9 and PCBP2 were competed away from the wild-type affinity column with excess competitor oligonucleotide. Human cellular proteins were bound to two separate RNA affinity columns that contained the wild-type ODC IRES RNA sequence. One of the affinity columns was treated with wash buffer while the second column was treated with 60 nmol (a 2-fold excess to column) of non-biotinylated, (competitor) oligonucleotide identical in sequence to the wild-type ODC IRES RNA. Proteins bound to both columns were eluted with 150, 250, 350, and 600mM NaCl. Each protein fraction was analyzed as described in (B) to generate the heat maps of ZNF9 and PCBP2.

Affinity columns containing either the wild-type or mutant IRES RE RNA were used to capture proteins, and the proteins were then eluted with increasing concentrations of salt. We fractionated and detected the eluted proteins using SDS-PAGE and silver staining (Figure 3-3A). The gel revealed several proteins that were present in both the wild-type and mutant eluates. In contrast, the mutant IRES RE failed to form any RNP complexes in our EMSA analysis. We speculate that many of the proteins present in both the wild-type and mutant affinity eluates bind to the streptavidin resin non-specifically. Additionally, the buffering environment is more stringent in the EMSA analysis compared to the affinity purification. Thus the EMSA analysis reveals only high-affinity interactions. Of particular interest were several additional proteins that were eluted from the wild-type affinity column but were absent from the mutant column. We pursued these candidate proteins that bind to the wild-type IRES RE, but not the mutant.

To directly identify proteins that were associated with both the wild-type and mutant IRES RE, we performed LC-MS/MS mass spectrometry on both sets of chromatography elutions (Link, 1999). The mass spectrometry data were processed and analyzed using our bioinformatic graphical comparative analysis software tools (BIGCAT) (Fleischer et al., 2006) The mass spectrometry analysis identified 219 individual human proteins.

To estimate the relative abundance of each protein from the mass spectrometry data, we used a normalized label-free method of quantification (Fleischer et al., 2006; Powell et al., 2004). A protein abundance factor (PAF)

was calculated for each identified protein to quantify its relative amount in the samples. PAF values in our samples ranged from 0 to 4.64. A PAF value of zero indicated that the protein was not identified in the sample.

We were specifically interested in those proteins that eluted preferentially from the wild-type RNA-affinity column (Figure 3-3B). The proteins ZNF9 and PCBP2 scored the highest PAF values among those proteins that bound to the wild-type IRES RE but not to the mutant. From the LC-MS/MS analysis, multiple, independent peptides ($n \geq 3$) were identified for both ZNF9 and PCBP2, strongly supporting these identifications. Although two protein isoforms of PCBP2 are predicted from alternative splicing of the cognate gene (Leffers et al., 1995), our LC-MS/MS analysis could not distinguish between the isoforms. Among all the proteins that associated with the wild-type but not the mutant IRES, ZNF9 had the highest PAF value (0.899 in the wild-type samples and 0 in the mutant samples). PCBP2 had PAF values of 0.523 in the wild-type samples and 0 in the mutant samples.

The LC MS-MS identifications of ZNF9 and PCBP2 are supported by the PAGE analysis of the same affinity purifications. Figure 3-3A shows silver-stained bands corresponding to the predicted mobilities of PCBP2 and ZNF9 in the proteins eluted from the wild-type IRES RE but not the mutant. In-gel digestion and LC-MS/MS analysis of these gel regions confirmed the bands as PCBP2 and ZNF9 respectively.

We next tested whether the ZNF9 and PCBP2 proteins could be competed away from the ODC IRES RE. A two-fold molar excess of non-

biotinylated wild-type ODC IRES RE RNA released a number of RNA-binding proteins from the wild-type RE affinity column. Importantly, both ZNF9 and PCBP2 were successfully competed away from the affinity column by the non-biotinylated oligonucleotide (Figure 3-3C). Therefore, both ZNF9 and PCBP2 were bound to the ODC wild-type IRES RE RNA.

Figure 3-4

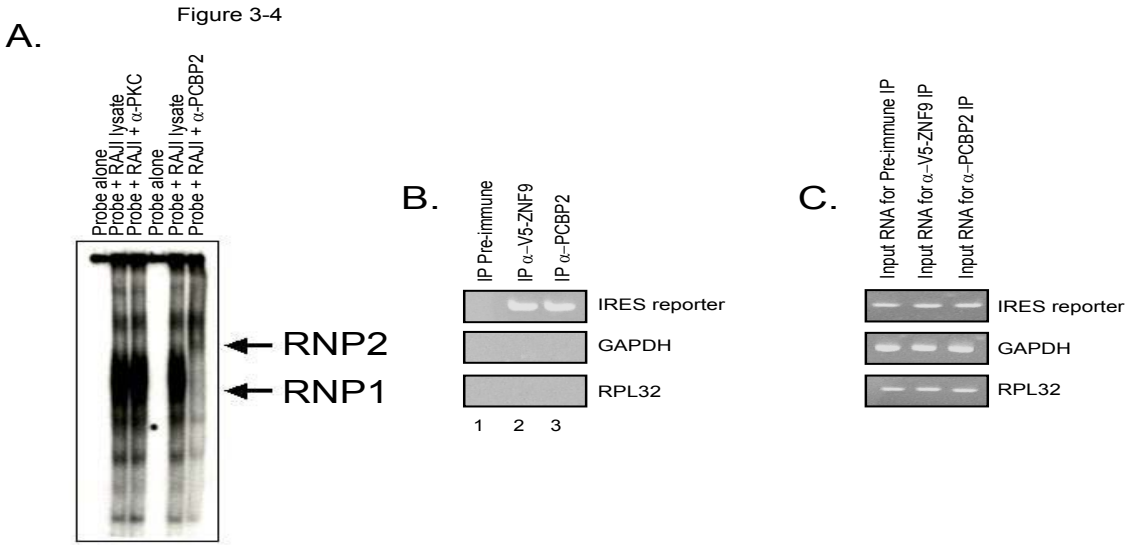

Figure 3-4: Biochemical analysis of interactions with the ODC IRES and binding proteins

(A) Radiolabeled oligonucleotide probes containing the wild-type ODC IRES RNA sequence were incubated with either depC-treated water (probe alone), human RAJI lymphocyte lysate, RAJI lysate and α-PKC antibodies, or RAJI lysate and α-PCBP2 antibodies. EMSA analysis was performed on all the reactions. Arrows point to the RNPs formed between RAJI lysate proteins and the oligonucleotide probe. Arrows pointing to RNP1 indicate the primary RNP formed between RAJI extracts and wild-type ODC IRES RNA. Arrows pointing to RNP2 indicate a second minor RNP that had a slower electrophoretic mobility (supershift) and specifically formed when α-PCBP2 antibodies were added to the EMSA reaction. **(B)** 293T cells were transfected with the ODC bicistronic reporter (lanes1 and 3), or the bicistronic reporter and pcDNA-ZNF9-V5 (lane 2). Cell extracts were immunoprecipitated with either pre-immune (lane 1), α-V5 (lane 2), or α-PCBP2 (lane 3) antibodies and analyzed for the presence of ODC IRES reporter, GAPDH, and RPL32 mRNAs by RT-PCR. **(C)** Ten-percent of the total extract mRNA in (B) was analyzed for the presence of ODC IRES reporter, GAPDH, and RPL32 mRNAs by RT-PCR.

PCBP2 and ZNF9 bind the ODC IRES.

We next used independent methods to validate the interactions of ZNF9 and PCBP2 with the ODC IRES RE. We used extracts from a human B-cell line for RNA EMSAs. Again, we found that the radiolabeled ODC IRES RE formed RNP complexes. Addition of α-PCBP2 polyclonal antibodies resulted in disruption of the primary RNP, and formation of a slightly larger supershifted RNP (Figure 3-4A). Only a fraction of the IRES-protein complexes were supershifted. We speculate that the α-PCBP2 antibodies mostly disrupt the interaction between the IRES RE and PCBP2. Similar results have been observed in other studies when antibodies were added to EMSA reactions (Lassar et al., 1991). Because the reduced electrophoretic mobility of the supershifted RNP was relatively small, we speculate that antibodies raised against PCBP2 are disrupting other interactions within the RNP. In a control reaction, an α-Protein Kinase C antibody did not produce a supershifted RNP (Figure 3-4A). These data, together with our proteomic analysis of ODC IRES binding proteins, support our conclusion that PCBP2 is a bonafide ODC IRES binding protein.

Because we failed to detect supershifted RNP complexes in EMSA experiments using ZNF9-V5 and α-V5 antibody (data not shown), we used immunoprecipitations and RT-PCR to validate biochemical interactions between ZNF9 or PCBP2 and the ODC IRES. First, ZNF9-V5 was immunoprecipitated from 293T cells expressing a bicistronic reporter mRNA containing the entire ODC IRES (5'UTR) (Pyronnet et al., 1996). RNA was extracted from the

precipitates, and the samples were analyzed by RT-PCR for the presence of the ODC IRES and mRNAs for GAPDH and RPL32 (controls). GAPDH is a highly abundant mRNA that is translated in a cap-dependent fashion, and the RPL32 mRNA contains a 5' terminal oligopyrimidine tract (TOP) (46). We identified the ODC IRES in the samples immunoprecipitated with an α-V5 antibody (Figure 3-4B). Using the α-PCBP2 antibodies, we found the ODC mRNA also co-immunoprecipitated with PCBP2 (Figure 3-4B). RT-PCR did not detect GAPDH and RPL32 in the precipitated samples (Figure 3-4B). Specificity of the interactions was demonstrated by the absence of the ODC IRES RT-PCR product in extracts immunoprecipitated using nonspecific polyclonal antibodies (Figure 3-4B). A loading control showed that all samples contained similar levels of the ODC IRES reporter, GAPDH, and RPL32 mRNAs prior to immunoprecipitation (Figure 3-4C). In combination, these experiments confirm that ZNF9 and PCBP2 specifically bind the ODC IRES.

Figure 3-5

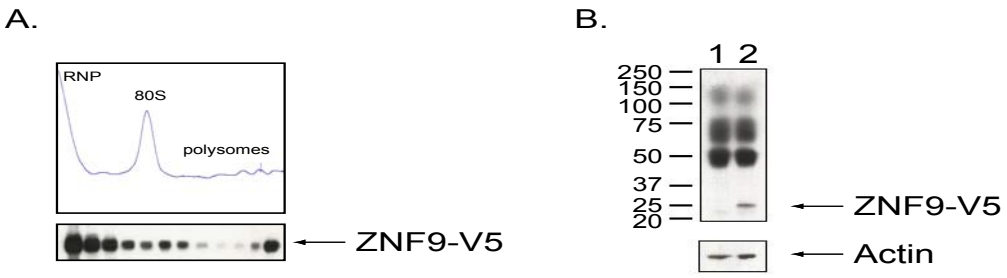

Figure 3-5: ZNF9 associates with ribosome-containing portions of a sucrose gradient and co-purifies with the ITAF PCBP2

(A) 293T cells were transfected with plasmids pcDNA-ZNF9-V5. Transfected cell extracts were fractionated over 7-47% sucrose gradients as previously described (Link et al., 2005). The UV-trace from the sucrose gradient shows the position of free ribonucleoproteins (RNP), 80S (monosomes), and polysomes (polyribosomes). Twelve fractions from the sucrose gradient were subjected to SDS-PAGE, immunoblotted, and probed for the V5 epitope (ZNF9). **(B)** 293T cells were either mock transfected with either no plasmid (lane 1), or transfected with plasmid pcDNA-ZNF9-V5 (lane 2). Extracts from both samples were immunoprecipitated with α-PCBP2 antibodies. Following immunoprecipitation, both samples were subjected to SDS-PAGE, immunoblotted, and probed with an antibody against the V5 epitope. Immunoreactivity above the 50KDa marker represents non-specific background proteins detected in both samples. As a loading control, extracts from both samples were probed for actin levels by immunoblotting prior to immunoprecipitation.

ZNF9 copurifies with the ITAF PCBP2 and partially co-localizes with the ribosomal density

PCBP2 has previously been shown to bind to and regulate the activity of cellular and viral IRESs (Blyn et al., 1996; Blyn et al., 1997; Evans et al., 2003; Gamarnik and Andino, 1997). Our results suggested that PCBP2 as well as ZNF9 are part of an ITAF complex that binds to the ODC IRES. We hypothesized that if ZNF9 is a cellular IRES-associated protein and functions in cap-independent translation, then ZNF9 should associate with mRNAs that are actively being translated. To test this model, we used sucrose gradient ultracentrifugation to separate particles containing the different ribosomal subunits and performed immunoblot analysis to identify ZNF9. Fractions from cells transfected with pcDNA-ZNF9-V5 were analyzed. We found that the ZNF9 protein partially co-localizes with the ribosome-and polysome-containing portion of the sucrose density gradient (Figure 3-5A). These data suggest that ZNF9 associates with both actively translating and ribosome-free mRNAs.

We also tested whether PCBP2 and ZNF9 copurify biochemically. By co-immunoprecipitation analysis, we found that PCBP2 and ZNF9 are biochemically associated (Figure 3-5B). Because PCBP2 is often associated with larger ITAF assemblies, we hypothesize that ZNF9 might also function as a novel component of ITAF complexes.

Figure 3-6

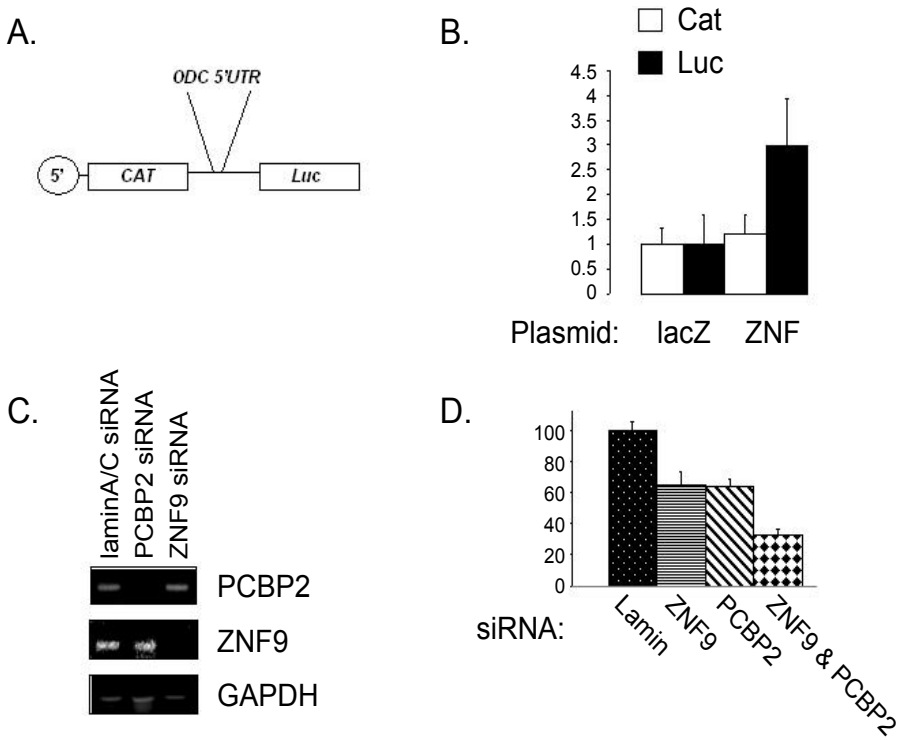

Figure 3-6: ZNF9 and PCBP2 enhance the translation of the ODC IRES

(A) Experiments utilized this bicistronic reporter construct for experimental results shown in (B) and (C) (Pyronnet et al., 2000). **(B)** 293T cells were co-transfected with a plasmid expressing the bicistronic reporter and either pcDNA3.1/V5-His-TOPO/lacZ or pcDNA-ZNF9-V5 expression plasmids. Following transfection, cells were lysed and assayed separately for luciferase and chloramphenicol-acetyl-transferase (CAT) activity. The white bars indicate CAT (cap-dependent) activity for cells that were co-transfected with the bicistronic reporter and either pcDNA3.1/V5-His-TOPO/lacZ (negative control) or pcDNA-ZNF9-V5. The black bars show the detected luciferase activity of cells transfected with the indicate regiment. Values on the y-axis indicate the fold difference in activity between cells transfected with pcDNA3.1/V5-His-TOPO/lacZ and cells transfected with pcDNA-ZNF9-V5. The activity of CAT and Luciferase for samples transfected with pcDNA3.1/V5-His-TOPO/lacZ was set to one. Error bars indicate the standard deviation. **(C)** RT-PCR showing the effectiveness of PCBP2 and ZNF9 siRNAs repressing expression of the endogenous mRNA levels. 293T cells were transfected with either lamin A/C, ZNF9, or PCBP2 siRNAs. Following transfection, RNA was isolated from cells with TRI-REAGENT, and RT-PCR was performed on each individual sample to amplify either GAPDH, ZNF9, or PCBP2 products. **(D)** 293T cells were co-transfected with the bicistronic reporter and lamin A/C, ZNF9, PCBP2, or PCBP2 and ZNF9 siRNAs combined. After co-transfection, cells were lysed and assayed separately for luciferase and CAT activity. IRES activity is calculated as a ratio of luciferase to CAT activity. The graph shows the % ODC IRES activity in each sample relative to samples transfected with lamin A/C control siRNAs. Error bars indicate the standard deviation.

The function of PCBP2 and ZNF9 in ODC IRES translation

ITAF proteins that bind to viral and cellular IRESs also enhance IRES activity (Blyn et al., 1997; Gamarnik and Andino, 1997; Gamarnik and Andino, 2000; Holcik and Korneluk, 2000; Hunt et al., 1999; Mitchell et al., 2001; Mitchell et al., 2005; Walter et al., 1999). Our data strongly suggested that PCBP2 and ZNF9 function as ITAFs of the ODC IRES. To test this hypothesis, we used a bicistronic reporter driven by the wild-type ODC IRES (Pyronnet et al., 2000) to determine whether ZNF9 plays a role in translation mediated by the ODC IRES (Figure 3-6). We overexpressed ZNF9 in 293T cells using plasmid pcDNA-ZNF9-V5 and found that overexpression of ZNF9 enhanced the activity of the ODC IRES 3-fold in comparison to controls (p value=0.013) (Figure 3-6B).

In a second set of experiments, we analyzed the function of endogenous ZNF9 and PCBP2 in the translation of the ODC IRES by transfecting cells with siRNAs targeting PCBP2 and ZNF9. In control experiments to test the effectiveness of the siRNAs, we found that siRNAs directed against PCBP2 and ZNF9 were effective at specifically reducing the PCBP2 and ZNF9 transcript levels (Figure 3-6C). These siRNAs also reduced expression of the ODC IRES reporter by 30% in comparison to control siRNAs (p value=0.043 for ZNF9 siRNAs and p value=0.020 for PCBP2 siRNAs) (Figure 3-6D). To determine whether PCBP2 and ZNF9 had an additive effect on ODC IRES activity, we transfected cells with a combination of both PCBP2 and ZNF9 siRNAs. The combination of PCBP2 and ZNF9 siRNAs reduced ODC IRES activity approximately 75% (p value= 0.001) (Figure 3-6D). Collectively, these data

suggest that PCBP2 and ZNF9 function as enhancers of the ODC IRES. These results provide evidence that ZNF9 functions as a novel component of a cellular ITAF complex.

Discussion

Previous studies of the ODC 5'UTR have led to the identification of an RNA element that is necessary for IRES activity (Pyronnet et al., 2000; Pyronnet et al., 2005). We performed a proteomic screen for proteins that bind to this regulatory element. We found that two nucleic acid-binding proteins PCBP2 and ZNF9 bind to this region of the ODC IRES. Additionally, we found that both PCBP2 and ZNF9 enhance the activity of the ODC IRES. Our results suggest that PCBP2 and ZNF9 function as IRES *trans*-acting factors. Importantly, these data show that the myotonic dystrophy type-2 protein ZNF9 can function as an IRES *trans*-acting factor.

Proteins that associate with the ODC IRES

The purpose of our proteomic screen was to identify proteins that specifically bind to the wild-type ODC IRES sequence element, but not a mutant IRES sequence. While PCBP2 and ZNF9 specifically bind the active form of the IRES RNA element, our mass spectrometry approach also identified proteins that are associated with both wild-type and mutant IRES sequences. Many of the apparently non-specific cellular proteins were detected from both affinity

columns. These proteins likely represent background binding to the streptavidin beads. Some of the proteins from both the wild-type and mutant RNA affinity columns are previously described RNA-binding proteins that may be involved in ITAF activity. Two of the proteins UNR and PTB have been shown to be ITAFs (Hunt et al., 1999; Mitchell et al., 2001). Therefore, it is possible that additional ITAFs interact with the ODC IRES element independently of the PY-tract by binding to the RNA sequence that is shared by both the wild-type and mutant ODC IRES (Pyronnet et al., 2000). We speculate that a combination of proteins including PCBP2, ZNF9, PTB, and UNR might function as a holo-ITAF complex to stimulate ODC IRES activity. Similar models of multiprotein ITAF complexes that assemble on IRESs have been described in other studies (Evans et al., 2003; Hunt et al., 1999; Mitchell et al., 2001).

PCBP2 and ZNF9 function as ODC ITAFs

Our proteomic screen revealed that PCBP2 and ZNF9 bind to the active form of the ODC IRES RE but not an inactive form. Because we were able to detect an interaction of ZNF9 with the ODC IRES by mass spectrometry and IP-RT-PCR approaches but not by EMSA, we speculate that ZNF9 might partially associate with the ODC IRES through protein-protein interactions. Because we observe co-immunoprecipitation between PCBP2 and ZNF9, it is possible that ZNF9 binds the ODC IRES through interactions with PCBP2.

To dissect the function of these two proteins in the translation of the ODC IRES, we utilized both overexpression and RNA-interference approaches.

Overexpression of ZNF9 in 293T cells enhanced the activity of the ODC IRES. Disruption of endogenous levels of ZNF9 and PCBP2 by RNA-interference also supported a role for these two proteins in enhancing the activity of the ODC IRES. Because the dual RNA-interference of PCBP2 and ZNF9 had an additive, but not a synergistic affect on ODC IRES activity, it is possible that ZNF9 and PCBP2 play redundant roles in ODC IRES translation. In contrast, the observation that PCBP2 and ZNF9 interact biochemically, and bind to and enhance the activity of the ODC IRES suggests that these two proteins function as part of a cellular ITAF complex.

Potential role of ZNF9 as an ITAF in type-2 myotonic dystrophy

Myotonic dystrophy is the most common adult form of muscular dystrophy. The disease effects approximately 1 in every 8,000 individuals (Cho and Tapscott, 2006). There are two types of myotonic dystrophy. Patients afflicted with either type 1 or 2 muscular dystrophy express symptoms that include myotonia, muscle weakness, cataracts, testicular atrophy, and defects in cardiac conduction (Cho and Tapscott, 2006). Both type 1 and type 2 myotonic dystrophy present strikingly similar symptoms in adults. However, type 1 myotonic dystrophy presents a congenital form, whereas type 2 does not. Type 1 myotonic dystrophy results from CTG expansions in the 3'UTR of DMPK, a gene that encodes a serine/threonine kinase (Brook et al., 1992). Type 2 myotonic dystrophy, is caused by tetranucleotide (CCTG) repeat expansions in the first intron of the ZNF9 gene (Liquori et al., 2001).

It is possible that these mutations in the ZNF9 gene cause changes in translation of mRNA's containing IRESs. However, the favored model of the CCTG expansions in type 2 myotonic dystrophy is that the long CCUG repeats in the ZNF9 RNA sequester essential cellular ribonucleoproteins (Kanadia et al., 2003; Kanadia et al., 2006). Sequestration of these RNPs is believed to disrupt an essential cellular process, such as RNA processing, leading to the disease symptoms.

We show that ZNF9 functions as an ITAF. Because it is possible that ZNF9 activates many unidentified cellular IRESs, disruption of ZNF9 function through genetic mutations should result in an abnormal profile of cellular proteins. Modifying specific cellular protein levels through a gain or loss of ZNF9 function might contribute to the pathogenesis of type 2 myotonic dystrophy. Identification of such changes in protein levels will lead to a better understanding of the targets of ZNF9 action.

Acknowledgements

We would like to thank Nahum Sonenberg and Raul Andino for sharing reagents. We would like to thank Jill McAfee, Dexter Duncan, and Jennifer Jennings for technical assistance. We would also like to thank Tracey Fleischer and Elizabeth Link for editorial assistance. This project was supported by NIH grant GM64779. V.R.G. was supported by NIH training grant T32 CA009385 and GM64779. A.J.L

was supported by NIH grants GM64779, HL68744, ES11993, and CA098131. In addition, A.J.L. was funded in part with Federal funds from the National Institute of Allergy and Infectious Diseases, National Institutes of Health, Department of Health and Human Services, under Contract No. HHSN266200400079C/N01-AI-40079.

CHAPTER V

SUMMARY AND CONCLUSIONS

This dissertation investigated several distinct and novel biological phenomena. The significance of each of these topics in biology will be discussed below. Additionally, I will discuss future lines of inquiry that other scientists may pursue based on this work. The discussion and summary section is broken into two parts. One part discusses the novel core ribosomal protein Asc1p. The second part discusses the discovery of internal ribosomal entry site *trans*-acting factors.

Part I: RACK1/Asc1p: a new subunit of the eukaryotic 40S

Link and Yates found that RACK1 was strongly associated with the ribosome and might actually be a core component of the 40S (Link et al., 1999). However, the association of RACK1 with the ribosome did not necessarily dictate that RACK1 was a core subunit of the ribosome. With Dr. Link's guidance, I performed an extensive series of molecular biology experiments and eventually concluded that RACK1 and Asc1p are indeed part of the core of the eukaryotic 40S. Later, Joachim Frank's structural biology group used cryo-electron-microscopy to confirm that Asc1p constituted a portion of the 40S mRNA exit channel (Sengupta et al., 2004). Therefore, our studies and those of Joachim Frank's group leave little doubt that RACK1/Asc1p is a core component of the

ribosome (Gerbasi et al., 2004; Sengupta et al., 2004). It should also be noted that the National Center for Biotechnology Information considers the function of RACK1 to be ribosomal in nature. Likewise, the *Saccharomyces* Genome Database lists Asc1p as a core component of the 40S subunit.

Cryo-EM analysis of bacterial, yeast, and human ribosomes has shown the differences and similarities in small subunit structure throughout evolution (Spahn et al., 2004). The most striking difference between the eukaryotic and prokaryotic small subunits is a large density near the mRNA exit channel. Because ribosomes deficient in Asc1p/RACK1 are lacking a majority of this density that is specific to the eukaryotic ribosome, Asc1p most likely evolved to perform a function that is specific to eukaryotes. Below, I will discuss the proposed functions of *ASC1* based on work performed in this dissertation.

The Role of RACK1 in Protein Synthesis

Many of the genes that encode ribosomal proteins are duplicated in eukaryotic genomes. Therefore, disruption of ribosomal gene function using homologous recombination often has no effect on translation. Yeast contains a single copy of the *ASC1* gene. I analyzed the function of Asc1p in translation using a yeast strain that had been disrupted by homologous recombination. Disruption of *ASC1* did not kill the yeast or result in a slow growth phenotype at 30°C (Gerbasi et al., 2004; Giaever et al., 2002). Disruption of genes performing critical functions in translational initiation is usually lethal in yeast (Giaever et al., 2002). This result would suggest that the Asc1p protein was not involved in

enhancing the process of translation. Instead, this growth phenotype suggested that *ASC1* was either not necessary for translation, effected the translation of only a small subset of genes, or was functioning as a suppressor of translation.

To dissect the function of *ASC1* in the translation process, I performed *in vitro* translation assays. To my surprise, I found that the Asc1p deficient ribosomes had higher translational activity (Gerbasi et al., 2004). As an additional assay to test the function of *ASC1 in vivo*, we analyzed yeast protein levels using 2D-difference in gel electrophoresis (2D-DIGE) (Gerbasi et al., 2004). The results of our 2D-DIGE analysis showed that *asc1*-deficient yeast had elevated protein levels relative to wild-type (Gerbasi et al., 2004). Additionally, complementation of the *asc1*-deficient yeast with *ASC1* on a low-copy yeast expression plasmid restored protein levels back to the wild-type state. Finally, complementation of the *asc1*-deficient yeast with mammalian RACK1 also restored protein levels back to the wild-type state. Collectively, the *in vitro* and *in vivo* experiments strongly suggested that RACK1 was a core ribosomal subunit that played a role in repressing the translation of a subset of mRNAs (Gerbasi et al., 2004).

Possible mechanisms of Asc1p mediated translational repression

Disruption of *ASC1* from yeast cells resulted in an up-regulation of protein levels for a subset of proteins. This was a surprising result because disruption of a core ribosomal subunit would be expected to modify the natural structure of the ribosome and possibly inhibit translational activity.

Translational control of core ribosomal subunits in prokaryotes is achieved through an auto-regulatory mechanism (Baughman and Nomura, 1983; Baughman and Nomura, 1984). When the synthesis of ribosomal proteins exceeds the synthesis of ribosomal RNA, core ribosomal subunits do not associate with the ribosome. As a mechanism to ensure that subunits are not synthesized in the absence of ribosomal RNA, free ribosomal proteins will repress the translation of their cognate mRNAs (Baughman and Nomura, 1983; Baughman and Nomura, 1984). Therefore, free ribosomal proteins can function as a repressor to inhibit the translation of their own mRNAs. Because core ribosomal proteins bind to specific RNA sequences and structures on the ribosomal RNA, it is possible that free core ribosome subunits might bind to other mRNAs that resemble ribosomal RNA sequences and structures. Therefore, it is possible that core ribosomal proteins function as *trans*-acting factors to repress the translation of mRNAs that do not code for ribosomal proteins.

In response to long term interferon gamma treatment, core subunits of the human ribosome dissociate and function as translational repressors (Mazumder et al., 2003; Sampath et al., 2004). Specifically, the ribosomal protein RPL13 has been shown to dissociate from the 60S subunit upon IFNγ treatment of cells (Mazumder et al., 2003). When RPL13 dissociates, it forms a new multi-protein component RNP complex (Sampath et al., 2004). This RNP complex is referred to as the interferon gamma inducible translational repressor complex (GAIT) (Sampath et al., 2003). The GAIT complex binds to RNA elements that exist in the 3'UTR of specific mRNAs. Examples of these mRNAs include the copper-

binding protein ceruloplasmin and the growth factor VEGF. Therefore, in both prokaryotes and higher eukaryotes there are examples of core ribosomal proteins functioning as repressors of translational activity.

Our studies suggested that *ASC1* played a repressive role in the translation of a specific subset of mRNAs. Our 2D-DIGE data suggested that *ASC1* suppressed the translation of a subset of mRNAs, and not the entire set of mRNAs expressed by the cell. This form of translational repression is consistent with past examples (Mazumder et al., 2003; Sampath et al., 2004). All examples of core ribosomal proteins functioning as repressors of mRNA translation require that the protein dissociate from the ribosome. Therefore, it is possible that Asc1p achieves translational repression by dissociating from the core 40S subunit. In this model, once Asc1p dissociates from the 40S it would have to bind to mRNAs and repress their translation.

It is conceivable that a ribosomal protein could function as a scaffold for proteins that repress translation. This may be the case for Asc1p because yeast that are null for *asc1* fail to recruit the translational regulatory protein Scp160 to ribosomes (Baum et al., 2004). Although this is just one example of a protein that is recruited to the 40S through Asc1p, it is possible that other unidentified proteins utilize Asc1p to associate with the ribosome. Therefore, it is possible that Asc1p functions as a scaffold for additional translational regulatory proteins.

Future Experiments to Discriminate Between Models of *ASC1*-mediated Translational Repression

When we perform sucrose gradient ultracentrifugation experiments, we find that Asc1p is exclusively associated with the ribosomal density. Therefore, if Asc1p is functioning as a translational repressor that is free of the ribosome, a relatively minor portion of the cellular Asc1p exists in the free-state. In order to discover mRNAs that associate with this small population of ribosome-free Asc1p, it will be necessary to concentrate free Asc1p from sucrose gradients. Immunoprecipitation of ribosome-free Asc1p followed by microarray analysis would potentially identify mRNAs associated with ribosome-free Asc1p. Follow-up experiments performed *in vitro* and *in vivo* should be designed to test the ability of Asc1p to repress the translation of the candidate target mRNAs.

If Asc1p is not functioning as a translational repressor in the ribosome-free state, it is possible that Asc1p is functions as a scaffolding protein for translational repressors as described above. To test this model, a comparative mass spectrometry based approach would be most useful. Specifically, the ribosome-associated proteins of *asc1*-deficient yeast should be analyzed using MUDPIT technology. As a comparative control, the ribosome-associated proteins of wild-type yeast should also be analyzed. Comparing the ribosome-associated proteins of wild-type and *asc1*-deficient yeast will result in the identification of any potential proteins that require the presence of Asc1p to associate with the 40S. Therefore, these proposed experiments are likely to provide further insight into the function of *ASC1* in translational repression.

Ssb1/2p and HSP70 chaperones in ribosome biogenesis and stability

Proteomic analysis of Asc1p-deficient ribosomes revealed an enrichment of the HSP70 chaperone protein Ssb1/2p. Ssb1/2p is one of a family of chaperone proteins that are referred to as chaperones linked to proteins synthesis (CLIPS) (Albanese et al., 2006). The function of CLIPS proteins are poorly understood. However, the common feature of CLIPS is their shared biochemical association with the ribosome (Albanese et al., 2006). There are two predominant theories to explain their association with the ribosome. First, that nascent polypeptides emerge from ribosomes dictates that chaperones must associate with the ribosome to fold these recently synthesized proteins. As such, it is postulated that CLIPS bind to the ribosome to fold nascent polypeptides. This function for CLIPS is supported experimentally because puromycin, a drug that prematurely terminates polypeptide chain elongation partially dissociates CLIPS from ribosomes (Nelson et al., 1992; Pfund et al., 1998).

As a second possibility, CLIPS might function to stabilize the structure of the ribosome (Nelson et al., 1992; Pfund et al., 1998; Woolford, 2002). Indeed, chaperones bind to multi-protein complexes to stabilize interactions between proteins and block the formation of non-productive interactions (Bukau and Horwich, 1998). Therefore, CLIPS chaperones, which include Ssb1/2p, most likely function to stabilize ribosome structure, fold nascent polypeptides, or both. The function of Ssb1/2p in chaperoning ribosome structure is supported experimentally because yeast deficient in SSB1/2 have disrupted polyribosomes

(Nelson et al., 1992). Additionally, another member of the HSP chaperone family chaperones yeast ribosome biogenesis (Meyer et al., 2007).

Discoveries made in this dissertation showed that Asc1p-deficient ribosomes are enriched in Ssb1/2p relative to wild-type or complemented ribosomes. Because Asc1p-deficient ribosomes represent an abundant, non-native multi-protein complex, it is possible that Ssb1/2p blocks unproductive interactions with this mutant 40S (Bukau and Horwich, 1998). Past studies have shown that Ssb1/2p binds to the ribosome in a conformation-dependent manner (Pfund et al., 1998). Therefore, results shown in this dissertation and elsewhere suggest that Ssb1/2p might function to stabilize ribosome structure.

ASC1 function in ribosome biogenesis

Proteomic analysis of Asc1p-deficient ribosomes revealed an enrichment of the HSP70 chaperone protein Ssb1/2p. The discovery that Asc1p-deficient ribosomes were enriched in Ssb1/2p led to the hypothesis that these mutant ribosomes might be unstable. Indeed, shifting *asc1*-deficient yeast to elevated growth temperatures disrupted ribosomes. Additional experiments showed that elevated temperatures disrupted nascent ribosome structure, but not pre-existing ribosomes. Therefore, *ASC1* facilitates ribosome biogenesis.

Eukaryotic ribosome biogenesis is a compartmentalized, multi-step process. The process requires over 100 different non-ribosomal proteins referred to as ribosome biogenesis *trans*-acting factors (Kressler et al., 1999; Warner, 2001; Woolford, 2002). Additionally, most of the core 40S ribosomal

proteins, with the exception of RPS22 and RPS29, have roles in yeast ribosome biogenesis(Ferreira-Cerca et al., 2005). Because *ASC1* facilitates ribosome biogenesis at elevated temperatures, Asc1p may have evolved to chaperone ribosome formation through stressful conditions.

Potential Mechanistic Roles of *ASC1* in Ribosome Biogenesis

Asc1p could facilitate nascent ribosome structure through several different mechanisms. Because *asc1*-deficient yeast lose nascent ribosomes at elevated temperatures, it is possible that *ASC1* evolved as part of the heat-shock response. During heat shock, Asc1p might function either directly or indirectly to chaperone ribosome formation at elevated temperatures. Because Asc1p lacks heat-shock-protein-related functional domains, it is unlikely that Asc1p performs an HSP-chaperone related function. Instead, the WD-repeat domains shared by Asc1p with other proteins have been primarily implicated in scaffolding protein-protein interactions. Therefore, it is possible that Asc1p scaffolds the association of chaperone-like protein(s) to the ribosome during biogenesis. Loss of this Asc1p-chaperone interaction may lead to the inability to repair ribosomes at elevated temperatures.

During eukaryotic ribosome biogenesis, a majority of ribosomal RNA processing occurs in the nucleolus (Kressler et al., 1999; Warner, 2001). However, the 18S rRNA (which is incorporated into the 40S subunit) is partially processed in the cytoplasm (Kressler et al., 1999; Warner, 2001). Specifically, the small subunit transports a 20S rRNA species from the nucleolus to the

cytoplasm where the 20S is subsequently cleaved into an 18S mature rRNA (Jakovljevic et al., 2004). Several mutants have been isolated that fail to convert the 20S into 18S rRNA (Ferreira-Cerca et al., 2005; Jakovljevic et al., 2004). These mutants often fail to export the developing 40S subunit from the nucleolus to the cytoplasm for completion of small subunit biogenesis (Ferreira-Cerca et al., 2005). Therefore, 40S transport out of the nucleolus is a critical step in the biogenesis of small subunits. It is possible that part of the ribosome-export sequence requires the chaperoning or scaffolding function of Asc1p at elevated temperatures.

Proposed Experiments to Identify the Mechanistic Role of *ASC1* in Ribosome Biogenesis

Ribosome biogenesis requires the step-wise processing of a single 35S precursor ribosomal RNA (Kressler et al., 1999). This ribosomal RNA is processed into 33S, 32S, 27S, 25.5S, 25S, 20S, and 5.8S rRNAs in the nucleolus (Warner, 2001). Because the ribosomal RNAs represent some of the most abundant RNA species in the cell, it is possible to isolate the precursor rRNA species. Radio-labeled uracil incorporates into ribosomal RNA during synthesis. Therefore, pulse-chase analysis of ribosomal RNA with uracil reveals the multiple ribosomal RNA precursors (de la Cruz et al., 2005; Ferreira-Cerca et al., 2005; Iouk et al., 2001; Jakovljevic et al., 2004). In ribosome biogenesis mutants, the processing of ribosomal RNA precursors is often stalled. If *ASC1* functions in ribosome biogenesis then it is possible that *asc1*-deficient yeast fail to perform one or more steps of ribosomal RNA processing. A pulse-chase

analysis of ribosomal RNA processing at either 30 or 39°C might reveal that *asc1*-deficient yeast fail to generate the appropriate terminal or precursor rRNA species.

If *asc1*-deficient yeast fail to process ribosomal RNA at the 20S-to-18S transition, *ASC1* is likely involved in one of two ribosome biogenesis steps. Because 20S rRNA processing occurs in the cytoplasm, a 20S-to18S processing defect might indicate that *ASC1* plays a critical role in transporting the developing 40S from the nucleolus to the cytoplasm. If this model is correct, then *asc1*-deficient yeast should accumulate 40S subunits in the nucleolus. However, if *asc1*-deficient yeast exhibit a defect in 20S-to-18S processing, but do not demonstrate a defect in 40S transport from the nucleolus, then it is likely that *ASC1* is critical for a stage of ribosome biogenesis that occurs in the cytoplasm.

Growth Behavior of ribosome-depleted *asc1*-deficient yeast suggest a role for ribosomes in cell proliferation

Because ribosomes are believed to be essential for survival, few studies have been able to gain an understanding of ribosome function. Of course, ribosomes have been caught-in-the-act of mRNA translation . However, the overall contribution of ribosomes to cellular homeostasis has remained elusive. Conflicting reports suggest that ribosomal proteins either slow or enhance processes that require cell proliferation (Amsterdam et al., 2004; Volarevic et al., 2000).

Yeast deficient in *asc1* exhibit a severely reduced ribosome population after growth at 39°C for 16 hours. At this point in the growth cycle, both wild-type

and mutant yeast contain reduced polyribosomes, suggesting that translational initiation is repressed. Introduction of the yeast to fresh media at 30°C results in the formation of polyribosomes immediately. However, *asc1*-deificent yeast exhibit a diminished pool of total ribosomes relative to wild-type that lasts 4-20 hours after introduction to the fresh media. These results show that *asc1*-deficient yeast are competent to initiate mRNA translation immediately, but replenish the ribosome pool at a latter time-point. Interestingly, a yeast strain with an *asc1*Δ background exhibits a lag in proliferation when recovering from growth at the NPT. Taken together, these results strongly suggest that the growth lag of *asc1*-deficient yeast is associated with a reduced ribosome density, but not repressed translational initiation. Therefore, this work further illustrates an association between ribosome density (per cell) and cell proliferation.

Link between ribosome biogenesis, cell proliferation, and Rapamycin treatment

The pharmacological compound Rapamycin (also known as Sirolimus), has many clinical applications (Shapiro et al., 2000; Stallone et al., 2005a; Stallone et al., 2005b). Rapamycin inhibits cell proliferation through mechanisms that are not entirely understood. The drug suppress the synthesis of proteins that encode components of the ribosome and ribosome biogenesis factors (Guertin et al., 2006; Tang et al., 2001). Therefore Rapamycin suppresses both cell proliferation and the synthesis of ribosomes. The studies described in this dissertation establish an association between ribosome density and cell proliferation. Taken together, work presented in this dissertation and elsewhere

suggests that Rapamycin might inhibit the potential for cells to proliferate by blocking ribosome biogenesis (Guertin et al., 2006; Tang et al., 2001; Volarevic et al., 2000).

Other Possible Functions for *ASC1* in Ribosome Function/Translation

The introduction of this dissertation outlines the differences between prokaryotic and eukaryotic mRNA translation and ribosome structure. Because eukaryotic small subunits have evolved large structural features that are absent from their prokaryotic counterparts, these new structures may be responsible for orchestrating aspects of translational initiation that are unique to eukaryotes (Spahn et al., 2004). That Asc1p is a large, recently evolved portion of the small subunit suggests that it may function during eukaryotic translational initiation. In support of this possibility, Dr. Leos Valasek has found that Asc1p is the only 40S protein that has an interaction with NIP1; a component of the eIF3 complex (*personal communication, unpublished data*). Because eIF3 forms a complex with eIF4F (the mRNA cap-binding complex), it is possible that Asc1p docks eIF3 on the ribosome. Therefore, *ASC1* may have a critical function in scaffolding interactions of the ribosome with the 5'end of mRNAs to initiate translation. However, there are several reasons why the results presented in this dissertation conflict with this possibility. First, *asc1*-deficient yeast do not exhibit a growth phenotype at 30°C. In sharp contrast, deletion of any eIF3 subunit, including NIP1, is lethal (Giaever et al., 2002). Conditional mutants of eIF3 also have strong defects in translational initiation (Jivotovskaya et al., 2006; Nielsen et al.,

2004). Therefore, if Asc1p is critical for docking eIF3 to the ribosome, then one would expect *asc1*-deficient yeast to exhibit a severe growth defect at 30°C.

Consistent with *ASC1* performing an important role in translation, *asc1*-deficient yeast fail to grow at 39°C. This defect is principally due to the failure of *asc1*-deficient yeast to form nascent ribosomes at the 39°C. Yeast deficient in *ASC1* appear to lose polyribosomes in proportion to monosomes at 39°C. Loss of polyribosomes, but not monosomes is an indicator of suppressed translational initiation. Because asc1-deficient yeast appear to have an equivalent loss of all ribosome species at the non-permissive temperature, it is unlikely that *ASC1* functions to stimulate translational initiation. Rather, this result suggests that *ASC1* is critical for ribosome biogenesis.

Part I Conclusion: Asc1p is part of the ribosome core and facilitates ribosome biogenesis

This dissertation provides some of the principal evidence that Asc1p and RACK1 are core components of the eukaryotic 40S ribosome. In addition, this dissertation shows that yeast deficient in *asc1* have elevated levels of specific proteins at 30°C. These proteins levels are elevated through a post-transcriptional mechanism, consistent with a role for Asc1p in the post-transcriptional repression of protein expression. When the growth temperature of *asc1*-deficient yeast is shifted to 39°C, the nascent ribosome population is diminished, suggesting that *ASC1* functions during ribosome biogenesis at elevated temperatures. Therefore, these studies establish Asc1p as a novel core component of the 40S subunit that functions to repress the expression of a

subset of mRNAs at 30°C, and facilitates the biogenesis of the ribosome at elevated temperatures. Future studies outlined above will define the precise mechanistic contribution of *ASC1* to translational repression and ribosome biogenesis.

Part II: Discovery of novel IRES RNP complexes

In the last portion of my dissertation research I wanted to pursue my own discovery-driven proteomic analysis. To this end, I chose to develop a protocol that would allow one to use RNA affinity chromatography combined with proteomic approaches to identify proteins that would bind to specific RNA sequences. As my model RNA, I used the ornithine decarboxylase Internal Ribosomal Entry Site (Pyronnet et al., 2000; Pyronnet et al., 2005). The ODC IRES had been mutated previously by Nahum Sonenberg's group (Pyronnet et al., 2000; Pyronnet et al., 2005). Mutagenesis of pyrimidine tracts in the 5'UTR of ODC resulted in a marked loss of IRES activity. Therefore, comparing proteins that would bind to the wild-type IRES RNA, but not the mutant IRES RNA, might lead to the discovery of IRES trans-acting-factors.

Mutation of the ODC IRES identified a regulatory element (RE) in the 5'UTR. This RE was 18 bases in length. I reasoned that this RNA could be coupled to chromatography beads in order to capture proteins that would bind the wild-type (active form) of the IRES. I also reasoned that a similar RNA affinity column containing the mutant (inactive form) of the ODC IRES RE might fail to form protein-RNA interactions that form on the wild-type affinity column.

Mass spectrometry analysis of the wild-type and mutant RNA-binding proteins showed that two proteins were abundantly and specifically associated with the wild-type IRES RNA. These two proteins were ZNF9 and PCBP2. Although ZNF9 was a protein with no official ascribed function, PCBP2 had been shown to function as an ITAF in several studies. Importantly, ZNF9 is mutated in patients with type-2 myotonic dystrophy (Liquori et al., 2001).

Additional biochemical experiments suggested that ZNF9 and PCBP2 were bona fide ODC IRES binding proteins. Further, loss-of-function and over-expression analyses suggested that PCBP2 and ZNF9 function to stimulate the cap-independent translation of the ODC IRES. Interestingly, ZNF9 and PCBP2 co-purified, and might function as part of a larger ITAF assembly.

Possible models of ZNF9-mutation-induced pathogenesis

Our proteomic screen and detailed molecular analysis suggests that the ZNF9 protein functions as an ITAF. If we apply a simplistic model of heritable disease to the ZNF9 gene, it is possible that mutations in ZNF9 disrupt cap-independent mRNA translation in type-2 myotonic dystrophy. Importantly, mice that are heterozygous mutants of ZNF9 share many of the human symptoms of myotonic dystrophy including: myotonic discharges, heart conduction abnormalities, and cataracts (Chen et al., 2007). Therefore, haploinsuffiency of ZNF9 in mice causes phenotypes that are consistent with myotonic dystrophy in humans.

The nature of the ZNF9 mutation has led to some disease models that ignore the natural function of the gene in the etiology of the disease. ZNF9 harbors tandem CCTG expansions in intron 1 of patients with type-2 myotonic dystrophy. Similarly, patients with type-1 myotonic dystrophy harbor tandem CTG expansions in a non-coding region of the DMPK gene (Brook et al., 1992; Carango et al., 1993). DMPK encodes a serine/threonine protein kinase whereas ZNF9 is expected to encode a nucleic acid binding protein (Liquori et al., 2001). Therefore, the genes that cause both forms of myotonic dystrophy harbor similar mutations in genes that are predicted to have divergent functions. From this observation, it is postulated that CTG-like expansions cause a gain-of-function phenotype in individuals with these mutations (Kanadia et al., 2003; Kanadia et al., 2006). Specifically, if these tandem CTG repeats are transcribed into CUG repeats, it is conceivable that CUG-RNA-binding proteins might be sequestered by these non-translated sequences. If this is the case, it would explain why the expansion mutations CTG and CCTG occur in genes with divergent functions but have the same outcome; the development of myotonic dystrophy like symptoms.

This dissertation describes a protocol that successfully couples RNA-affinity chromatography to LC-MS/MS mass spectrometry analysis. The RNA-toxicity model in myotonic dystrophy postulates that CUG-binding proteins are sequestered in the nuclei of patients with the disease. Subsequent loss of CUG-binding protein function might disrupt essential cellular processes such as RNA splicing and export. If this model is correct, then a common group of proteins

should bind to tandem repeats of either CUG or CCUG. The proteomic approach used in this dissertation to discover IRES-binding proteins can be applied to the discovery of proteins that bind to both CUG and CCUG sequences. Additionally, this approach can be used to identify proteins that uniquely bind to either CUG or CCUG repeats. After the shared and unique CUG or CCUG-binding proteins are identified, mice that are null for individual CUG-binding proteins can be tested for their ability to recapitulate the disease. Because there are additional forms of myotonic dystrophy for which the effected genes are not known, this approach may pinpoint the etiology of these other type(s) of dystrophy.

Future Studies of ODC IRES-binding Proteins

During my screen of ODC IRES RNA-binding proteins, I found proteins that were specifically associated with the wild-type RNA, but not the mutant (inactive) IRES RNA. A number of the proteins that bound to both the wild-type and mutant (inactive) IRES RNA are established ITAFs. For example, poly-pyrimidine tract binding protein (PTB) and upstream of N-ras (UNR) were associated with both wild-type and mutant RNAs. Therefore, a number of the proteins identified in our screen bind to the wild-type and inactive ODC IRES and are established ITAFs. I put forward the possibility that these proteins might also function as ITAFs of the ODC IRES. Additionally, it is possible that these proteins function as part of a larger holo-ITAF complex with PCBP2 and ZNF9 to stimulate the cap-independent translation of the ODC IRES.

Part II: Conclusion: ZNF9 and PCBP2 are ITAFs that stimulate the ODC IRES

The combination of RNA affinity chromatography and mass spectrometry defined proteins that specially bind an active wild-type ODC IRES but not a mutant form of the IRES. These proteins, PCBP2 and ZNF9 associate biochemically and function as ITAFs. That ZNF9 is mutated in patients with type-2 myotonic dystrophy raises the intriguing possibility that IRES-dependent mRNA translation is disrupted in the disease. In consideration of these discoveries, future studies will pursue this possibility.

References

Alban, A., David, S. O., Bjorkesten, L., Andersson, C., Sloge, E., Lewis, S., and Currie, I. (2003). A novel experimental design for comparative two-dimensional gel analysis: two-dimensional difference gel electrophoresis incorporating a pooled internal standard. Proteomics *3*, 36-44.

Albanese, V., Yam, A. Y., Baughman, J., Parnot, C., and Frydman, J. (2006). Systems analyses reveal two chaperone networks with distinct functions in eukaryotic cells. Cell *124*, 75-88.

Amsterdam, A., Sadler, K. C., Lai, K., Farrington, S., Bronson, R. T., Lees, J. A., and Hopkins, N. (2004). Many ribosomal protein genes are cancer genes in zebrafish. PLoS Biol *2*, E139.

Angenstein, F., Evans, A. M., Settlage, R. E., Moran, S. T., Ling, S. C., Klintsova, A. Y., Shabanowitz, J., Hunt, D. F., and Greenough, W. T. (2002). A receptor for activated C kinase is part of messenger ribonucleoprotein complexes associated with polyA-mRNAs in neurons. J Neurosci *22*, 8827-8837.

Asano, K., Phan, L., Krishnamoorthy, T., Pavitt, G. D., Gomez, E., Hannig, E. M., Nika, J., Donahue, T. F., Huang, H. K., and Hinnebusch, A. G. (2002). Analysis and reconstitution of translation initiation in vitro. Methods Enzymol *351*, 221-247.

Ashe, M. P., De Long, S. K., and Sachs, A. B. (2000). Glucose depletion rapidly inhibits translation initiation in yeast. Mol Biol Cell *11*, 833-848.

Audhya, A., Foti, M., and Emr, S. D. (2000). Distinct roles for the yeast phosphatidylinositol 4-kinases, Stt4p and Pik1p, in secretion, cell growth, and organelle membrane dynamics. Mol Biol Cell *11*, 2673-2689.

Baughman, G., and Nomura, M. (1983). Localization of the target site for translational regulation of the L11 operon and direct evidence for translational coupling in Escherichia coli. Cell *34*, 979-988.

Baughman, G., and Nomura, M. (1984). Translational regulation of the L11 ribosomal protein operon of Escherichia coli: analysis of the mRNA target site using oligonucleotide-directed mutagenesis. Proc Natl Acad Sci U S A *81*, 5389-5393.

Baum, S., Bittins, M., Frey, S., and Seedorf, M. (2004). Asc1p, a WD40-domain containing adaptor protein, is required for the interaction of the RNA-binding protein Scp160p with polysomes. Biochem J *380*, 823-830.

Blyn, L. B., Swiderek, K. M., Richards, O., Stahl, D. C., Semler, B. L., and Ehrenfeld, E. (1996). Poly(rC) binding protein 2 binds to stem-loop IV of the poliovirus RNA 5' noncoding region: identification by automated liquid chromatography-tandem mass spectrometry. Proc Natl Acad Sci U S A *93*, 11115-11120.

Blyn, L. B., Towner, J. S., Semler, B. L., and Ehrenfeld, E. (1997). Requirement of poly(rC) binding protein 2 for translation of poliovirus RNA. J Virol *71*, 6243-6246.

Brodskii, L. I., Ivanov, V. V., Kalaidzidis Ia, L., Leontovich, A. M., Nikolaev, V. K., Feranchuk, S. I., and Drachev, V. A. (1995). [GeneBee-NET: An Internet based server for biopolymer structure analysis]. Biokhimiia *60*, 1221-1230.

Brodsky, L. I., Drachev, A. L., Leontovich, A. M., and Feranchuk, S. I. (1993). A novel method of multiple alignment of biopolymer sequences. Biosystems *30*, 65-79.

Brook, J. D., McCurrach, M. E., Harley, H. G., Buckler, A. J., Church, D., Aburatani, H., Hunter, K., Stanton, V. P., Thirion, J. P., Hudson, T., and et al. (1992). Molecular basis of myotonic dystrophy: expansion of a trinucleotide (CTG) repeat at the 3' end of a transcript encoding a protein kinase family member. Cell *69*, 385.

Bukau, B., and Horwich, A. L. (1998). The Hsp70 and Hsp60 chaperone machines. Cell *92*, 351-366.

Carango, P., Noble, J. E., Marks, H. G., and Funanage, V. L. (1993). Absence of myotonic dystrophy protein kinase (DMPK) mRNA as a result of a triplet repeat expansion in myotonic dystrophy. Genomics *18*, 340-348.

Ceci, M., Gaviraghi, C., Gorrini, C., Sala, L. A., Offenhauser, N., Marchisio, P. C., and Biffo, S. (2003). Release of eIF6 (p27BBP) from the 60S subunit allows 80S ribosome assembly. Nature *426*, 579-584.

Chang, B. Y., Conroy, K. B., Machleder, E. M., and Cartwright, C. A. (1998). RACK1, a receptor for activated C kinase and a homolog of the beta subunit of G proteins, inhibits activity of src tyrosine kinases and growth of NIH 3T3 cells. Mol Cell Biol *18*, 3245-3256.

Chantrel, Y., Gaisne, M., Lions, C., and Verdiere, J. (1998). The transcriptional regulator Hap1p (Cyp1p) is essential for anaerobic or heme-deficient growth of Saccharomyces cerevisiae: Genetic and molecular characterization of an extragenic suppressor that encodes a WD repeat protein. Genetics *148*, 559-569.

Chen, C. Y., and Sarnow, P. (1995). Initiation of protein synthesis by the eukaryotic translational apparatus on circular RNAs. Science *268*, 415-417.

Chen, W., Liang, Y., Deng, W., Shimizu, K., Ashique, A. M., Li, E., and Li, Y. P. (2003). The zinc-finger protein CNBP is required for forebrain formation in the mouse. Development *130*, 1367-1379.

Chen, W., Wang, Y., Abe, Y., Cheney, L., Udd, B., and Li, Y. P. (2007). Haploinsuffciency for Znf9 in Znf9(+/-) Mice Is Associated with Multiorgan Abnormalities Resembling Myotonic Dystrophy. J Mol Biol.

Chersi, A., Dzionara, M., Donner, D., and Wittman, H. G. (1968). Ribosomal proteins. IV. Isolation, amino acid compositions, peptide maps and molecular weights of yeast ribosomal proteins. Mol Gen Genet *101*, 82-88.

Cho, D. H., and Tapscott, S. J. (2006). Myotonic dystrophy: Emerging mechanisms for DM1 and DM2. Biochim Biophys Acta.

Cho, D. H., and Tapscott, S. J. (2007). Myotonic dystrophy: Emerging mechanisms for DM1 and DM2. Biochim Biophys Acta *1772*, 195-204.

Choi, S. K., Lee, J. H., Zoll, W. L., Merrick, W. C., and Dever, T. E. (1998). Promotion of met-tRNAiMet binding to ribosomes by yIF2, a bacterial IF2 homolog in yeast. Science *280*, 1757-1760.

Christianson, T. W., Sikorski, R. S., Dante, M., Shero, J. H., and Hieter, P. (1992). Multifunctional yeast high-copy-number shuttle vectors. Gene *110*, 119-122.

Cox, E. A., Bennin, D., Doan, A. T., O'Toole, T., and Huttenlocher, A. (2003). RACK1 regulates integrin-mediated adhesion, protrusion, and chemotactic cell migration via its Src-binding site. Mol Biol Cell *14*, 658-669.

Creusot, F., Verdiere, J., Gaisne, M., and Slonimski, P. P. (1988). CYP1 (HAP1) regulator of oxygen-dependent gene expression in yeast. I. Overall organization of the protein sequence displays several novel structural domains. J Mol Biol *204*, 263-276.

Crick, F. (1970). Central dogma of molecular biology. Nature *227*, 561-563.

Crick, F. H. (1958). On protein synthesis. Symp Soc Exp Biol *12*, 138-163.

Crosio, C., Boyl, P. P., Loreni, F., Pierandrei-Amaldi, P., and Amaldi, F. (2000). La protein has a positive effect on the translation of TOP mRNAs in vivo. Nucleic Acids Res *28*, 2927-2934.

Culver, G. M., and Noller, H. F. (1999). Efficient reconstitution of functional Escherichia coli 30S ribosomal subunits from a complete set of recombinant small subunit ribosomal proteins. Rna *5*, 832-843.

de la Cruz, J., Sanz-Martinez, E., and Remacha, M. (2005). The essential WD-repeat protein Rsa4p is required for rRNA processing and intra-nuclear transport of 60S ribosomal subunits. Nucleic Acids Res *33*, 5728-5739.

Dell, E. J., Connor, J., Chen, S., Stebbins, E. G., Skiba, N. P., Mochly-Rosen, D., and Hamm, H. E. (2002). The betagamma subunit of heterotrimeric G proteins interacts with RACK1 and two other WD repeat proteins. J Biol Chem *277*, 49888-49895.

Dever, T. E., Feng, L., Wek, R. C., Cigan, A. M., Donahue, T. F., and Hinnebusch, A. G. (1992). Phosphorylation of initiation factor 2 alpha by protein kinase GCN2 mediates gene-specific translational control of GCN4 in yeast. Cell *68*, 585-596.

Dosil, M., and Bustelo, X. R. (2004). Functional characterization of Pwp2, a WD family protein essential for the assembly of the 90 S pre-ribosomal particle. J Biol Chem *279*, 37385-37397.

Doudna, J. A., and Rath, V. L. (2002). Structure and function of the eukaryotic ribosome: the next frontier. Cell *109*, 153-156.

Dzionara, M., Kaltschmidt, E., and Wittmann, H. G. (1970). Ribosomal proteins. 8. Molecular weights of isolated ribosomal proteins of Escherichia coli. Proc Natl Acad Sci U S A *67*, 1909-1913.

Elbashir, S. M., Harborth, J., Lendeckel, W., Yalcin, A., Weber, K., and Tuschl, T. (2001). Duplexes of 21-nucleotide RNAs mediate RNA interference in cultured mammalian cells. Nature *411*, 494-498.

Evans, J. R., Mitchell, S. A., Spriggs, K. A., Ostrowski, J., Bomsztyk, K., Ostarek, D., and Willis, A. E. (2003). Members of the poly (rC) binding protein family stimulate the activity of the c-myc internal ribosome entry segment in vitro and in vivo. Oncogene *22*, 8012-8020.

Fatica, A., and Tollervey, D. (2002). Making ribosomes. Curr Opin Cell Biol *14*, 313-318.

Ferreira-Cerca, S., Poll, G., Gleizes, P. E., Tschochner, H., and Milkereit, P. (2005). Roles of eukaryotic ribosomal proteins in maturation and transport of pre-18S rRNA and ribosome function. Mol Cell *20*, 263-275.

Fillingame, R. H., Jorstad, C. M., and Morris, D. R. (1975). Increased cellular levels of spermidine or spermine are required for optimal DNA synthesis in lymphocytes activated by concanavalin A. Proc Natl Acad Sci U S A *72*, 4042-4045.

Fleischer, T. C., Weaver, C. M., McAfee, K. J., Jennings, J. L., and Link, A. J. (2006). Systematic identification and functional screens of uncharacterized proteins associated with eukaryotic ribosomal complexes. Genes Dev *20*, 1294-1307.

Friedman, D. B., Hill, S., Keller, J. W., Merchant, N. B., Levy, S. E., Coffey, R. J., and Caprioli, R. M. (2004). Proteome analysis of human colon cancer by two-dimensional difference gel electrophoresis and mass spectrometry. Proteomics *4*, 793-811.

Fromont-Racine, M., Senger, B., Saveanu, C., and Fasiolo, F. (2003). Ribosome assembly in eukaryotes. Gene *313*, 17-42.

Furuichi, Y., Morgan, M., Muthukrishnan, S., and Shatkin, A. J. (1975a). Reovirus messenger RNA contains a methylated, blocked 5'-terminal structure: m-7G(5')ppp(5')G-MpCp. Proc Natl Acad Sci U S A *72*, 362-366.

Furuichi, Y., Muthukrishnan, S., and Shatkin, A. J. (1975b). 5'-Terminal m-7G(5')ppp(5')G-m-p in vivo: identification in reovirus genome RNA. Proc Natl Acad Sci U S A *72*, 742-745.

Furuichi, Y., Muthukrishnan, S., Tomasz, J., and Shatkin, A. J. (1976). Caps in eukaryotic mRNAs: mechanism of formation of reovirus mRNA 5'-terminal m7GpppGm-C. Prog Nucleic Acid Res Mol Biol *19*, 3-20.

Gallina, A., Rossi, F., and Milanesi, G. (2001). Rack1 binds HIV-1 Nef and can act as a Nef-protein kinase C adaptor. Virology *283*, 7-18.

Gamarnik, A. V., and Andino, R. (1997). Two functional complexes formed by KH domain containing proteins with the 5' noncoding region of poliovirus RNA. Rna *3*, 882-892.

Gamarnik, A. V., and Andino, R. (2000). Interactions of viral protein 3CD and poly(rC) binding protein with the 5' untranslated region of the poliovirus genome. J Virol *74*, 2219-2226.

Garrels, J. I., McLaughlin, C. S., Warner, J. R., Futcher, B., Latter, G. I., Kobayashi, R., Schwender, B., Volpe, T., Anderson, D. S., Mesquita-Fuentes, R., and Payne, W. E. (1997). Proteome studies of Saccharomyces cerevisiae: identification and characterization of abundant proteins. Electrophoresis *18*, 1347-1360.

Geijsen, N., Spaargaren, M., Raaijmakers, J. A., Lammers, J. W., Koenderman, L., and Coffer, P. J. (1999). Association of RACK1 and PKCbeta with the common beta-chain of the IL-5/IL-3/GM-CSF receptor. Oncogene *18*, 5126-5130.

Gerbasi, V., Lutsenko, S., and Lewis, E. J. (2003). A mutation in the ATP7B copper transporter causes reduced dopamine beta-hydroxylase and norepinephrine in mouse adrenal. Neurochem Res *28*, 867-873.

Gerbasi, V. R., Weaver, C. M., Hill, S., Friedman, D. B., and Link, A. J. (2004). Yeast Asc1p and mammalian RACK1 are functionally orthologous core 40S ribosomal proteins that repress gene expression. Mol Cell Biol *24*, 8276-8287.

Ghaemmaghami, S., Huh, W. K., Bower, K., Howson, R. W., Belle, A., Dephoure, N., O'Shea, E. K., and Weissman, J. S. (2003). Global analysis of protein expression in yeast. Nature *425*, 737-741.

Giaever, G., Chu, A. M., Ni, L., Connelly, C., Riles, L., Veronneau, S., Dow, S., Lucau-Danila, A., Anderson, K., Andre, B.*, et al.* (2002). Functional profiling of the Saccharomyces cerevisiae genome. Nature *418*, 387-391.

Gingras, A. C., Raught, B., and Sonenberg, N. (1999). eIF4 initiation factors: effectors of mRNA recruitment to ribosomes and regulators of translation. Annu Rev Biochem *68*, 913-963.

Granneman, S., and Baserga, S. J. (2004). Ribosome biogenesis: of knobs and RNA processing. Exp Cell Res *296*, 43-50.

Guertin, D. A., Guntur, K. V., Bell, G. W., Thoreen, C. C., and Sabatini, D. M. (2006). Functional genomics identifies TOR-regulated genes that control growth and division. Curr Biol *16*, 958-970.

Guillemot, F., Billault, A., and Auffray, C. (1989). Physical linkage of a guanine nucleotide-binding protein-related gene to the chicken major histocompatibility complex. Proc Natl Acad Sci U S A *86*, 4594-4598.

Harnpicharnchai, P., Jakovljevic, J., Horsey, E., Miles, T., Roman, J., Rout, M., Meagher, D., Imai, B., Guo, Y., Brame, C. J.*, et al.* (2001). Composition and functional characterization of yeast 66S ribosome assembly intermediates. Mol Cell *8*, 505-515.

Held, W. A., Ballou, B., Mizushima, S., and Nomura, M. (1974). Assembly mapping of 30 S ribosomal proteins from Escherichia coli. Further studies. J Biol Chem *249*, 3103-3111.

Hellen, C. U., and Sarnow, P. (2001). Internal ribosome entry sites in eukaryotic mRNA molecules. Genes Dev *15*, 1593-1612.

Hennig, E. E., Butruk, E., and Ostrowski, J. (2001). RACK1 protein interacts with Helicobacter pylori VacA cytotoxin: the yeast two-hybrid approach. Biochem Biophys Res Commun *289*, 103-110.

Hermanto, U., Zong, C. S., Li, W., and Wang, L. H. (2002). RACK1, an insulin-like growth factor I (IGF-I) receptor-interacting protein, modulates IGF-I-dependent integrin signaling and promotes cell spreading and contact with extracellular matrix. Mol Cell Biol *22*, 2345-2365.

Higo, K., Otaka, E., and Osawa, S. (1982). Purification and characterization of 30S ribosomal proteins from Bacillus subtilis: correlation to Escherichia coli 30S proteins. Mol Gen Genet *185*, 239-244.

Hinnebusch, A. G. (1985). A hierarchy of trans-acting factors modulates translation of an activator of amino acid biosynthetic genes in Saccharomyces cerevisiae. Mol Cell Biol *5*, 2349-2360.

Hinnebusch, A. G. (2005). Translational regulation of GCN4 and the general amino acid control of yeast. Annu Rev Microbiol *59*, 407-450.

Hoffmann, B., Mosch, H. U., Sattlegger, E., Barthelmess, I. B., Hinnebusch, A., and Braus, G. H. (1999). The WD protein Cpc2p is required for repression of

Gcn4 protein activity in yeast in the absence of amino-acid starvation. Mol Microbiol *31*, 807-822.

Holcik, M., and Korneluk, R. G. (2000). Functional characterization of the X-linked inhibitor of apoptosis (XIAP) internal ribosome entry site element: role of La autoantigen in XIAP translation. Mol Cell Biol *20*, 4648-4657.

Holmes, L. E., Campbell, S. G., De Long, S. K., Sachs, A. B., and Ashe, M. P. (2004). Loss of translational control in yeast compromised for the major mRNA decay pathway. Mol Cell Biol *24*, 2998-3010.

Hosokawa, K., Fujimura, R. K., and Nomura, M. (1966). Reconstitution of functionally active ribosomes from inactive subparticles and proteins. Proc Natl Acad Sci U S A *55*, 198-204.

Huang, P., Gautschi, M., Walter, W., Rospert, S., and Craig, E. A. (2005). The Hsp70 Ssz1 modulates the function of the ribosome-associated J-protein Zuo1. Nat Struct Mol Biol *12*, 497-504.

Hunt, S. L., Hsuan, J. J., Totty, N., and Jackson, R. J. (1999). unr, a cellular cytoplasmic RNA-binding protein with five cold-shock domains, is required for internal initiation of translation of human rhinovirus RNA. Genes Dev *13*, 437-448.

Hunt, S. L., and Jackson, R. J. (1999). Polypyrimidine-tract binding protein (PTB) is necessary, but not sufficient, for efficient internal initiation of translation of human rhinovirus-2 RNA. Rna *5*, 344-359.

Iizuka, N., Najita, L., Franzusoff, A., and Sarnow, P. (1994). Cap-dependent and cap-independent translation by internal initiation of mRNAs in cell extracts prepared from Saccharomyces cerevisiae. Mol Cell Biol *14*, 7322-7330.

Inada, T., Winstall, E., Tarun, S. Z., Jr., Yates, J. R., 3rd, Schieltz, D., and Sachs, A. B. (2002). One-step affinity purification of the yeast ribosome and its associated proteins and mRNAs. Rna *8*, 948-958.

Iouk, T. L., Aitchison, J. D., Maguire, S., and Wozniak, R. W. (2001). Rrb1p, a yeast nuclear WD-repeat protein involved in the regulation of ribosome biosynthesis. Mol Cell Biol *21*, 1260-1271.

Ishiguro, J. (1976). Study on proteins from yeast cytoplasmic ribosomes by two-dimensional gel electrophoresis. Mol Gen Genet *145*, 73-79.

Ishikawa, H. (1977). Evolution of ribosomal RNA. Comp Biochem Physiol B *58*, 1-7.

Jakovljevic, J., de Mayolo, P. A., Miles, T. D., Nguyen, T. M., Leger-Silvestre, I., Gas, N., and Woolford, J. L., Jr. (2004). The carboxy-terminal extension of yeast ribosomal protein S14 is necessary for maturation of 43S preribosomes. Mol Cell *14*, 331-342.

Jang, S. K., Davies, M. V., Kaufman, R. J., and Wimmer, E. (1989). Initiation of protein synthesis by internal entry of ribosomes into the 5' nontranslated region of encephalomyocarditis virus RNA in vivo. J Virol *63*, 1651-1660.

Jansen, R., Bussemaker, H. J., and Gerstein, M. (2003). Revisiting the codon adaptation index from a whole-genome perspective: analyzing the relationship between gene expression and codon occurrence in yeast using a variety of models. Nucleic Acids Res *31*, 2242-2251.

Ji, H., Fraser, C. S., Yu, Y., Leary, J., and Doudna, J. A. (2004). Coordinated assembly of human translation initiation complexes by the hepatitis C virus internal ribosome entry site RNA. Proc Natl Acad Sci U S A *101*, 16990-16995.

Jivotovskaya, A. V., Valasek, L., Hinnebusch, A. G., and Nielsen, K. H. (2006). Eukaryotic translation initiation factor 3 (eIF3) and eIF2 can promote mRNA binding to 40S subunits independently of eIF4G in yeast. Mol Cell Biol *26*, 1355-1372.

Johannes, G., Carter, M. S., Eisen, M. B., Brown, P. O., and Sarnow, P. (1999). Identification of eukaryotic mRNAs that are translated at reduced cap binding complex eIF4F concentrations using a cDNA microarray. Proc Natl Acad Sci U S A *96*, 13118-13123.

Johannes, G., and Sarnow, P. (1998). Cap-independent polysomal association of natural mRNAs encoding c-myc, BiP, and eIF4G conferred by internal ribosome entry sites. Rna *4*, 1500-1513.

Jorgensen, P., Rupes, I., Sharom, J. R., Schneper, L., Broach, J. R., and Tyers, M. (2004). A dynamic transcriptional network communicates growth potential to ribosome synthesis and critical cell size. Genes Dev *18*, 2491-2505.

Kaltschmidt, E., and Wittmann, H. G. (1970). Ribosomal proteins. XII. Number of proteins in small and large ribosomal subunits of Escherichia coli as determined by two-dimensional gel electrophoresis. Proc Natl Acad Sci U S A *67*, 1276-1282.

Kanadia, R. N., Johnstone, K. A., Mankodi, A., Lungu, C., Thornton, C. A., Esson, D., Timmers, A. M., Hauswirth, W. W., and Swanson, M. S. (2003). A muscleblind knockout model for myotonic dystrophy. Science *302*, 1978-1980.

Kanadia, R. N., Shin, J., Yuan, Y., Beattie, S. G., Wheeler, T. M., Thornton, C. A., and Swanson, M. S. (2006). Reversal of RNA missplicing and myotonia after muscleblind overexpression in a mouse poly(CUG) model for myotonic dystrophy. Proc Natl Acad Sci U S A *103*, 11748-11753.

Kief, D. R., and Warner, J. R. (1981). Coordinate control of syntheses of ribosomal ribonucleic acid and ribosomal proteins during nutritional shift-up in Saccharomyces cerevisiae. Mol Cell Biol *1*, 1007-1015.

Kiely, P. A., Sant, A., and O'Connor, R. (2002). RACK1 is an insulin-like growth factor 1 (IGF-1) receptor-interacting protein that can regulate IGF-1-mediated Akt activation and protection from cell death. J Biol Chem *277*, 22581-22589.

Koehler, J. A., and Moran, M. F. (2001). RACK1, a protein kinase C scaffolding protein, interacts with the PH domain of p120GAP. Biochem Biophys Res Commun *283*, 888-895.

Kozak, M. (1978). How do eucaryotic ribosomes select initiation regions in messenger RNA? Cell *15*, 1109-1123.

Kozak, M. (1980a). Evaluation of the "scanning model" for initiation of protein synthesis in eucaryotes. Cell *22*, 7-8.

Kozak, M. (1980b). Role of ATP in binding and migration of 40S ribosomal subunits. Cell *22*, 459-467.

Kozak, M., and Shatkin, A. J. (1976). Characterization of ribosome-protected fragments from reovirus messenger RNA. J Biol Chem *251*, 4259-4266.

Kozak, M., and Shatkin, A. J. (1978). Identification of features in 5' terminal fragments from reovirus mRNA which are important for ribosome binding. Cell *13*, 201-212.

Kressler, D., Linder, P., and de La Cruz, J. (1999). Protein trans-acting factors involved in ribosome biogenesis in Saccharomyces cerevisiae. Mol Cell Biol *19*, 7897-7912.

Kruiswijk, T., and Planta, R. J. (1974). Analysis of the protein composition of yeast ribosomal subunits by two-dimensional polyacrylamide gel electrophoresis. Mol Biol Rep *1*, 409-415.

Kubota, T., Yokosawa, N., Yokota, S., and Fujii, N. (2002). Association of mumps virus V protein with RACK1 results in dissociation of STAT-1 from the alpha interferon receptor complex. J Virol *76*, 12676-12682.

Kuyumcu-Martinez, N. M., and Cooper, T. A. (2006). Misregulation of alternative splicing causes pathogenesis in myotonic dystrophy. Prog Mol Subcell Biol *44*, 133-159.

Kwast, K. E., Burke, P. V., and Poyton, R. O. (1998). Oxygen sensing and the transcriptional regulation of oxygen-responsive genes in yeast. J Exp Biol *201*, 1177-1195.

LaMuraglia, G. M., Lacaine, F., and Malt, R. A. (1986). High ornithine decarboxylase activity and polyamine levels in human colorectal neoplasia. Ann Surg *204*, 89-93.

Lassar, A. B., Davis, R. L., Wright, W. E., Kadesch, T., Murre, C., Voronova, A., Baltimore, D., and Weintraub, H. (1991). Functional activity of myogenic HLH proteins requires hetero-oligomerization with E12/E47-like proteins in vivo. Cell *66*, 305-315.

Leffers, H., Dejgaard, K., and Celis, J. E. (1995). Characterisation of two major cellular poly(rC)-binding human proteins, each containing three K-homologous (KH) domains. Eur J Biochem *230*, 447-453.

Leger-Silvestre, I., Milkereit, P., Ferreira-Cerca, S., Saveanu, C., Rousselle, J. C., Choesmel, V., Guinefoleau, C., Gas, N., and Gleizes, P. E. (2004). The ribosomal protein Rps15p is required for nuclear exit of the 40S subunit precursors in yeast. Embo J *23*, 2336-2347.

Liliental, J., and Chang, D. D. (1998). Rack1, a receptor for activated protein kinase C, interacts with integrin beta subunit. J Biol Chem *273*, 2379-2383.

Link, A. J. (1999). Autoradiography of 2-D gels. Methods Mol Biol *112*, 285-290.

Link, A. J., Eng, J., Schieltz, D. M., Carmack, E., Mize, G. J., Morris, D. R., Garvik, B. M., and Yates, J. R., 3rd (1999). Direct analysis of protein complexes using mass spectrometry. Nat Biotechnol *17*, 676-682.

Link, A. J., Fleischer, T. C., Weaver, C. M., Gerbasi, V. R., and Jennings, J. L. (2005). Purifying protein complexes for mass spectrometry: applications to protein translation. Methods *35*, 274-290.

Liquori, C. L., Ricker, K., Moseley, M. L., Jacobsen, J. F., Kress, W., Naylor, S. L., Day, J. W., and Ranum, L. P. (2001). Myotonic dystrophy type 2 caused by a CCTG expansion in intron 1 of ZNF9. Science *293*, 864-867.

Liu, Z., Sekito, T., Epstein, C. B., and Butow, R. A. (2001). RTG-dependent mitochondria to nucleus signaling is negatively regulated by the seven WD-repeat protein Lst8p. Embo J *20*, 7209-7219.

Lopez-Bergami, P., Habelhah, H., Bhoumik, A., Zhang, W., Wang, L. H., and Ronai, Z. (2005). RACK1 mediates activation of JNK by protein kinase C [corrected]. Mol Cell *19*, 309-320.

Manuell, A. L., Yamaguchi, K., Haynes, P. A., Milligan, R. A., and Mayfield, S. P. (2005). Composition and structure of the 80S ribosome from the green alga Chlamydomonas reinhardtii: 80S ribosomes are conserved in plants and animals. J Mol Biol *351*, 266-279.

Martinez, M. E., O'Brien, T. G., Fultz, K. E., Babbar, N., Yerushalmi, H., Qu, N., Guo, Y., Boorman, D., Einspahr, J., Alberts, D. S., and Gerner, E. W. (2003). Pronounced reduction in adenoma recurrence associated with aspirin use and a polymorphism in the ornithine decarboxylase gene. Proc Natl Acad Sci U S A *100*, 7859-7864.

Mazumder, B., Sampath, P., Seshadri, V., Maitra, R. K., DiCorleto, P. E., and Fox, P. L. (2003). Regulated release of L13a from the 60S ribosomal subunit as a mechanism of transcript-specific translational control. Cell *115*, 187-198.

McAfee, K. J., Duncan, D. T., Assink, M., and Link, A. J. (2006). Analyzing proteomes and protein function using graphical comparative analysis of tandem mass spectrometry results. Mol Cell Proteomics *5*, 1497-1513.

McCahill, A., Warwicker, J., Bolger, G. B., Houslay, M. D., and Yarwood, S. J. (2002). The RACK1 scaffold protein: a dynamic cog in cell response mechanisms. Mol Pharmacol *62*, 1261-1273.

McCormack, A. L., Schieltz, D. M., Goode, B., Yang, S., Barnes, G., Drubin, D., and Yates, J. R., 3rd (1997). Direct analysis and identification of proteins in mixtures by LC/MS/MS and database searching at the low-femtomole level. Anal Chem *69*, 767-776.

Meerovitch, K., Pelletier, J., and Sonenberg, N. (1989). A cellular protein that binds to the 5'-noncoding region of poliovirus RNA: implications for internal translation initiation. Genes Dev *3*, 1026-1034.

Meerovitch, K., Svitkin, Y. V., Lee, H. S., Lejbkowicz, F., Kenan, D. J., Chan, E. K., Agol, V. I., Keene, J. D., and Sonenberg, N. (1993). La autoantigen enhances and corrects aberrant translation of poliovirus RNA in reticulocyte lysate. J Virol *67*, 3798-3807.

Meyer, A. E., Hung, N. J., Yang, P., Johnson, A. W., and Craig, E. A. (2007). The specialized cytosolic J-protein, Jjj1, functions in 60S ribosomal subunit biogenesis. Proc Natl Acad Sci U S A *104*, 1558-1563.

Mikulits, W., Pradet-Balade, B., Habermann, B., Beug, H., Garcia-Sanz, J. A., and Mullner, E. W. (2000). Isolation of translationally controlled mRNAs by differential screening. Faseb J *14*, 1641-1652.

Mitchell, S. A., Brown, E. C., Coldwell, M. J., Jackson, R. J., and Willis, A. E. (2001). Protein factor requirements of the Apaf-1 internal ribosome entry segment: roles of polypyrimidine tract binding protein and upstream of N-ras. Mol Cell Biol *21*, 3364-3374.

Mitchell, S. A., Spriggs, K. A., Bushell, M., Evans, J. R., Stoneley, M., Le Quesne, J. P., Spriggs, R. V., and Willis, A. E. (2005). Identification of a motif that mediates polypyrimidine tract-binding protein-dependent internal ribosome entry. Genes Dev *19*, 1556-1571.

Mitchell, S. A., Spriggs, K. A., Coldwell, M. J., Jackson, R. J., and Willis, A. E. (2003). The Apaf-1 internal ribosome entry segment attains the correct structural conformation for function via interactions with PTB and unr. Mol Cell *11*, 757-771.

Mizushima, S., and Nomura, M. (1970). Assembly mapping of 30S ribosomal proteins from E. coli. Nature *226*, 1214.

Morinaga, T., Funatsu, G., Funatsu, M., and Wittman, H. G. (1976). Primary structure of the 16S rRNA binding protein S15 from Escherichia coli ribosomes. FEBS Lett *64*, 307-309.

Mourton, T., Hellberg, C. B., Burden-Gulley, S. M., Hinman, J., Rhee, A., and Brady-Kalnay, S. M. (2001). The PTPmu protein-tyrosine phosphatase binds and recruits the scaffolding protein RACK1 to cell-cell contacts. J Biol Chem *276*, 14896-14901.

Mumberg, D., Muller, R., and Funk, M. (1995). Yeast vectors for the controlled expression of heterologous proteins in different genetic backgrounds. Gene *156*, 119-122.

Nelson, R. J., Ziegelhoffer, T., Nicolet, C., Werner-Washburne, M., and Craig, E. A. (1992). The translation machinery and 70 kd heat shock protein cooperate in protein synthesis. Cell *71*, 97-105.

Nielsen, K. H., Szamecz, B., Valasek, L., Jivotovskaya, A., Shin, B. S., and Hinnebusch, A. G. (2004). Functions of eIF3 downstream of 48S assembly impact AUG recognition and GCN4 translational control. Embo J *23*, 1166-1177.
Nierhaus, K. H. (1991). The assembly of prokaryotic ribosomes. Biochimie *73*, 739-755.

Nilsson, J., Sengupta, J., Frank, J., and Nissen, P. (2004). Regulation of eukaryotic translation by the RACK1 protein: a platform for signalling molecules on the ribosome. EMBO Rep *5*, 1137-1141.

Nissen, P., Hansen, J., Ban, N., Moore, P. B., and Steitz, T. A. (2000). The structural basis of ribosome activity in peptide bond synthesis. Science *289*, 920-930.

Noller, H. F., and Chaires, J. B. (1972). Functional modification of 16S ribosomal RNA by kethoxal. Proc Natl Acad Sci U S A *69*, 3115-3118.

Noller, H. F., Hoffarth, V., and Zimniak, L. (1992). Unusual resistance of peptidyl transferase to protein extraction procedures. Science *256*, 1416-1419.

Nomura, M., and Lowry, C. V. (1967). PHAGE f2 RNA-DIRECTED BINDING OF FORMYLMETHIONYL-TRNA TO RIBOSOMES AND THE ROLE OF 30S RIBOSOMAL SUBUNITS IN INITIATION OF PROTEIN SYNTHESIS. Proc Natl Acad Sci U S A *58*, 946-953.

Nomura, M., and Traub, P. (1968). Structure and function of Escherichia coli ribosomes. 3. Stoichiometry and rate of the reconstitution of ribosomes from subribosomal particles and split proteins. J Mol Biol *34*, 609-619.

Nordeen, S. K., Green, P. P., 3rd, and Fowlkes, D. M. (1987). A rapid, sensitive, and inexpensive assay for chloramphenicol acetyltransferase. DNA *6*, 173-178.

O'Brien, T. G., Megosh, L. C., Gilliard, G., and Soler, A. P. (1997). Ornithine decarboxylase overexpression is a sufficient condition for tumor promotion in mouse skin. Cancer Res *57*, 2630-2637.

Olson, M. V., Dutchik, J. E., Graham, M. Y., Brodeur, G. M., Helms, C., Frank, M., MacCollin, M., Scheinman, R., and Frank, T. (1986). Random-clone strategy for genomic restriction mapping in yeast. Proc Natl Acad Sci U S A *83*, 7826-7830.

Otaka, E., Higo, K., and Osawa, S. (1982). Isolation of seventeen proteins and amino-terminal amino acid sequences of eight proteins from cytoplasmic ribosomes of yeast. Biochemistry *21*, 4545-4550.

Ozaki, T., Watanabe, K., Nakagawa, T., Miyazaki, K., Takahashi, M., and Nakagawara, A. (2003). Function of p73, not of p53, is inhibited by the physical interaction with RACK1 and its inhibitory effect is counteracted by pRB. Oncogene *22*, 3231-3242.

Palade, G. E. (1955). A small particulate component of the cytoplasm. J Biophys Biochem Cytol *1*, 59-68.

Pelletier, J., and Sonenberg, N. (1988). Internal initiation of translation of eukaryotic mRNA directed by a sequence derived from poliovirus RNA. Nature *334*, 320-325.

Pestov, D. G., Stockelman, M. G., Strezoska, Z., and Lau, L. F. (2001). ERB1, the yeast homolog of mammalian Bop1, is an essential gene required for maturation of the 25S and 5.8S ribosomal RNAs. Nucleic Acids Res *29*, 3621-3630.

Pestova, T. V., Borukhov, S. I., and Hellen, C. U. (1998). Eukaryotic ribosomes require initiation factors 1 and 1A to locate initiation codons. Nature *394*, 854-859.

Pestova, T. V., and Hellen, C. U. (2003). Translation elongation after assembly of ribosomes on the Cricket paralysis virus internal ribosomal entry site without initiation factors or initiator tRNA. Genes Dev *17*, 181-186.

Pfund, C., Lopez-Hoyo, N., Ziegelhoffer, T., Schilke, B. A., Lopez-Buesa, P., Walter, W. A., Wiedmann, M., and Craig, E. A. (1998). The molecular chaperone Ssb from Saccharomyces cerevisiae is a component of the ribosome-nascent chain complex. Embo J *17*, 3981-3989.

Pickering, B. M., Mitchell, S. A., Spriggs, K. A., Stoneley, M., and Willis, A. E. (2004). Bag-1 internal ribosome entry segment activity is promoted by structural changes mediated by poly(rC) binding protein 1 and recruitment of polypyrimidine tract binding protein 1. Mol Cell Biol *24*, 5595-5605.

Planta, R. J., and Mager, W. H. (1998). The list of cytoplasmic ribosomal proteins of Saccharomyces cerevisiae. Yeast *14*, 471-477.

Powell, D. W., Weaver, C. M., Jennings, J. L., McAfee, K. J., He, Y., Weil, P. A., and Link, A. J. (2004). Cluster analysis of mass spectrometry data reveals a novel component of SAGA. Mol Cell Biol *24*, 7249-7259.

Pyronnet, S., Pradayrol, L., and Sonenberg, N. (2000). A cell cycle-dependent internal ribosome entry site. Mol Cell *5*, 607-616.

Pyronnet, S., Pradayrol, L., and Sonenberg, N. (2005). Alternative splicing facilitates internal ribosome entry on the ornithine decarboxylase mRNA. Cell Mol Life Sci *62*, 1267-1274.

Pyronnet, S., and Sonenberg, N. (2001). Cell-cycle-dependent translational control. Curr Opin Genet Dev *11*, 13-18.

Pyronnet, S., Vagner, S., Bouisson, M., Prats, A. C., Vaysse, N., and Pradayrol, L. (1996). Relief of ornithine decarboxylase messenger RNA translational repression induced by alternative splicing of its 5' untranslated region. Cancer Res *56*, 1742-1745.

Qin, X., and Sarnow, P. (2004). Preferential translation of internal ribosome entry site-containing mRNAs during the mitotic cycle in mammalian cells. J Biol Chem *279*, 13721-13728.

Rajavashisth, T. B., Taylor, A. K., Andalibi, A., Svenson, K. L., and Lusis, A. J. (1989). Identification of a zinc finger protein that binds to the sterol regulatory element. Science *245*, 640-643.

Raught, B., Gingras, A. C., and Sonenberg, N. (2001). The target of rapamycin (TOR) proteins. Proc Natl Acad Sci U S A *98*, 7037-7044.

Reinhardt, J., and Wolff, T. (2000). The influenza A virus M1 protein interacts with the cellular receptor of activated C kinase (RACK) 1 and can be phosphorylated by protein kinase C. Vet Microbiol *74*, 87-100.

Rigas, A. C., Ozanne, D. M., Neal, D. E., and Robson, C. N. (2003). The scaffolding protein RACK1 interacts with androgen receptor and promotes cross-talk through a protein kinase C signaling pathway. J Biol Chem *278*, 46087-46093.

Riles, L., Dutchik, J. E., Baktha, A., McCauley, B. K., Thayer, E. C., Leckie, M. P., Braden, V. V., Depke, J. E., and Olson, M. V. (1993). Physical maps of the six smallest chromosomes of Saccharomyces cerevisiae at a resolution of 2.6 kilobase pairs. Genetics *134*, 81-150.

Rodal, A. A., Tetreault, J. W., Lappalainen, P., Drubin, D. G., and Amberg, D. C. (1999). Aip1p interacts with cofilin to disassemble actin filaments. J Cell Biol *145*, 1251-1264.

Ron, D., Chen, C. H., Caldwell, J., Jamieson, L., Orr, E., and Mochly-Rosen, D. (1994). Cloning of an intracellular receptor for protein kinase C: a homolog of the beta subunit of G proteins. Proc Natl Acad Sci U S A *91*, 839-843.

Ron, D., Jiang, Z., Yao, L., Vagts, A., Diamond, I., and Gordon, A. (1999). Coordinated movement of RACK1 with activated betaIIPKC. J Biol Chem *274*, 27039-27046.

Rudra, D., and Warner, J. R. (2004). What better measure than ribosome synthesis? Genes Dev *18*, 2431-2436.

Rudra, D., Zhao, Y., and Warner, J. R. (2005). Central role of Ifh1p-Fhl1p interaction in the synthesis of yeast ribosomal proteins. Embo J *24*, 533-542.

Rychlik, J. L., Gerbasi, V., and Lewis, E. J. (2003). The interaction between dHAND and Arix at the dopamine beta-hydroxylase promoter region is independent of direct dHAND binding to DNA. J Biol Chem *278*, 49652-49660.

Sachs, A. B., Sarnow, P., and Hentze, M. W. (1997). Starting at the beginning, middle, and end: translation initiation in eukaryotes. Cell *89*, 831-838.

Sadygov, R. G., Eng, J., Durr, E., Saraf, A., McDonald, H., MacCoss, M. J., and Yates, J. R., 3rd (2002). Code developments to improve the efficiency of automated MS/MS spectra interpretation. J Proteome Res *1*, 211-215.

Sampath, P., Mazumder, B., Seshadri, V., and Fox, P. L. (2003). Transcript-selective translational silencing by gamma interferon is directed by a novel structural element in the ceruloplasmin mRNA 3' untranslated region. Mol Cell Biol *23*, 1509-1519.

Sampath, P., Mazumder, B., Seshadri, V., Gerber, C. A., Chavatte, L., Kinter, M., Ting, S. M., Dignam, J. D., Kim, S., Driscoll, D. M., and Fox, P. L. (2004). Noncanonical function of glutamyl-prolyl-tRNA synthetase: gene-specific silencing of translation. Cell *119*, 195-208.

Sanders, S. L., Jennings, J., Canutescu, A., Link, A. J., and Weil, P. A. (2002). Proteomics of the Eukaryotic Transcription Machinery: Identification of Proteins Associated with Components of Yeast TFIID by Multidimensional Mass Spectrometry. Mol Cell Biol *22*, 4723-4738.

Saveanu, C., Namane, A., Gleizes, P. E., Lebreton, A., Rousselle, J. C., Noaillac-Depeyre, J., Gas, N., Jacquier, A., and Fromont-Racine, M. (2003). Sequential protein association with nascent 60S ribosomal particles. Mol Cell Biol *23*, 4449-4460.

Schaper, S., Fromont-Racine, M., Linder, P., de la Cruz, J., Namane, A., and Yaniv, M. (2001). A yeast homolog of chromatin assembly factor 1 is involved in early ribosome assembly. Curr Biol *11*, 1885-1890.

Schechtman, D., and Mochly-Rosen, D. (2001). Adaptor proteins in protein kinase C-mediated signal transduction. Oncogene *20*, 6339-6347.

Sengupta, J., Nilsson, J., Gursky, R., Spahn, C. M., Nissen, P., and Frank, J. (2004). Identification of the versatile scaffold protein RACK1 on the eukaryotic ribosome by cryo-EM. Nat Struct Mol Biol *11*, 957-962.

Shapiro, A. M., Lakey, J. R., Ryan, E. A., Korbutt, G. S., Toth, E., Warnock, G. L., Kneteman, N. M., and Rajotte, R. V. (2000). Islet transplantation in seven patients with type 1 diabetes mellitus using a glucocorticoid-free immunosuppressive regimen. N Engl J Med *343*, 230-238.

Sharp, P. M., and Li, W. H. (1987). The codon Adaptation Index--a measure of directional synonymous codon usage bias, and its potential applications. Nucleic Acids Res *15*, 1281-1295.

Shatkin, A. J. (1976). Capping of eucaryotic mRNAs. Cell *9*, 645-653.

Shatkin, A. J. (1985). mRNA cap binding proteins: essential factors for initiating translation. Cell *40*, 223-224.

Sherman, F., Fink, G. R., and Hicks, J. B. (1986). Laboratory Course Manual for Methods in Yeast Genetics (Cold Spring Harbor, NY, Cold Spring Harbor Press).

Shine, J., and Dalgarno, L. (1975). Determinant of cistron specificity in bacterial ribosomes. Nature *254*, 34-38.

Shor, B., Calaycay, J., Rushbrook, J., and McLeod, M. (2003). Cpc2/RACK1 is a ribosome-associated protein that promotes efficient translation in Schizosaccharomyces pombe. J Biol Chem *278*, 49119-49128.

Singh, R., Valcarcel, J., and Green, M. R. (1995). Distinct binding specificities and functions of higher eukaryotic polypyrimidine tract-binding proteins. Science *268*, 1173-1176.

Slessareva, J. E., Routt, S. M., Temple, B., Bankaitis, V. A., and Dohlman, H. G. (2006). Activation of the phosphatidylinositol 3-kinase Vps34 by a G protein alpha subunit at the endosome. Cell *126*, 191-203.

Smith, T. F., Gaitatzes, C., Saxena, K., and Neer, E. J. (1999). The WD repeat: a common architecture for diverse functions. Trends Biochem Sci *24*, 181-185.

Sonenberg, N., Morgan, M. A., Testa, D., Colonno, R. J., and Shatkin, A. J. (1979a). Interaction of a limited set of proteins with different mRNAs and protection of 5'-caps against pyrophosphatase digestion in initiation complexes. Nucleic Acids Res *7*, 15-29.

Sonenberg, N., Rupprecht, K. M., Hecht, S. M., and Shatkin, A. J. (1979b). Eukaryotic mRNA cap binding protein: purification by affinity chromatography on sepharose-coupled m7GDP. Proc Natl Acad Sci U S A *76*, 4345-4349.

Spahn, C. M., Beckmann, R., Eswar, N., Penczek, P. A., Sali, A., Blobel, G., and Frank, J. (2001). Structure of the 80S ribosome from Saccharomyces cerevisiae--tRNA-ribosome and subunit-subunit interactions. Cell *107*, 373-386.

Spahn, C. M., Jan, E., Mulder, A., Grassucci, R. A., Sarnow, P., and Frank, J. (2004). Cryo-EM visualization of a viral internal ribosome entry site bound to human ribosomes: the IRES functions as an RNA-based translation factor. Cell *118*, 465-475.

Spence, J., Gali, R. R., Dittmar, G., Sherman, F., Karin, M., and Finley, D. (2000). Cell cycle-regulated modification of the ribosome by a variant multiubiquitin chain. Cell *102*, 67-76.

Stallone, G., Infante, B., Schena, A., Battaglia, M., Ditonno, P., Loverre, A., Gesualdo, L., Schena, F. P., and Grandaliano, G. (2005a). Rapamycin for treatment of chronic allograft nephropathy in renal transplant patients. J Am Soc Nephrol *16*, 3755-3762.

Stallone, G., Schena, A., Infante, B., Di Paolo, S., Loverre, A., Maggio, G., Ranieri, E., Gesualdo, L., Schena, F. P., and Grandaliano, G. (2005b). Sirolimus for Kaposi's sarcoma in renal-transplant recipients. N Engl J Med *352*, 1317-1323.

Stebbins, E. G., and Mochly-Rosen, D. (2001). Binding specificity for RACK1 resides in the V5 region of beta II protein kinase C. J Biol Chem *276*, 29644-29650.

Stoneley, M., and Willis, A. E. (2004). Cellular internal ribosome entry segments: structures, trans-acting factors and regulation of gene expression. Oncogene *23*, 3200-3207.

Tang, H., Hornstein, E., Stolovich, M., Levy, G., Livingstone, M., Templeton, D., Avruch, J., and Meyuhas, O. (2001). Amino acid-induced translation of TOP mRNAs is fully dependent on phosphatidylinositol 3-kinase-mediated signaling, is partially inhibited by rapamycin, and is independent of S6K1 and rpS6 phosphorylation. Mol Cell Biol *21*, 8671-8683.

Tarun, S. Z., Jr., and Sachs, A. B. (1995). A common function for mRNA 5' and 3' ends in translation initiation in yeast. Genes Dev *9*, 2997-3007.

Tarun, S. Z., Jr., Wells, S. E., Deardorff, J. A., and Sachs, A. B. (1997). Translation initiation factor eIF4G mediates in vitro poly(A) tail-dependent translation. Proc Natl Acad Sci U S A *94*, 9046-9051.

Tcherkasowa, A. E., Adam-Klages, S., Kruse, M. L., Wiegmann, K., Mathieu, S., Kolanus, W., Kronke, M., and Adam, D. (2002). Interaction with factor associated

with neutral sphingomyelinase activation, a WD motif-containing protein, identifies receptor for activated C-kinase 1 as a novel component of the signaling pathways of the p55 TNF receptor. J Immunol *169*, 5161-5170.

Traub, P., Hosokawa, K., Craven, G. R., and Nomura, M. (1967). Structure and function of E. coli ribosomes, IV. Isolation and characterization of functionally active ribosomal proteins. Proc Natl Acad Sci U S A *58*, 2430-2436.

Traub, P., and Nomura, M. (1968a). Structure and function of E. coli ribosomes. V. Reconstitution of functionally active 30S ribosomal particles from RNA and proteins. Proc Natl Acad Sci U S A *59*, 777-784.

Traub, P., and Nomura, M. (1968b). Structure and function of Escherichia coli ribosomes. I. Partial fractionation of the functionally active ribosomal proteins and reconstitution of artificial subribosomal particles. J Mol Biol *34*, 575-593.

Traub, P., Soll, D., and Nomura, M. (1968). Structure and function of Escherichia coli ribosomes. II. Translational fidelity and efficiency in protein synthesis of a protein-deficient subribosomal particle. J Mol Biol *34*, 595-608.

Tschochner, H., and Hurt, E. (2003). Pre-ribosomes on the road from the nucleolus to the cytoplasm. Trends Cell Biol *13*, 255-263.

Tutton, P. J., and Barkla, D. H. (1986). Comparison of the effects of an ornithine decarboxylase inhibitor on the intestinal epithelium and on intestinal tumors. Cancer Res *46*, 6091-6094.

van Nocker, S., and Ludwig, P. (2003). The WD-repeat protein superfamily in Arabidopsis: conservation and divergence in structure and function. BMC Genomics *4*, 50.

Velculescu, V. E., Zhang, L., Zhou, W., Vogelstein, J., Basrai, M. A., Bassett, D. E., Jr., Hieter, P., Vogelstein, B., and Kinzler, K. W. (1997). Characterization of the yeast transcriptome. Cell *88*, 243-251.

Vilardell, J., and Warner, J. R. (1997). Ribosomal protein L32 of Saccharomyces cerevisiae influences both the splicing of its own transcript and the processing of rRNA. Mol Cell Biol *17*, 1959-1965.

Volarevic, S., Stewart, M. J., Ledermann, B., Zilberman, F., Terracciano, L., Montini, E., Grompe, M., Kozma, S. C., and Thomas, G. (2000). Proliferation, but not growth, blocked by conditional deletion of 40S ribosomal protein S6. Science *288*, 2045-2047.

Walter, B. L., Nguyen, J. H., Ehrenfeld, E., and Semler, B. L. (1999). Differential utilization of poly(rC) binding protein 2 in translation directed by picornavirus IRES elements. Rna *5*, 1570-1585.

Warner, J. R. (2001). Nascent ribosomes. Cell *107*, 133-136.

Warner, J. R., and Gorenstein, C. (1978). The ribosomal proteins of Saccharomyces cerevisiae. Methods Cell Biol *20*, 45-60.

Washburn, M. P., Wolters, D., and Yates, J. R., 3rd (2001). Large-scale analysis of the yeast proteome by multidimensional protein identification technology. Nat Biotechnol *19*, 242-247.

Wilson, J. E., Pestova, T. V., Hellen, C. U., and Sarnow, P. (2000). Initiation of protein synthesis from the A site of the ribosome. Cell *102*, 511-520.

Winzeler, E. A., Shoemaker, D. D., Astromoff, A., Liang, H., Anderson, K., Andre, B., Bangham, R., Benito, R., Boeke, J. D., Bussey, H.*, et al.* (1999). Functional characterization of the S. cerevisiae genome by gene deletion and parallel analysis. Science *285*, 901-906.

Wodicka, L., Dong, H., Mittmann, M., Ho, M. H., and Lockhart, D. J. (1997). Genome-wide expression monitoring in Saccharomyces cerevisiae. Nat Biotechnol *15*, 1359-1367.

Woolford, J. (2002). Chaperoning ribosome assembly. Mol Cell *10*, 8-10.

Yan, W., Schilke, B., Pfund, C., Walter, W., Kim, S., and Craig, E. A. (1998). Zuotin, a ribosome-associated DnaJ molecular chaperone. Embo J *17*, 4809-4817.

Yang, Q., and Sarnow, P. (1997). Location of the internal ribosome entry site in the 5' non-coding region of the immunoglobulin heavy-chain binding protein (BiP) mRNA: evidence for specific RNA-protein interactions. Nucleic Acids Res *25*, 2800-2807.

Yarwood, S. J., Steele, M. R., Scotland, G., Houslay, M. D., and Bolger, G. B. (1999). The RACK1 signaling scaffold protein selectively interacts with the cAMP-specific phosphodiesterase PDE4D5 isoform. J Biol Chem *274*, 14909-14917.

Yik, J. H., Chen, R., Nishimura, R., Jennings, J. L., Link, A. J., and Zhou, Q. (2003). Inhibition of P-TEFb (CDK9/Cyclin T) kinase and RNA polymerase II transcription by the coordinated actions of HEXIM1 and 7SK snRNA. Mol Cell *12*, 971-982.

Zinker, S., and Warner, J. R. (1976). The ribosomal proteins of Saccharomyces cerevisiae. Phosphorylated and exchangeable proteins. J Biol Chem *251*, 1799-1807.